

# MScMM

MASTER IN  
**MEDICAL  
MICROBIOLOGY**

**MARGARIDA REÇONHA MARQUES**  
BSc in Molecular and Cellular Biology

**Characterization of biofilm  
formation by bacteria associated  
with the midgut of *Anopheles*  
mosquito, vector of malaria**

October, 2023



**Universidade Nova de Lisboa**  
**Instituto de Tecnologia Química e Biológica António  
Xavier**

**Characterization of biofilm formation by bacteria  
associated with the midgut of *Anopheles*  
mosquito, vector of malaria**

**Author:** Margarida Reçonha Marques

**Supervisor:** Prof. Dr. Henrique Silveira, Instituto de Higiene e Medicina Tropical, Universidade Nova de Lisboa

**Co-Supervisors:** Dr. Sofia Santos Costa, Instituto de Higiene e Medicina Tropical, Universidade Nova de Lisboa; Dr. Sandra N. Pinto, Instituto Superior Técnico, Universidade de Lisboa

A thesis submitted to fulfil the requirements for completing the degree of Master in Medical Microbiology

**October, 2023**



INSTITUTO DE HIGIENE E  
MEDICINA TROPICAL  
DESDE 1902



## Communications

The results obtained from this Dissertation were accepted for communications in two national scientific meetings:

- **Margarida Marques**, Sofia Santos Costa, Sandra N. Pinto, Henrique Silveira, 2023. Characterization of biofilm formation by bacteria associated with the midgut of *Anopheles* mosquito, vector of malaria. Congress of Microbiology and Biotechnology 2023, 7<sup>th</sup> - 9<sup>th</sup> December 2023, Universidade da Beira Interior, Covilhã, Portugal. Oral communication.
- **Margarida Marques**, Sofia Santos Costa, Sandra N. Pinto, Henrique Silveira, 2023. Characterization of biofilm formation by bacteria associated with the midgut of *Anopheles* mosquito, vector of malaria. 3rd iBB Workshop, 13<sup>th</sup> November 2023, Instituto Superior Técnico, Lisboa, Portugal. Poster presentation.

## **Acknowledgments**

I would like to express my sincere gratitude to everyone who contributed in any way to this project:

To my supervisor, Prof. Dr. Henrique Silveira, and my Co-supervisors, Dr. Sofia Costa and Dr. Sandra Pinto, for their orientation, receptiveness, availability and transmitted knowledge, which contributed decisively to my scientific and personal development.

To the Scientific Committee of the XI Medical Microbiology Master Degree, as a representative of all those involved in it, for the knowledge transmitted over these two years, in particular to the Instituto de Tecnologia Química e Biológica António Xavier for coordinating this edition.

To all the researchers and laboratory colleagues, from both Instituto de Higiene e Medicina Tropical and Instituto Superior Técnico, who, although not directly involved in my work, helped me and were essential to its development. Thank you very much for your integration and help throughout this year.

To all my friends for their encouragement, emotional support and for being there whenever I needed them. A special thank you to Joana and Maria, whom I thank for the moments of sharing, critical reflection and friendship, which have been essential throughout this experience.

To all my family, especially my parents, Fátima and Mário, and my brother Gonçalo, who have accompanied me throughout this journey. Thank you for your unconditional love and support, for always encouraging me to fight for my principles and convictions, and for showing me the value of hard work and commitment. Without them it wouldn't have been possible.

## Abstract

Malaria is the most prevalent vector-borne disease, caused by *Plasmodium* parasites, transmitted by female *Anopheles* mosquitoes. One malaria control approach involves the *Anopheles* midgut microbiota manipulation. According to the literature, *Pseudomonas* spp. may reduce *Plasmodium* infection in *Anopheles* mosquitoes, which could be associated with their high capacity of biofilm production. Bacterial biofilms at the midgut epithelium may restrict the ookinetes' movement, therefore with potential application as a malaria transmission blocking tool.

This work focuses on the capacity of bacteria isolated from *Anopheles* midguts to form biofilms and their characterization, with emphasis on *Pseudomonas* and *Serratia* species. *Anopheles* midguts were macerated and plated in different selective and non-selective media. Morphologically distinct colonies were characterized by Gram staining and oxidase test, and identified by 16S rDNA Sanger sequencing. Selected isolates were further studied regarding their antibiotic susceptibility profiles by disc diffusion/E-tests and their ability to produce biofilms in different media. Isolates of interest were subjected to whole genome sequencing (WGS).

Biofilms were characterized by microbiological and biophysical tools, including quantification of biofilm maximum height using confocal microscopy.

We identified ten bacterial genera colonizing the midgut of six *Anopheles* species, including *Serratia* and *Pseudomonas*. WGS of *Serratia marcescens* and *Pseudomonas mendocina* isolates revealed the carriage of relevant biofilm-related genes and partly corroborated antibiotic resistance phenotypes. We observed that *S. marcescens* isolates formed poorly structured biofilms. In contrast, *P. mendocina* produced highly thick and heterogenous biofilms ( $39.00 \pm 22.44$   $\mu\text{m}$  maximum height), which were highly dependent on growth conditions. Moreover, the ability of the *P. mendocina* isolate to efficiently colonize the *An. stephensi* midgut was confirmed in 72-hours colonization assays.

Overall, our results highlight that the isolated *P. mendocina* has potential as a tool for the development of malaria control strategies. Further research is needed to comprehend biofilm formation mechanisms and its impact on malaria transmission.

**Keywords:** Malaria control, microbiota, *Pseudomonas* spp., *Serratia marcescens*, bacterial biofilms.

## Resumo

A malária é uma doença causada por parasitas do género *Plasmodium*, transmitidos por mosquitos do género *Anopheles*. Uma abordagem de controlo da malária envolve a manipulação da microbiota do intestino médio dos *Anopheles*. Segundo a literatura, *Pseudomonas* spp. poderão reduzir a infeção por *Plasmodium* em *Anopheles*, o que poderá estar associado à sua elevada capacidade de produção de biofilmes.

Este trabalho foca-se no estudo da capacidade das bactérias isoladas do intestino médio dos *Anopheles* em formar biofilmes e na sua caracterização, com destaque para espécies de *Pseudomonas* e *Serratia*.

Os intestinos médios dos *Anopheles* foram macerados e semeados em diferentes meios de cultura. Colónias morfológicamente distintas foram caracterizadas e identificadas por coloração de Gram, teste de oxidase e sequenciação de Sanger do gene 16S rDNA. Os isolados selecionados foram estudados quanto aos seus perfis de suscetibilidade a antibióticos e à sua capacidade de produção de biofilmes. Os isolados de interesse foram sujeitos a sequenciação total do genoma.

Os biofilmes foram caracterizados por ensaios microbiológicos e biofísicos, incluindo a quantificação da altura máxima dos biofilmes por microscopia confocal. Identificou-se dez géneros bacterianos em seis espécies de *Anopheles*, incluindo *Serratia* e *Pseudomonas*. A sequenciação total do genoma de *Serratia marcescens* e *Pseudomonas mendocina* revelou a presença de genes relacionados com a formação de biofilmes. Observou-se que os isolados de *S. marcescens* formaram biofilmes pouco estruturados. A *P. mendocina* produziu biofilmes espessos e heterogéneos ( $39,00 \pm 22,44$   $\mu\text{m}$  de altura máxima), sendo altamente dependente das condições de crescimento. Adicionalmente, a capacidade de colonização da *P. mendocina* no intestino médio de *An. stephensi* foi confirmada em ensaios de colonização de 72 horas.

Os resultados destacam que o isolado de *P. mendocina* tem potencial para o desenvolvimento de estratégias de controlo da malária. No entanto, é necessária investigação adicional para compreender os mecanismos de formação dos biofilmes e o seu impacto na transmissão da malária.

**Palavras-chave:** Controlo da malária, microbiota, *Pseudomonas* spp., *Serratia marcescens*, biofilmes bacterianos.

## Table of contents:

<b>Communications .....</b>	<b>i</b>
<b>Acknowledgments .....</b>	<b>ii</b>
<b>Abstract.....</b>	<b>iii</b>
<b>Resumo.....</b>	<b>iv</b>
<b>List of Figures.....</b>	<b>vii</b>
<b>List of Tables .....</b>	<b>ix</b>
<b>Abbreviations and Acronyms .....</b>	<b>x</b>
<b>1. Introduction.....</b>	<b>1</b>
1.1. Malaria .....	1
1.2. <i>Anopheles</i> mosquitoes as vectors of malaria.....	2
1.3. <i>Plasmodium</i> parasite life cycle and their hosts .....	4
1.4. <i>Anopheles</i> mosquito microbiota and the transmission of malaria.....	7
1.5. Therapeutic potential of gut microbiota transgenesis .....	12
1.6. Challenges associated with microbiota modulation as prevention of malaria transmission .....	15
1.7. <i>Pseudomonas</i> species and their potential for biofilm formation.....	16
1.8. Objectives.....	19
<b>2. Materials and Methods.....</b>	<b>20</b>
2.1. Culture media and solutions used .....	20
2.2. Bacterial isolation from the microbiota midgut of <i>Anopheles</i> mosquitoes .....	22
2.2.1. <i>Anopheles</i> species analyzed.....	22
2.2.2. Dissection of mosquitoes midguts.....	23
2.2.3. Isolation of bacteria from mosquitoes midguts .....	24
2.3. Identification of bacteria isolated from <i>Anopheles</i> midgut microbiota.....	25
2.4. Evaluation of antibiotic susceptibility profiles of bacteria from the <i>Anopheles</i> midgut microbiota .....	27

2.5. Colonization assay of <i>Anopheles stephensi</i> midgut with <i>Pseudomonas</i> sp. ....	29
2.6. Whole genome sequencing of bacteria isolated from the midgut .....	30
2.6.1. Bioinformatic analysis of sequences resulting from the WGS.....	31
2.7. Determination of bacterial growth curves .....	32
2.8. Analysis of biofilm formation potential .....	32
2.8.1. Analysis of biofilm formation by confocal microscopy .....	32
2.8.2. Quantitative analysis of adhesion and biofilm formation using the crystal violet assay .....	33
2.8.3. Evaluation of metabolic activity of biofilm-growing bacteria by a resazurin reduction fluorometric assay .....	34
2.8.4. Evaluation of Colony Forming Units of different biofilms.....	35
<b>3. Results and Discussion.....</b>	<b>36</b>
3.1. Bacteria isolation from <i>Anopheles</i> mosquitoes midguts .....	36
3.2. Antibiotic susceptibility profiles of bacteria isolated from mosquito midgut.....	43
3.3. Colonization of the midgut of <i>Anopheles stephensi</i> with <i>Pseudomonas</i> sp.....	46
3.4. Analysis of whole genome sequencing results.....	49
3.5. Determination of bacterial growth curves .....	56
3.6. Potential of biofilm production by bacteria isolated from the midgut of <i>Anopheles</i> .....	58
3.6.1. Analysis of biofilm formation by confocal microscopy .....	58
3.6.2. Quantitative analysis of adhesion and biofilm formation using the crystal violet assay .....	67
3.6.3. Evaluation of metabolic activity of biofilm-growing bacteria by a resazurin reduction fluorometric assay .....	68
3.6.4. Evaluation of Colony Forming Units of different biofilms.....	73
<b>4. Conclusions.....</b>	<b>76</b>
<b>5. Bibliographic References .....</b>	<b>81</b>
<b>6. Annexes .....</b>	<b>101</b>

## List of Figures

<b>Figure 1</b> – Global distribution of malaria and respective density of registered cases.. ...	4
<b>Figure 2</b> – Replicative cycle of the <i>Plasmodium</i> parasite.....	6
<b>Figure 3</b> – Anatomy of an <i>Anopheles</i> mosquito.....	6
<b>Figure 4</b> – Schematic representation of <i>Pseudomonas aeruginosa</i> biofilm formation..	17
<b>Figure 5</b> – Colonization of <i>Anopheles stephensi</i> midguts by <i>Pseudomonas</i> sp.....	49
<b>Figure 6</b> – Representative growth curves of the selected bacteria isolated from <i>Anopheles</i> ’ midguts.....	57
<b>Figure 7</b> – Representative confocal microscopy images of biofilms formed during 3 hours in different culture conditions.....	60
<b>Figure 8</b> – Representative confocal microscopy images of biofilms formed during 24 hours in different culture conditions.....	62
<b>Figure 9</b> – Influence of FBS in Schneider medium on biofilm formation.....	63
<b>Figure 10</b> – Biofilm height captured by confocal microscopy. ....	65
<b>Figure 11</b> – Influence of the incubation temperature on biofilm formation by <i>P. mendocina</i> .....	66
<b>Figure 12</b> – Adhesion assay at 3 hours of biofilm incubation.. ....	68
<b>Figure 13</b> – Chemical reaction and emission/absorption spectra on which the metabolic assay is based. ....	69
<b>Figure 14</b> – Metabolic assay in relation to the medium.....	71
<b>Figure 15</b> – Metabolic assay in relation to the bacterial isolate.....	72
<b>Figure 16</b> – Counting of CFU/mL of the different bacterial biofilms.. ....	75

<b>Figure S1</b> – Phylogenetic Analysis resulting from the Comprehensive Genome Analysis Service of the BV-BRC online program, referring to the <i>P. mendocina</i> isolate.....	101
<b>Figure S2</b> – Phylogenetic Analysis resulting from the Comprehensive Genome Analysis Service of the BV-BRC online program, referring to the <i>S. marcescens</i> isolates .....	102
<b>Figure S3</b> – Schematic representation of the genomic alignment between the sequences of the <i>S. marcescens</i> isolates resulting from whole genome sequencing. ...	103
<b>Figure S4</b> – Representative confocal microscopy images of 24 hours <i>S. marcescens</i> An. steph A7-A1 biofilms.....	104
<b>Figure S5</b> – Representative confocal microscopy images of 24 hours <i>S. marcescens</i> An. col A9-C4 biofilms. ....	105
<b>Figure S6</b> – Representative confocal microscopy images of 24 hours <i>P. aeruginosa</i> ATCC 27853 biofilms. ....	106

## List of Tables

<b>Table 1</b> – Composition of the culture media used throughout the project. ....	20
<b>Table 2</b> – Composition of the solutions used throughout the project. ....	22
<b>Table 3</b> – General conditions of each assay for isolating bacteria from the midgut of <i>Anopheles</i> . ....	23
<b>Table 4</b> – Sequences of universal primers used for amplification and sequencing of 16S rDNA. ....	26
<b>Table 5</b> – Program for amplification by PCR of 16S rDNA. ....	27
<b>Table 6</b> – Antibiotics tested, and respective class, for evaluation of antibiotic susceptibility profiles by the disk diffusion method. ....	28
<b>Table 7</b> – Antibiotics tested, and respective class, for evaluation of antibiotic susceptibility profiles by the E-test method. ....	29
<b>Table 8</b> – List of bacteria isolated from the midgut of <i>Anopheles</i> mosquitoes per assay. ....	39
<b>Table 9</b> – Antibiotic susceptibility profiles of <i>S. marcescens</i> isolates tested by the disk diffusion method. ....	45
<b>Table 10</b> – Antibiotic susceptibility profiles of <i>Pseudomonas</i> isolate tested by the E-test method. ....	46
<b>Table 11</b> – <i>In silico</i> analysis of the sequences resulting from whole genome sequencing. ....	54
<b>Table 12</b> – Prediction of antimicrobial susceptibility phenotype based on whole genome sequencing. ....	55

## Abbreviations and Acronyms

AMR	Antimicrobial Resistance
ATCC	American Type Culture Collection
CFU	Colony Forming Units
DNA	Deoxyribonucleic Acid
FBS	Fetal Bovine Serum
IZD	Inhibition Zone Diameter
LB	Luria-Bertani broth
MHA	Muller-Hinton Agar
MHB	Muller-Hinton Broth
MIC	Minimum Inhibitory Concentration
PBS	Phosphate Buffered Saline
PCR	Polymerase Chain Reaction
PIA	<i>Pseudomonas</i> Isolation Agar
ROS	Reactive Oxygen Species
RPMI	Roswell Park Memorial Institute
RPMI*	RPMI medium supplemented with HEPES, albumax, hypoxanthine and NaHCO <sub>3</sub>
Schneider+FBS	Schneider's <i>Drosophila</i> Medium supplemented with 20% (v/v) FBS
TSB	Tryptic Soy Broth
TSBG	TSB medium supplemented with 0.25% glucose
WGS	Whole Genome Sequencing

# 1. Introduction

## 1.1. Malaria

Malaria is a disease resulting from infection by protozoan parasites of the genus *Plasmodium*. The transmission of this disease occurs through the bite of *Anopheles* mosquitoes that are infected with the parasite and which, when they make a blood meal in a human individual, transmit the parasite into their bloodstream (Cowman *et al.*, 2016; Garcia, 2010).

There are several *Plasmodium* species capable of causing infection and disease in humans, the most relevant being *Plasmodium vivax*, in terms of geographical distribution (it is the species with the most impact outside the African continent) (Milner, 2018) and *Plasmodium falciparum*, in terms of severity of the disease caused (Gething *et al.*, 2012; Meibalan & Marti, 2017). The *P. falciparum* species is the most dominant in Africa, where the vast majority of cases are reported (in 2021, about 95% of malaria cases occurred in Africa) (World Health Organization, 2022).

Malaria is the most prevalent vector-borne disease and has the highest mortality impact in the world, with most deaths occurring in children (CDC, 2023; Milner, 2018). This disease is endemic in several countries, especially tropical and sub-tropical areas in Africa, Asia, and Central and South America. In 2021, there were an estimated 247 million malaria cases (in 84 endemic countries), resulting in about 619 000 deaths, mostly children in sub-Saharan Africa (World Health Organization, 2022). Most people infected with the parasite may only develop mild symptoms, such as fever and chills, but the disease can reach more severe, life-threatening stages, depending on the species of *Plasmodium* responsible for the infection and the host's own immune system (Cowman *et al.*, 2016; Milner, 2018). As a result, it is of great medical and economic relevance to develop strategies to control malaria, particularly with regard to its transmission.

In Europe, malaria has already been eradicated, but in many countries, it remains a public health problem (Nájera *et al.*, 2011). Although in Europe the parasite is no longer circulating in nature, it is equally important to study the main vectors on this continent, since there is always the possibility of imported cases from other continents resulting in the re-introduction of the parasite into the mosquito populations in Europe (Birnberg *et*

*al.*, 2021). In addition, the intense climate change that has been observed may also contribute to the establishment of mosquito populations in regions that previously did not have the temperature/humidity conditions to allow this to happen (Hertig, 2019).

## **1.2. *Anopheles* mosquitoes as vectors of malaria**

As above mentioned, parasites of the genus *Plasmodium* are transmitted to humans through a bite by mosquitoes of the genus *Anopheles*. This genus of mosquitoes harbors more than 400 species and, in general, are of great medical importance because they act as vectors of human and animal pathogens. There are about 30-40 *Anopheles* species that can transmit *Plasmodium* parasites (CDC, 2023; Cohuet *et al.*, 2010).

Like all mosquitoes, they go through different stages throughout their life cycle. The eggs are laid in the aquatic environment, and it is also there that the larval and pupal forms develop. It is only when mosquitoes reach the adult stage that the transition to the terrestrial environment occurs, where they can interact with humans and other animals. A striking feature of all mosquito-borne diseases is that only females can transmit the pathogen because only they feed on blood (CDC, 2023).

*Anopheles* mosquitoes have a worldwide distribution, with the exception of Antarctica, and the *Anopheles* species associated with malaria transmission depends on the geographic region and the environment of the region itself (Figure 1). In the African continent the main vectors of malaria belong to the *Anopheles gambiae* s.l. complex, which includes the main vectors *An. gambiae* s.s., *An. coluzzii* and *An. arabiensis*, and also *An. funestus* s.s. (belonging to the *An. funestus* s.l. complex) (Sinka *et al.*, 2012; Wiebe *et al.*, 2017). In Central and South America, *An. darlingi* and *An. aquasalis* are species associated with transmission of the parasite (Conn *et al.*, 2018; Laporta *et al.*, 2015; Sinka *et al.*, 2012; Torres *et al.*, 2022). *An. stephensi* is the most relevant malaria vector in urban areas in Asia, while in rural areas malaria transmission is more associated with *An. culicifacies* (Kumar *et al.*, 2012; Sinka *et al.*, 2011, 2012). In all these regions there are other species of *Anopheles* that can also act as secondary vectors of malaria. Although malaria is no longer endemic on the European continent, registering mostly imported cases, there are still populations of mosquitoes capable of transmitting the

parasite, of several species of *Anopheles*. Species such as *An. atroparvus* and *An. labranchiae* are examples of possible malaria vectors in Europe (Bertola *et al.*, 2022; Hertig, 2019; Sinka *et al.*, 2012).

Regardless of its worldwide distribution, these mosquitoes have a preference for tropical and sub-tropical regions, where the combination of temperature and humidity conditions is most favorable (CDC, 2023). Malaria transmission also occurs only under specific temperature and humidity conditions, which is why endemic countries are usually tropical/sub-tropical regions (Figure 1). For example, the *P. falciparum* parasite, cannot complete its infection cycle in the *Anopheles* mosquito at temperatures below 20°C (CDC, 2023).

Males usually live for about a week, feeding primarily on sugary nectars from plants. Adult females usually live between one to two weeks and can reach up to a month if the weather conditions are optimal. However, the vast majority of females live a short time, depending additionally on whether they succeed to feed on blood from a vertebrate host. Therefore, only a small proportion of females can live long enough to transmit malaria, as the extrinsic incubation period (the period of time it takes from the blood meal containing *Plasmodium* gametocytes until the mosquito becomes infective) can be up to fifteen days, for some *Plasmodium* species. Females also feed on sugary nectars to ensure that they obtain energy, but a blood meal is required for egg laying to occur, since the *Anopheles* species are anautogenic (CDC, 2023).

Since there are no anti-malarial vaccines yet, one of the main strategies to prevent transmission of the parasite is to control mosquito populations with insecticides (Greenwood *et al.*, 2008). When this approach fails and human infection occurs, anti-malarial drugs are usually used to treat the infection. Consequently, there has been a significant increase in mosquito resistance to commonly used insecticides (Dondorp *et al.*, 2010; Hemingway *et al.*, 2016; Ranson & Lissenden, 2016), and of the parasite to the anti-malarial drugs (Cheeseman *et al.*, 2012; Zoure *et al.*, 2020). Therefore, the emergence of new strategies that work around these issues are essential.

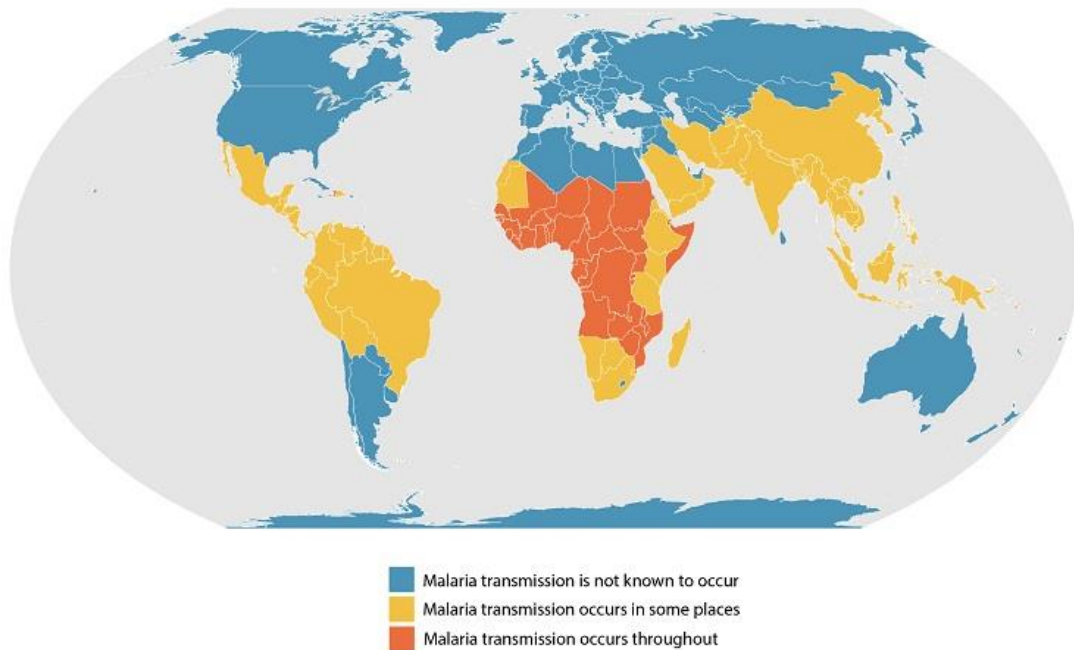


**Figure 1 - Global distribution of malaria and respective density of registered cases.**  
 Reproduced from CDC, 2020a.

Mosquitoes play a fundamental role in the ecosystem. Besides being central pollinating agents when they feed on the plants nectars, they serve as food for various organisms, both in the terrestrial environment in their adult phase (for example, by birds and bats), and in the aquatic environment in their larval phase (for example, by frogs and fish) (Wang & Jacobs-Lorena, 2013). Thus, the ideal strategy for mosquito-borne disease control would involve turning them in ineffective vectors, and not eliminate them from the ecosystems (Wang & Jacobs-Lorena, 2013). In the case of malaria, this is possible by developing methods that allow the parasite to be blocked/eliminated before the mosquito becomes infective, i.e. by attacking the stages that develop in the midgut of the mosquito (Abraham & Jacobs-Lorena, 2004).

### **1.3. *Plasmodium* parasite life cycle and their hosts**

Human malaria parasites depend on two cycles in two different hosts for their transmission in a population. When a human individual is bitten by an infected female *Anopheles* mosquito, sporozoites are introduced into the body, which first infect the liver

cells, where a series of parasite changes occur, resulting in the release of merozoites into the bloodstream. This form of the parasite infects the red blood cells, where it reproduces asexually, increasing the number of infected red blood cells (CDC, 2023). *P. falciparum* can modify the surface of red blood cells with adhesins, which results in its adhesion to the epithelium, to platelets, or to other red blood cells (Milner, 2018). It should be noted that it is the parasite stages that develop in the bloodstream that are responsible for the clinical manifestations of malaria (CDC, 2023). As the infection progresses, some parasites enter their sexual phase, where gametocytes (microgametocytes and macrogametocytes) are formed (Figure 2).

The gametocytes can be ingested along with a blood meal by a female *Anopheles* mosquito (Figure 3). In the lumen of the mosquito midgut, the microgametocytes (male) and macrogametocytes (female) fuse to form a flattened, mobile zygote (ookinete). This mobile form of the parasite passes through the epithelium of the mosquito midgut (about 18-36 hours after blood ingestion) reaching the basal lamina where it matures into an oocyst (Bahia *et al.*, 2014; Romoli & Gendrin, 2018). Normally after 8-15 days (depending on the *Plasmodium* species) the maturation of the oocyst occurs, on the basal side of the midgut (Yordanova *et al.*, 2018). The oocyst ruptures and releases the sporozoites into the hemolymph which, in turn, travel to the salivary glands. From this point on, the mosquito becomes infective and can transmit the parasite to a new vertebrate host (Figure 2).

Given the medical importance associated with mosquitoes, efforts have been made to understand and identify the factors that contribute to restrict the vectorial capacity of the mosquito, so they can be used for the development of new strategies to control pathogen transmission (Yordanova *et al.*, 2018). The vectorial capacity of mosquitoes depends on several factors, such as susceptibility to the pathogen, but also on population size, egg-laying capacity and biting frequency, all of which influence malaria transmission in a given geographic region (Chattopadhyay *et al.*, 2022; Smith & McKenzie, 2004).

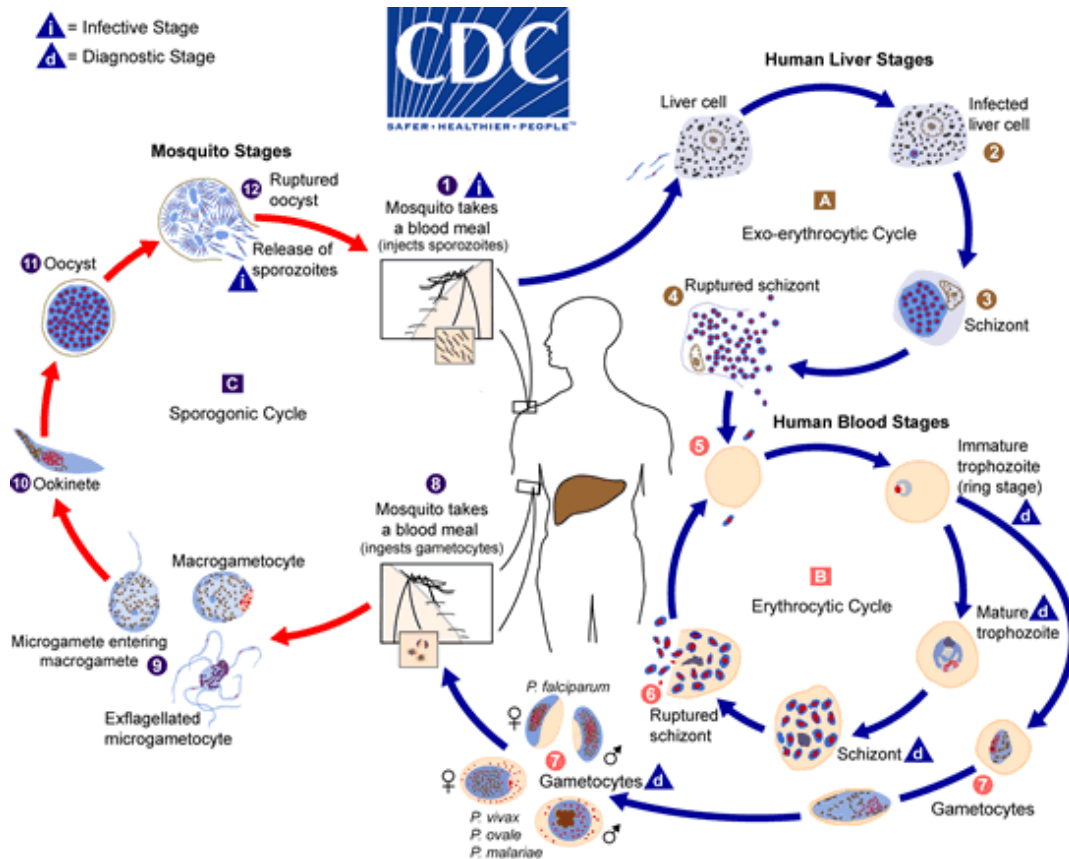


**Figure 2 - Replicative cycle of the *Plasmodium* parasite.** Representation of the development cycle of the infectious agent of malaria, in the *Anopheles* mosquito and the human host. Reproduced from CDC, 2020b.

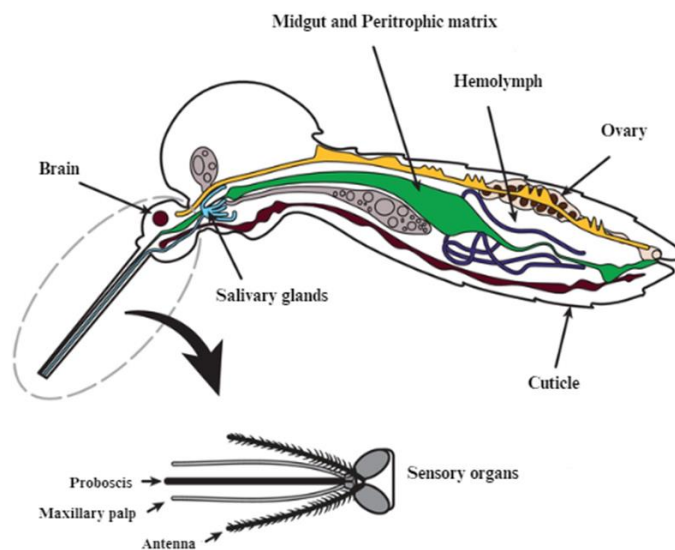


**Figure 3 - Anatomy of an *Anopheles* mosquito.** Representative scheme of the main internal organs of an *Anopheles* mosquito. Adapted from Hugo & Birrell, 2018.

For more complex organisms, there is a strong association of symbiont microorganisms with physiological processes of the host organism. This is also true for mosquitoes. The microbiota of the mosquito has an impact on its physiological processes and on the development of the *Plasmodium* parasite (Yordanova *et al.*, 2018).

#### **1.4. *Anopheles* mosquito microbiota and the transmission of malaria**

Microbiota is the term used to describe the community of microorganisms that inhabit a particular physiological environment, in or on the body of more complex organisms. It is a complex ecosystem of its own that includes bacteria, archaea, fungi, protozoa, and viruses (Gendrin & Christophides, 2013). The composition of an individual organism's microbiota is influenced by numerous factors, such as the surrounding environment, diet, and others. It is also known that these microorganisms influence and are essential for many physiological processes of the host (Das De *et al.*, 2022; Romoli & Gendrin, 2018). In the case of humans, several associations between changes in the microbiota and the development of some diseases are already known, as well as the potential for manipulating the microbiota to assist in the treatment of some of these conditions. It is thought that in the mosquito the same principle applies, i.e., the microbiota has an influence on the infection of the mosquito by *Plasmodium*, and its manipulation may be a promising method to control the infection (Huang *et al.*, 2020; Sharma *et al.*, 2020; Wang *et al.*, 2017).

*Anopheles* mosquitoes have symbiont microorganisms associated with various organs such as midgut, sexual organs, and salivary glands (Romoli & Gendrin, 2018), which have an influence on several physiological processes of the mosquito. As such, the interaction of these microorganisms with the mosquito and the parasite itself influences the establishment of the infection and consequently its transmissibility.

Several bacterial species of the mosquito microbiota have already been described to have anti-*Plasmodium* effect. This inhibitory effect on parasite development can be direct, by producing effector molecules that interact directly with the parasite (Bahia *et al.*, 2014; Dong *et al.*, 2009; Meister *et al.*, 2009; Wang *et al.*, 2017), or indirect, by activating immune mechanisms of the mosquito, which in turn lead to parasite elimination (Bai *et*

*al.*, 2019; Blumberg *et al.*, 2013; Cirimotich *et al.*, 2011; Dong *et al.*, 2009; Meister *et al.*, 2009; Rodgers *et al.*, 2017; Yordanova *et al.*, 2018).

One of the essential stages in the parasite's development in the mosquito takes place in the mosquito's midgut. The midgut of the mosquito is an immunocompetent organ, and the midgut microbiota is responsible for the basal immunity of mosquitoes, which is activated to prevent systemic infection by these bacteria. The presence of microorganisms (either pathogens or commensals) will result in an immune response by the arthropod (Rani *et al.*, 2009). This bacteria-induced immunity often results in the production of immune effectors with anti-*Plasmodium* activity (Bahia *et al.*, 2014).

The malaria parasite undergoes selective pressure throughout its life cycle within the mosquito, with the greatest bottleneck occurring when the ookinetes pass through the midgut epithelium (Taylor, 1999), where the parasite must overcome the mosquito immune system and the microorganisms of the mosquito midgut. Once the ookinetes begin to develop in the midgut, there will be a drastic reduction in their quantity due to the mosquito's immune system and interaction with the symbiont microorganisms (Dong *et al.*, 2009). The ookinetes that manage to survive, will ensure the continuity of the parasite's life cycle. Thus, the immune system of the mosquito and its commensal microorganisms are major influencers of its vectorial capacity, assuming a relevant role in the interaction between vector and parasite (Cirimotich *et al.*, 2011).

The microbiota of mosquitoes is highly influenced by the environment and, as in humans, varies slightly from individual to individual, although some bacteria are transmitted to offspring by the vertical route (Birnberg *et al.*, 2021; Dennison *et al.*, 2014; Gendrin & Christophides, 2013; Hegde *et al.*, 2018). Beside this, the microbiota of the mosquito also changes throughout its life cycle due to physiological and habitat changes (Birnberg *et al.*, 2021; Pereira *et al.*, 2021). The microbiota influences various physiological processes throughout the life cycle of the mosquito, such as larval development, fertility, immunity of the mosquito, and digestion of the blood meal (Das De *et al.*, 2022; Silva *et al.*, 2021). Thus, it will influence the susceptibility to infection by the *Plasmodium* parasite.

The development of the larval and pupal stages to the adult mosquito requires the transition from aquatic to terrestrial environment. In this process, a profound metamorphosis of the mosquito physiology occurs. In the larval stage, the mosquito

acquires its microbiota mostly from the aquatic environment, and it is at this stage that the microbial diversity is the highest (Birnberg *et al.*, 2021). When they pupate, there is a loss of bacterial communities, because they are expelled together with the larval peritrophic matrix during the molting from larvae to pupa (Gao *et al.*, 2020). However, the greatest loss of microbiota occurs when new adults emerge (where microbiota diversity is the lowest throughout the life cycle), as there is an almost complete sterilization of the midgut of the mosquitoes, with few bacterial genera being transmitted to the adult stage (Moll *et al.*, 2001; Yordanova *et al.*, 2018). On the other hand, adult mosquitoes also acquire some bacterial communities from the breeding water (reacquiring some of the bacteria that constituted the larval microbiota) and from sugar nectars they ingest, which may also alter the relative amounts of bacteria already present (Lindh *et al.*, 2008; Manda *et al.*, 2007; Yordanova *et al.*, 2018). Consequently, the composition of the microbiota of each mosquito will be highly dependent on its specific environment and geographic region, and its feeding habits.

The mosquito microbiota is known to include bacteria (Birnberg *et al.*, 2021; Manguin *et al.*, 2013; Rani *et al.*, 2009; Zoure *et al.*, 2020), fungi (Ricci, Damiani, *et al.*, 2011; Ricci, Mosca, *et al.*, 2011) and viruses (Gao *et al.*, 2020; O'neill *et al.*, 1995). Bacteria are the most common, best researched and known communities. In the case of the eukaryotic component of the microbiota, its study and identification (usually based on sequencing of the 18S rRNA coding gene) is hampered by interference from the chromosomal deoxyribonucleic acid (DNA) of the mosquito itself (Gendrin & Christophides, 2013).

No obligatory symbionts of *Anopheles* mosquitoes have yet been discovered, according to the different studies focusing on their microbiota. The nutritional function of midgut commensals is one of the main focuses of these studies. What is most interesting is that the influence on metabolism is not restricted to the mosquito. In a study in which *Anopheles* mosquitoes were fed with radioactively labeled *Pseudomonas* sp., the radioactive signal spread throughout the mosquito's body. Additionally, *Plasmodium* parasite that infected the mosquito also had radioactive signals in its oocysts and sporozoites, indicating that the gut microbiota plays a role in the parasite's metabolism as well (Gendrin & Christophides, 2013).

The microbiota of the *Anopheles* midgut is dominated by Gram-negative bacteria, and the most commonly identified phylum is *Pseudomonadota* (previously known as *Proteobacteria*), corresponding to more than 90% of the bacteria (Birnberg *et al.*, 2021; Das De *et al.*, 2022; Zoure *et al.*, 2020).

Several studies emphasize the fact that the microbiota of laboratory reared mosquitoes is relatively less diverse when compared to wild mosquitoes (Boissière *et al.*, 2012; Rani *et al.*, 2009; Romoli & Gendrin, 2018; Wang *et al.*, 2011). However, genera found in laboratory mosquitoes are also present in the wild ones, suggesting that laboratory mosquitoes colonies maintain some bacterial communities after laboratory adaptation (Wang *et al.*, 2011).

Numerous studies identified the bacterial genera associated with the midgut flora of *Anopheles*, mostly by culture methods or 16S rDNA sequencing. Some families frequently associated with the gut microbiota of *Anopheles* mosquitoes are *Enterobacteriaceae* (mainly genera *Enterobacter* and *Klebsiella*), *Pseudomonadaceae* (mainly genus *Pseudomonas*), *Yersiniaceae* (mainly genus *Serratia* and *Ewingella*), *Acetobacteraceae* (mainly genera *Acetobacter* and *Asaia*) and *Weeksellaceae* (mainly genera *Elizabethkingia* and *Chryseobacterium*) (Osei-Poku *et al.*, 2012; Romoli & Gendrin, 2018). In total, studies in both laboratory-reared and field-collected mosquitoes have identified over 98 bacterial genera with significant abundance in the midgut microbiota. Of these, 41 genera were found in more than one *Anopheles* species. *Pseudomonas* was the most frequently isolated genus, followed by *Aeromonas*, *Asaia*, *Comamonas*, *Elizabethkingia*, *Enterobacter*, *Klebsiella*, *Pantoea*, and *Serratia* (Gendrin & Christophides, 2013). No bacterial genus was isolated in all the experiments considered so, from what is known so far, there is no specific bacterial species that are considered obligate symbionts in *Anopheles* mosquitoes.

The mosquito midgut microbiota is relatively complex and undergoes considerable changes with the ingestion of a blood meal (which is stored and digested in the midgut), where there is a large expansion and proliferation of certain bacterial communities (about 100 to 1000 times) (Cirimotich *et al.*, 2011; Das De *et al.*, 2022; Romoli & Gendrin, 2018). The study by Das De *et al.*, (2022), using metagenomic analyses of *An. culicifacies* fed only with sugar, showed that the gut microbiota is dominated by bacteria from the

*Enterobacteriaceae* family (such as *Klebsiella pneumoniae*, *Salmonella enterica*, *Escherichia coli*), *Pseudomonadaceae* family (namely *Pseudomonas* genus) and *Moraxellaceae* family (namely *Acinetobacter* genus). The same analysis but on blood fed mosquitoes revealed a suppression of *Enterobacteriaceae*, accompanied by a considerable expansion of *Pseudomonadaceae* (reaching percentages of 40% of the total microbiota), including *P. mosselii*, *P. aeruginosa*, *P. chlororaphi* and *P. monteilii* species. The increased representation of *Pseudomonas* species is likely related to an increased diet-derived tryptophan consumption for serotonin production, which is a likely cause for the appetite loss that occurs after a blood meal (Das De *et al.*, 2022; Jenkins *et al.*, 2016). The introduction of the parasite into the mosquito happens at the time of a blood meal, so there is a greater chance of the parasite coming into contact with bacteria (or with metabolites resulting from bacteria) that expand after the ingestion of blood. Thus, the natural expansion of some bacteria in the presence of the parasite is an advantage to be explored for the malaria control strategies.

This expansion/proliferation is due to the female alternating meals between sugary nectars (for nutrient supply) and blood (for oviposition) (Yordanova *et al.*, 2018). The ingestion of blood results in physiological and oxidative changes in the midgut. The abundance of nutrients, namely proteins and lipids from the blood, induces a metabolic change, which leads to massive proliferation of most bacteria, inducing an increase in the expression of genes related to immune responses (Dong *et al.*, 2009), which contributes to the anti-*Plasmodium* effects. Furthermore, blood ingestion also results in increased levels of reactive oxygen species (ROS) in the mosquito hemolymph, activating ROS detoxification defenses, i.e., also leading to the activation of immune mechanisms, which ultimately also act against the parasite (Cirimotich *et al.*, 2011; Molina-Cruz *et al.*, 2008; Oliveira *et al.*, 2012).

Bacteria of the genera *Asaia*, *Enterobacter*, *Pantoea*, *Serratia* and *Pseudomonas* have already been proposed as promising candidates for symbiotic malaria control agents, using paratransgenesis, in *Anopheles* species belonging to the *Anopheles gambiae* s.l. group (which includes the main species of *Anopheles* that transmit malaria on the African continent) (Buck *et al.*, 2016; Capone *et al.*, 2013; Osei-Poku *et al.*, 2012).

The study by Birnberg *et al.*, (2021) analyzed the microbiota of the midgut of wild *An. atroparvus* from Spain and after their domestication in the laboratory. It describes that the highest bacterial diversity is observed in the larvae stage. *Pantoea*, *Thorsellia*, *Serratia*, *Asaia* and *Pseudomonas* were the dominant genera found in field captured females. After domestication in laboratory colonies, the most prevalent bacterial genera were *Asaia* and *Pseudomonas*. Of the 22 bacterial genera identified as the core microbiota of these mosquitoes, *Serratia* and *Pseudomonas* were the most prevalent throughout the various mosquito stages analyzed (Birnberg *et al.*, 2021).

Kalappa *et al.*, (2018) identified *Acinetobacter*, *Pseudomonas*, *Prevotella*, *Corynebacterium*, *Veillonella* and *Bacillus* as the most prevalent genera in laboratory *An. stephensi* in India, also finding that antibiotic treatment of these same mosquitoes results in increased susceptibility to *Plasmodium berghei* infection. The study by Chavshin *et al.*, (2012) identified 5 major genera in the midgut microbiota of *An. stephensi* in Iran (*Pseudomonas*, *Alcaligenes*, *Bordetella*, *Myroides*, and *Aeromonas*).

A clear predominance of *Pseudomonadota* (mainly *Gammaproteobacteria*) in the midgut microbiota of *Anopheles* is found in most studies reviewed. It is also verified that the associations between bacterial species and *Plasmodium* infection inhibition are usually made with Gram-negative bacteria, while Gram-positive bacteria are not associated with this beneficial effect.

### **1.5. Therapeutic potential of gut microbiota transgenesis**

The development of malaria control strategies continues to be an important topic of focus as malaria remains the vector-borne disease that causes the most deaths in the world (World Health Organization, 2022). With increasing resistance occurring in the parasite to anti-malarial drugs (Cheeseman *et al.*, 2012) and in mosquitoes to insecticides (Dondorp *et al.*, 2010; Ranson & Lissenden, 2016), the development of new strategies that rely on different approaches and mechanisms is urgently needed. One of the innovative strategies to control malaria transmission is to modulate and manipulate the microbiota associated with *Anopheles* mosquitoes so that they become resistant or, at least, less susceptible, to *Plasmodium* infection, because if the vector is less likely to

become infected, this directly results in a decrease of malaria cases in humans (Zoure *et al.*, 2020).

Therefore, there has been an increasing interest in the paratransgenesis strategy. This strategy consists of genetically modifying symbionts of the organism to decrease vector competence towards a particular pathogen (Wilke & Marrelli, 2015).

Efforts have been made to find the best bacterial candidate to be used for paratransgenesis strategies. In addition to the anti-*Plasmodium* effect, that the bacteria from the microbiota may have naturally, paratransgenesis involves modifying these bacteria to potentiate this effect, namely by the heterologous expression of immune genes with known negative effect on the development of the various parasite stages (Wang *et al.*, 2017). An important aspect of this strategy is that the symbiont used in the process must have the minimum fitness cost to the mosquito, so that the symbiont bacteria is not eliminated by natural selection (Wang *et al.*, 2017).

Another central aspect, which is perhaps one of the most challenging, is that, for the long-term success of this methodology, it is necessary for the bacteria to efficiently colonize the mosquito midgut and be perpetuated to the offspring over generations (Wang *et al.*, 2017), for a successful introduction into the wild population. As already discussed, few bacterial populations are transmitted between the early stages of the mosquito life cycle and its adult form, so this issue is one of the most challenging problems researchers face in developing these strategies. Thus, it is relatively complicated to ensure that the genetically modified bacteria are guaranteed to be transmitted between developmental stages of the mosquito. Nonetheless, a part of the bacteria of the midgut microbiota undergoes a large numerical expansion after ingestion of a blood meal by the mosquito. As such, it is expected that possible genetically modified bacteria introduced into the mosquito microbiota will also undergo this expansion, as well as their effector molecules (Wang *et al.*, 2017).

Several paratransgenesis strategies have already been attempted in experimental studies, using an *Escherichia coli* strain modified to produce anti-*Plasmodium* molecules on its surface (Riehle *et al.*, 2007). However, this strategy proved inefficient as the bacteria could not efficiently colonize the mosquito midgut and, consequently, the effector molecules could not reach their targets (Riehle *et al.*, 2007). Wang *et al.*, (2012) described

an attempt to use *Pantoea agglomerans* modified to secrete anti-*Plasmodium* effector molecules, but this study could not overcome the problem of spreading the bacteria throughout the population/generations (Wang *et al.*, 2012).

Another application of this strategy has been described for a strain of *Serratia marcescens* (*Serratia* AS1), isolated from the ovaries of *An. stephensi* from a laboratory colony, which had been genetically modified to express anti-*Plasmodium* effector genes (Wang *et al.*, 2017). The introduction of *Serratia* AS1 into the midgut microbiota of *An. stephensi* did not affect the fitness of the mosquito, and had no negative influence on lifespan, fecundity, fertility, and blood-feeding behavior. The *Serratia* AS1 strain was able to colonize the midgut of the mosquito and was found to increase dramatically (about 200x) after blood ingestion. An interesting fact is that this bacterium was also found in the hemolymph and ovaries of the mosquito, which facilitates its possible vertical transmission to offspring. In addition, it was also found on the surface of the eggs, which also turns out to be a mean of transmission of the bacteria, since they can be ingested by the larvae when they hatch (Wang *et al.*, 2017).

The presence of *Serratia* AS1 was also found in the accessory glands of males, indicating that this bacterium can be transmitted horizontally through mating. Since the bacterium is also present in the hemolymph, it was able to continue proliferating in the midgut of the adult mosquito after the extensive metamorphosis that occurs when adult mosquitoes emerge (transstadial transmission). Thus, this bacterium could be maintained in the mosquito population by various transmission routes, and it was found that it was maintained for at least three consecutive generations, making this strain a suitable candidate for paratransgenesis (Wang *et al.*, 2017). This study also showed the ability of this bacterium to heterologously produce several anti-*Plasmodium* effector molecules with various mechanisms of action. The infection assays concluded that the recombinant strains with several combinations of effector molecules were able to efficiently inhibit the development of *P. falciparum* and, at the same time, did not result in a negative impact on mosquito fitness. This study was a proof of concept that the genetically modified *Serratia* AS1 can function as a malaria control strategy. However, one of the challenges that remains is the transmission of the bacterium between different mosquito populations in nature. The authors point out as a possible dissemination strategy the placement of the bacterium in waters where mosquitoes normally lay their eggs (Wang *et al.*, 2017).

## **1.6. Challenges associated with microbiota modulation as prevention of malaria transmission**

There are some conflicting studies concerning the association of the presence of certain bacterial genera with the inhibition of *Plasmodium* infection in the mosquito (Romoli & Gendrin, 2018). This demonstrates the necessity to develop more appropriate and cross-sectional study models for investigations into the microbiota of *Anopheles* mosquitoes. One of the challenges in these studies is the great diversity of the microbiota between individuals of the same mosquito species (Boissière *et al.*, 2012; Coon *et al.*, 2014; Djadid *et al.*, 2011; Manguin *et al.*, 2013; Osei-Poku *et al.*, 2012; Rani *et al.*, 2009; Terenius *et al.*, 2008), making it difficult to generalize the findings of the various studies. Another limitation in the current studies of mosquito microbiota is their sole focus on bacterial communities, due to the difficulties associated with studying the viral and eukaryotic components of the microbiota. However, it is important to keep in mind that these non-bacterial communities probably also interact and influence parasite development (Belda *et al.*, 2017).

The phase of the parasite's life cycle where it undergoes the greatest immune pressure is during the crossing of the midgut epithelium by the ookinetes, where the greatest reduction in *Plasmodium* numbers occurs. As such, most studies focus on the description and identification of the microbiota of the mosquito midgut. However, a deeper knowledge of the microbiota associated with the other organs, such as the salivary glands and reproductive organs, is also relevant. The microbial communities of the salivary glands have a great potential for interaction with the parasites that managed to escape the immunological bottleneck in the midgut. On the other hand, microbial communities in the reproductive organs of mosquitoes, may influence reproductive success, immunity, lifespan and may be more easily transmitted to the offspring (vertically) or horizontally during mating. There are already some studies focusing on the microbiota of salivary glands and reproductive organs that highlight some differences in the abundance and diversity of microbial communities in the various mosquito organs (Gimonneau *et al.*, 2014; Segata *et al.*, 2016; Sharma *et al.*, 2014; Tchioffo *et al.*, 2016). However, according to Tchioffo *et al.*, (2016), rather than being uniquely influenced by the insect's organ, the microbiota of each mosquito is more strongly influenced by the history of the individual organism.

### **1.7. *Pseudomonas* species and their potential for biofilm formation**

The genus *Pseudomonas* is composed by Gram-negative, bacillus-shape, ubiquitous, metabolically very diverse bacteria that require relatively simple nutritional conditions (Radovanovic *et al.*, 2020). They are usually mobile, with one or more polar flagella, and are facultative anaerobic bacteria. Although there are some species that do not produce the cytochrome oxidase enzyme, the vast majority of *Pseudomonas* spp. are oxidase-positive, which makes the oxidase test useful for distinguishing this genus from bacteria of the order *Enterobacterales* (which are oxidase-negative). Certain species are pathogenic to humans, animals and plants, most of which are opportunistic (Palleroni, 2015).

Species of the genus *Pseudomonas* are often producers of biofilms. Biofilms are communities of microorganisms adhered to a surface, embedded in an extracellular matrix produced by the bacteria themselves, with both beneficial and problematic potentials for various areas of medicine and industry (Yan & Bassler, 2019). This characteristic is mainly studied and well characterized in the case of the species *Pseudomonas aeruginosa*, an opportunistic pathogen, in which biofilm production is related to severe disease in humans, normally immunocompromised. However, there are studies showing the great ability of other species belonging to this genus to produce biofilms, namely environmental species, which are not usually associated with disease in humans or other animals (Radovanovic *et al.*, 2020; Silverio *et al.*, 2022).

*P. aeruginosa* is a model organism for studying biofilms. The model described for this microorganism explains that biofilm formation begins by the adhesion of planktonic cells to a surface, where microcolony formation occurs, followed by the formation of a mature biofilm. Finally, the dispersion of cells from the biofilm to occupy new surfaces occurs (Ma *et al.*, 2009; Stoodley *et al.*, 2002) (Figure 4).

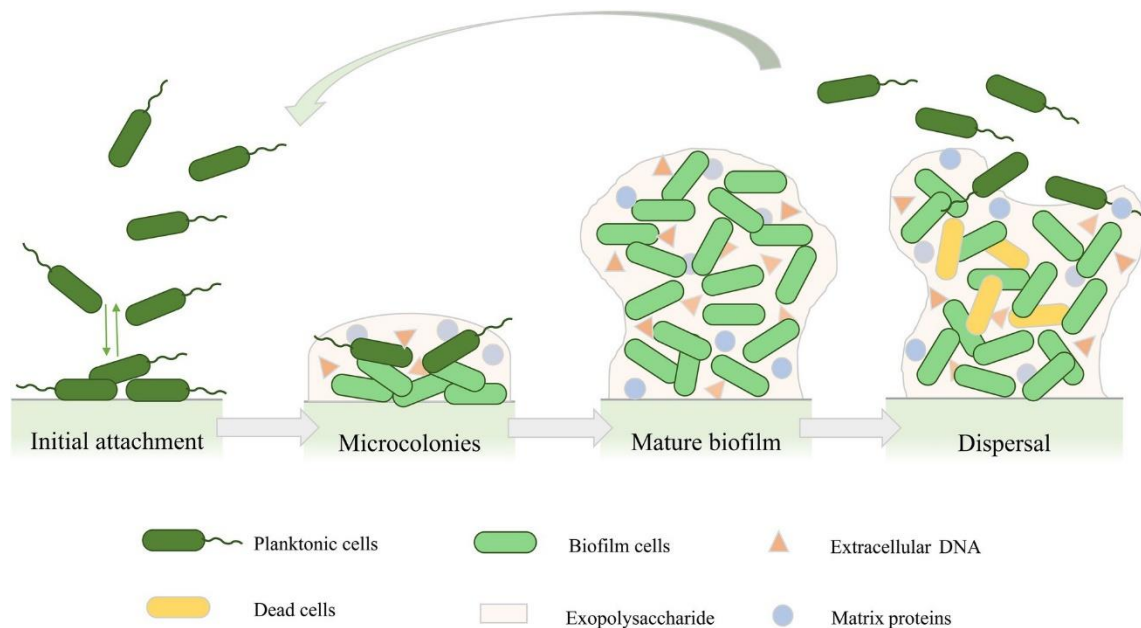


**Figure 4 – Schematic representation of *Pseudomonas aeruginosa* biofilm formation.** This process includes the four general steps: initial adhesion, microcolonies formation, formation of a mature biofilm and, finally, dispersal of the biofilm cells. In addition to the bacterial cells, the main components of the extracellular matrix of the *P. aeruginosa* biofilm are also indicated: exopolysaccharides, proteins and extracellular nucleic acids. Reproduced from Yin *et al.*, 2022.

The structuring of bacterial cells in biofilms allows them to have different groups of cells specialized in different processes, which is also related to the fact that there are different microenvironments within a biofilm, with different local conditions of nutrient availability, pH, humidity, redox conditions, etc. In other words, these structures and conditions allow a "division of labor", in which the various products of the metabolisms are released into the extracellular matrix and shared by the entire bacterial community of the biofilm. These structures and the conditions of low availability of nutrients and oxygen in some areas of the biofilm allow some cells to be in a state of metabolic dormancy, i.e. metabolically inactive, and are responsible for part of the tolerance/protection associated with biofilms to most antimicrobial agents and the host immune system, in addition to allowing a saving of resources by the bacterial community (Lewis, 2008; Tremblay *et al.*, 2014; Yan & Bassler, 2019).

Bacterial communities in biofilms are structured and maintained by an extracellular matrix that has as its general composition, polysaccharides, proteins, and extracellular nucleic acids (Ma *et al.*, 2009) (Figure 4). This matrix is essential to the maintenance of

the biofilm structure and also to the interaction between various bacterial sub-populations, as well as in tolerance mechanisms and genetic material exchange (Harmsen *et al.*, 2010). In addition, the biofilm matrix acts as a physical barrier to the entry of compounds with antimicrobial properties and factors of the host immune system (Drenkard, 2003). Thus, by the same principle, a bacterial biofilm present in the midgut epithelium of mosquitoes may function as a barrier to the passage of *Plasmodium* ookinetes through the midgut epithelium, essential to the process of maturation into oocysts that occurs in the developmental cycle of the parasite.

Bacterial communities in the midgut microbiota of mosquitoes are thought to live and grow in a biofilm mode, however, this hypothesis has not yet been studied closely enough (Chattopadhyay *et al.*, 2022; Jiang *et al.*, 2023; Ramirez *et al.*, 2014). Although biofilm formation is already recognized as an intrinsic feature of many bacteria, this formation always depends on many factors and conditions. Thus, it is necessary to test the ability of bacteria from the mosquito microbiota to produce biofilms *in vitro*, but it is also essential that this ability is studied *in vivo*, to understand the specific interactions and conditions that might enhance this ability. In addition, it is known that most naturally occurring biofilms are composed by more than one bacterial species, and within the midgut of the mosquito, given the existing bacterial diversity, biofilms are also likely to be polymicrobial, making it even more challenging to study and understand the mechanisms that lead to their formation.

From what is described in the literature, the genus *Pseudomonas* is among the most abundant in the midgut microbiota of *Anopheles* mosquitoes. This brings relevance to the study of biofilm formation by bacteria of this genus and isolated from the midgut of *Anopheles*, as it may be a starting point for the use of bacteria of this genus as candidates for paratransgenesis, which in some way contributes to the reduction of malaria transmission.

## 1.8. Objectives

Malaria is a major medical burden in many developing countries (CDC, 2023; World Health Organization, 2022). Consequently, the search for new strategies that overcome the problems associated with the strategies that are currently at the center of malaria prevention/treatment (insecticides and antimalarial drugs) is extremely important. One of the innovative strategies to prevent malaria transmission is known as paratransgenesis and consists of the genetic manipulation of microorganisms from the microbiota of *Anopheles* mosquitoes, in order to block the development cycle of *Plasmodium* inside the mosquito (Wilke & Marrelli, 2015; Zoure *et al.*, 2020). To this end, it is essential to study the microbial communities that live in association with *Anopheles* mosquitoes, as well as exploring possible bacterial features that can be explored for blocking malaria transmission. One feature that could be associated with blocking the parasite's development inside the mosquito is the formation of bacterial biofilms in the epithelium of the *Anopheles* midgut (Chattopadhyay *et al.*, 2022; Jiang *et al.*, 2023).

The main goal of this thesis is to analyze the potential for biofilm formation by bacteria isolated from the midgut of *Anopheles* mosquitoes from laboratory colonies. In particular, this study is expected to highlight the potential of *Pseudomonas* species as a potential target in the development of strategies to control malaria transmission.

In order to fulfill the above main goal, isolation of bacteria from the midgut of mosquitoes based on traditional culture methods was carried out. Although the focus of this study is mosquitoes from laboratory colonies, it is expected a relatively high level of bacterial diversity, and, in some way, distinctive between the different species of *Anopheles*. The experimental design was directed towards the isolation of species of the genus *Pseudomonas*, which was set in the begin as the main focus of this work. In addition, we also wanted to identify part of the composition of the bacterial flora of the midgut of various *Anopheles* species to obtain a more detail information on the relevance of each species. Subsequently, several microbiological and biophysical tests were carried out to characterize the biofilm-forming potential of a *Pseudomonas* species and *Serratia* species. The potential for biofilm formation was investigated under various *in vitro* conditions, including conditions that would mimic the environment in which the bacteria are found inside the mosquito.

## 2. Materials and Methods

### 2.1. Culture media and solutions used

All culture media (Table 1) and solutions (Table 2) were prepared with demineralized water and autoclaved at 121°C for 15 minutes.

**Table 1 - Composition of the culture media used throughout the project.**

Culture medium	Composition (per liter)
<b>Mueller-Hinton agar (MHA)<sup>1</sup></b>	2 g Beef extract; 17.5 g Acid Hydrolysate of Casein; 1.5 g Starch; 17 g Agar; pH: 7.3 ± 0.2
<b>Muller-Hinton Broth (MHB)<sup>1</sup></b>	2 g Beef extract; 17.5 g Acid digest of Casein; 1.5 g Starch; pH: 7.3 ± 0.1
<b><i>Pseudomonas</i> Isolation Agar (PIA)<sup>1</sup></b>	20 g Peptone; 1.4 g Magnesium Chloride; 10 g Potassium Sulfate; 25 mg Irgasan <sup>TM</sup> ; 13.6 g Agar; pH: 7.0 ± 0.2
<b>MacConkey II agar (MacConkey)<sup>2</sup></b>	17 g Pancreatic digest of Gelatin; 3 g Peptones (meat and Casein); 10 g Lactose; 1.5 g Bile Salts; 5 g Sodium Chloride; 13.5 g Agar; 0.03 g Neutral red; 1 mg Crystal Violet; pH: 7.1 ± 0.2
<b>CHROMagar<sup>TM</sup> <i>Pseudomonas</i><sup>3</sup></b>	15 g Agar; 20 g Peptone; 8 g Salts; 2.5 g Chromogenic mix; pH: 7.5 ± 0.2
<b>Blood agar (7% sheep blood)<sup>4</sup></b>	15 g Proteose Peptone; 2.5 g Liver Digest; 5 g Sodium Chloride; 5 g Yeast Extract; 14 g Agar; 70 mL Defibrinated Sheep Blood; pH: 7.2 ± 0.2
<b>Luria-Bertani Broth (LB)<sup>5</sup></b>	10 g SELECT Peptone 140; 5 g SELECT Yeast Extract; 10 g NaCl; pH: 7.3 ± 0.2
<b>Tryptic Soy Broth (TSB)<sup>6</sup></b>	17 g Pancreatic digest of Casein; 3 g Papaic digest of Soybean; 2.5 g Dextrose; 5 g Sodium Chloride; 2.5 g Dipotassium Phosphate; pH: 7.3 ± 0.2
<b>Tryptic Soy Broth + glucose<sup>7</sup></b>	TSB medium; 2.5 g glucose; pH: 7.3 ± 0.2

(<sup>1</sup>): BD Difco<sup>TM</sup>, Franklin Lakes, Nova Jersey, USA; (<sup>2</sup>): BD BBL<sup>TM</sup>, Franklin Lakes, Nova Jersey, USA; (<sup>3</sup>): CHROMagar<sup>TM</sup>, Kanto Chemical Co, Tokyo, Japan; (<sup>4</sup>): LiofilChem, Roseto degli Abruzzi (TE), Italy; (<sup>5</sup>): NZYTech, Lisbon, Portugal; (<sup>6</sup>): BD Bacto<sup>TM</sup>, Franklin Lakes, Nova Jersey, USA; (<sup>7</sup>): Scharlab, Sentmenat, Spain.

**Table 1 (continuation) - Composition of the culture media used throughout the project.**

Culture medium	Composition (per liter)
<b>Roswell Park Memorial Institute (RPMI)<sup>8</sup></b>	10 mg Glycine; 0.2 g L-Arginine; 50 mg L-Asparagine; 20 mg L-Aspartic acid; 65 mg L-Cystine 2HCl; 20 mg L-Glutamic Acid; 0.3 g L-Glutamine; 15 mg L-Histidine; 20 mg L-Hydroxyproline; 50 mg L-Isoleucine; 50 mg L-Leucine; 40 mg L-Lysine hydrochloride; 15 mg L-Methionine; 15 mg L-Phenylalanine; 20 mg L-Proline; 30 mg L-Serine; 20 mg L-Threonine; 5 mg L-Tryptophan; 29 mg L-Tyrosine disodium salt dihydrate; 20 mg L-Valine; 0.2 mg Biotin; 3 mg Choline chloride; 0.25 mg D-Calcium pantothenate; 1 mg Folic Acid; 1 mg Niacinamide; 1 mg Para-Aminobenzoic Acid; 1 mg Pyridoxine hydrochloride; 0.2 mg Riboflavin; 1 mg Thiamine hydrochloride; 0.005 mg Vitamin B12; 35 mg i-Inositol; 0.1 g Calcium nitrate; 48.84 mg Magnesium Sulfate; 0.4 g Potassium Chloride; 2 g Sodium Bicarbonate; 6 g Sodium Chloride; 0.8 g Sodium Phosphate dibasic; 2 g D-Glucose (Dextrose); 1 mg Glutathione (reduced); 5 mg Phenol Red; pH: 7.4 ± 0.2
<b>Roswell Park Memorial Institute supplemented (RPMI*)</b>	RPMI medium; 5.94 g HEPES; 5 g Albumax; 0.05 g hypoxanthine; 38 mL NaHCO <sub>3</sub> ; pH: 7.4 ± 0.2
<b>Schneider's <i>Drosophila</i> Medium<sup>8</sup></b>	0.25 g Glycine; 0.4 g L-Arginine; 0.4 g L-Aspartic acid; 0.06 g L-Cysteine; 0.1 g L-Cystine; 0.8 g L-Glutamic Acid; 1.8 g L-Glutamine; 0.4 g L-Histidine; 0.15 g L-Isoleucine; 0.15 g L-Leucine; 1.65 g L-Lysine hydrochloride; 0.8 g L-Methionine; 0.15 g L-Phenylalanine; 1.7 g L-Proline; 0.25 g L-Serine; 0.35 g L-Threonine; 0.1 g L-Tryptophan; 0.5 g L-Tyrosine; 0.3 g L-Valine; 0.5 g beta-Alanine; 0.6 g Calcium Chloride; 1.8069 g Magnesium Sulfate; 1.6 g Potassium Chloride; 0.45 Potassium Phosphate monobasic; 0.4 g Sodium Bicarbonate; 2.1 g Sodium Chloride; 0.701 g Sodium Phosphate dibasic; 0.2 g Alpha-Ketoglutaric acid; 2 g D-Glucose (Dextrose); 0.1 g Fumaric acid; 0.1 g Malic acid; 0.1 g Succinic acid; 2 g Trehalose; 2 g Yeastolate; pH: 7.4 ± 0.2
<b>Schneider's <i>Drosophila</i> Medium + Fetal Bovine Serum (FBS)<sup>9</sup></b>	Schneider's <i>Drosophila</i> Medium; 20% (v/v) FBS; pH: 7.4 ± 0.2

(<sup>8</sup>): Gibco™ Thermo Scientific, Waltham, Massachusetts, USA; (<sup>9</sup>) Sigma-Aldrich, St. Louis, Missouri, USA.

**Table 2 - Composition of the solutions used throughout the project.**

<b>Solutions</b>	<b>Composition</b>
<b>Phosphate Buffered Saline (PBS)<sup>1</sup></b>	137 mM NaCl; 2.7 mM KCl; 10 mM phosphate buffer; pH: 7.4 ± 0.05
<b>TE buffer</b>	10 mM TrisHCl <sup>2</sup> ; 1 mM EDTA <sup>3</sup> ; pH: 8± 0.2
<b>Physiological Saline Solution</b>	0.85% (p/v) NaCl <sup>4</sup>

(<sup>1</sup>): VWR Life Science, Avantor, Radnor, Pennsylvania, USA; (<sup>2</sup>): NZYTech, Lisbon, Portugal; (<sup>3</sup>): Sigma-Aldrich, St. Louis, Missouri, USA; (<sup>4</sup>): Merck KGaA, Darmstadt, Germany

## **2.2. Bacterial isolation from the microbiota midgut of *Anopheles* mosquitoes**

The main goal of this work was the characterization of biofilm production by *Pseudomonas* spp. isolated from *Anopheles* midgut. Thereby, bacterial isolation procedures were conducted to increase the likelihood of isolating *Pseudomonas* species, using selective media [*Pseudomonas* isolation agar (PIA) and CHROMagar *Pseudomonas*] for this purpose, in addition to the non-selective medium (Mueller-Hinton agar, MHA). Despite the use of selective media for *Pseudomonas*, these commercial media are more targeted to clinically relevant species, such as *Pseudomonas aeruginosa*, which makes isolation of environmental species difficult. Therefore, an enrichment step in non-selective media (Mueller-Hinton broth, MHB) was introduced aimed at increasing the relative amounts of the various bacteria to increase the likelihood of isolating the species of interest.

### **2.2.1. *Anopheles* species analyzed**

The various assays to isolate bacteria covered the different *Anopheles* species maintained at Instituto de Higiene e Medicina Tropical (IHMT, Lisbon, Portugal) laboratory colonies (*Anopheles stephensi*, *Anopheles atroparvus*, *Anopheles gambiae* and *Anopheles coluzzii*), as well as two laboratory species from Brazil (*Anopheles darlingi* and *Anopheles aquasalis*), under different feeding conditions (Table 3).

**Table 3 - General conditions of each assay for isolating bacteria from the midgut of *Anopheles*.** Assays performed for the isolation of bacteria from the midgut of mosquitoes, with the respective species of *Anopheles*, the nutritional conditions of the mosquitoes and presence or absence of the enrichment step in liquid medium. It is also indicated the solid culture media used for the isolation of the bacterial species in each assay.

Assay (#)	<i>Anopheles</i> ' species	Pre-blood-fed	Enrichment step**	Isolation culture media used
1	<i>Anopheles stephensi</i> ♀	No	No	- MHA - PIA
2	<i>Anopheles atroparvus</i> ♀	No	No	
3	<i>Anopheles stephensi</i> ♀	Yes	No	
4	<i>Anopheles stephensi</i> ♀	No	No	- MHA - PIA - MacConkey
5	<i>Anopheles stephensi</i> ♀	Yes (artificial diet)	No	
6	<i>Anopheles stephensi</i> ♂	No	No	
7	<i>Anopheles stephensi</i> ♂	No	Yes	- MHA - PIA - MacConkey
8	<i>Anopheles stephensi</i> ♀	Yes	Yes	
9	<i>Anopheles coluzzii</i> ♀	Yes	Yes	- MHA - PIA - MacConkey - CHROMagar <i>Pseudomonas</i> - Blood agar
10	<i>Anopheles darlingi</i> ♂*	No	Yes	
11	<i>Anopheles darlingi</i> ♀*	No	Yes	
12	<i>Anopheles gambiae</i> ♀	Yes	Yes	
13	<i>Anopheles aquasalis</i> ♂*	No	Yes	
14	<i>Anopheles aquasalis</i> ♀*	No	Yes	

*Anopheles* species indicated with \* are mosquitoes from laboratory colonies in Brazil (preserved dry, so the dissection was of the entire abdomen and not just the midgut). The symbols ♀ (female) and ♂ (male) identify the gender of the mosquitoes used in each assay. The enrichment step (\*\*) was performed in non-selective liquid medium for 24 hours after midgut dissection. MHA - Muller Hinton II agar; PIA - *Pseudomonas* isolation agar; MacConkey - MacConkey II agar; CHROMagar *Pseudomonas*; Blood agar - Blood agar Base (Sheep Blood 7%).

### 2.2.2. Dissection of mosquitoes midguts

All the necessary material for dissection was autoclaved (121°C for 15 minutes) or washed with 70% ethanol. All procedures were conducted in a sterile environment.

Pools of ten living adult mosquitoes were collected from the respective colony. Mosquitoes were anesthetized by placing them at  $-4^{\circ}\text{C}$  for 1 minute. To reduce any possible contamination, the mosquito's surface was sterilized by rinsing in 10% sodium hypochlorite for 1 minute, followed by 1 minute in 75% ethanol and finally 1 minute in sterile Phosphate Buffered Saline (PBS) (Table 2). Dissections were performed under a binocular magnifier. Each mosquito was dissected in a drop of sterile PBS on a sterilized slide and each midgut was placed in another drop of sterile PBS. A pool of 10 midguts each was collected into 200  $\mu\text{L}$  of sterile PBS. Pools of ten living adult mosquitoes from the laboratory colony from Brazil were sterilized on the outside only 30 seconds (instead of 1 minute), due to their preservation conditions (dry), and the area dissected was the entire abdomen and not just the midgut.

Each pool was homogenized using a motorized sterile pestle for about 1 minute. The samples were stored at  $4^{\circ}\text{C}$  until plating each homogenate.

### **2.2.3. Isolation of bacteria from mosquitoes midguts**

Throughout the various attempts to isolate bacteria from the midgut of *Anopheles* mosquitoes, the culture media for isolation were varied (Table 3). Initially, only a non-selective medium (MHA) and a selective medium for *Pseudomonas* spp. (PIA) were used. The PIA medium confers preferential selection of *Pseudomonas* spp. because it contains Irgasan (Triclosan), which is a broad-spectrum antimicrobial agent that has no effect against *Pseudomonas* spp., while inhibiting other Gram-negative and Gram-positive bacteria. The CHROMagar *Pseudomonas* medium is a chromogenic culture medium, suitable for the growth of *Pseudomonas* species, where they should appear with a greenish pigmentation, while *Enterobacteriaceae* are inhibited or show a violet pigmentation.

The MacConkey medium was used for the preferential isolation of Gram-negative bacteria, which is due to the presence in its composition of bile salts and crystal violet, which act as inhibitors of Gram-positive bacteria. This medium also allows to differentiate bacteria according to their capacity to ferment lactose, allowing a preliminary analysis of the characteristics of the isolated bacteria. The Blood Agar

medium (Sheep Blood 7%) allows the growth of more fastidious microorganisms and the detection of hemolytic activity by certain bacterial species.

For assays 1-6, ten-fold serial dilutions of the pooled midgut macerates were prepared in PBS and 100  $\mu$ L aliquots of the  $10^{-4}$ ,  $10^{-5}$  and  $10^{-6}$  dilutions were plated on the different media (three replicates per dilution per medium) (Table 3).

For assays 7-14, an enrichment step was performed in non-selective liquid medium (MHB), where the pooled midgut macerate was added to 5 mL of MHB and incubated at 37°C with 180 rpm agitation for 18-20 hours. Following this, ten-fold serial dilutions of the overnight culture were prepared in PBS and 100  $\mu$ L aliquots of the  $10^{-6}$ ,  $10^{-7}$  and  $10^{-8}$  dilutions were plated on the different media (three replicates per dilution per medium) (Table 3).

All plates were incubated at 37°C for 18-20 hours. In assays where very small colonies were observed, the plates were left at room temperature for further 24 hours.

### **2.3. Identification of bacteria isolated from *Anopheles* midgut microbiota**

From each plate, morphologically distinct colonies were selected and transferred to non-selective media (MHA) and selective media (PIA and CHROMagar *Pseudomonas*) to obtain pure cultures. From each pure culture, stocks were prepared by transferring the entire region of confluent growth, which was resuspended in media supplemented with 10% (v/v) glycerol (Sigma-Aldrich) and kept at -80°C.

A presumptive identification of each bacterium was performed by analyses of the colony morphological characteristics, Gram staining and oxidase test.

For the Gram staining, a drop of sterile water was placed on a glass microscope slide and an isolated colony was suspended in the drop of water. The bacteria were fixed by heat and the smear was flooded sequentially with crystal violet for 1 minute, Lugol's iodine solution for 1 minute, 100% ethanol for 20 seconds and, finally, fuchsin for 1 minute. Each reagent was washed with tap water. Afterwards, the slide was left to dry, and the smear was observed using a microscope (CH30RF200, Olympus Optical Co, Shinjuku, Tokyo, Japan).

The detection of cytochrome oxidase in the different bacteria was evaluated using the oxidase test strip method (Bactident<sup>R</sup> Oxidase, Sigma-Aldrich). The strip tip, impregnated with a redox indicator, was rubbed directly in one isolated colony. After 5-10 minutes, a change in the strip tip color, from white/colorless to violet indicates a positive result (presence of oxidase), while a no color change represents a negative result.

For bacteria with the desired characteristics (Gram-negative, oxidase-positive) or other bacteria of interest, a molecular identification was performed by 16S rDNA sequencing. First, for total DNA extraction, 3-4 single colonies were removed with a sterile plastic loop and resuspended in 0.5 mL of TE buffer (Table 2) + 1% Triton X-100 (Sigma-Aldrich) + 180 µg/mL proteinase K (NZYTech). The cellular suspensions were incubated at 56°C on a heat block for one hour, and then at 100°C for 10 minutes. The cellular suspensions were then cooled on ice and centrifuged at 13.000 rpm (MicroStar12, VWR Life Science, Avantor) for five minutes. The supernatants (which contain the total DNA) were collected and transferred to new 1.5 mL tubes. All total DNA samples were stored at -20°C.

Amplification of an internal region of the 16S rDNA gene (492 bp) was performed in 25 µL reaction mixtures containing 1X buffer NZY Tech (NZYTech), 1.75 mM MgCl<sub>2</sub> (NZYTech), 0.2 mM dNTPs (NZYTech), 0.4 µM of each universal primer (27f and 519r, MWG-Biotech AG, Ebersberg, Germany) (Table 4), 0.75 U of NZY Taq-II Polymerase (NZYTech) and 5 µL of total DNA. Total DNA of *Staphylococcus pseudintermedius* DSM21284<sup>T</sup> (known to amplify from previous experiences) was used as positive control and for negative control sterile water was added to the master mix.

All PCR reactions were performed in an UNO II thermocycler (Biometra, Gottingen, Germany) using the amplification program described in Table 5.

**Table 4 - Sequences of universal primers used for amplification and sequencing of 16S rDNA.**

<b>Universal primer</b>	<b>Primer sequence</b>	<b>Reference</b>
<b>27f</b>	5'- AGAGTTTGATCMTGGCTCAG - 3'	Lane, 1991
<b>519r</b>	5'- GWATTACCGCGGCKGCTG - 3'	Lane <i>et al.</i> , 1985

**Table 5 – Program for amplification by PCR of 16S rDNA.**

<b>Initial denaturation</b>	<b>Denaturation</b>	<b>Hybridization</b>	<b>Elongation</b>	<b>Final elongation</b>
94°C	94°C	50°C	72°C	72°C
5 min	30 s	45 s	45 s	5 min
1 cycle	<b>35 cycles</b>			1 cycle

The amplification products (5 µL) were analyzed by 1% (p/v) agarose (NZYTech) gel electrophoresis, using 1 Kb Gene Ruler DNA Ladder (Thermo Fisher Scientific, Waltham, Massachusetts, USA) as molecular weight size marker and using GreenSafe Premium (NZYTech) as nucleic acid stain. The electrophoresis was carried out at 90 V for 40 minutes and the agarose gel was then visualized under UV light in a Gel-Doc XR (Bio-Rad Laboratories, Milan, Italy).

To identify the bacterial species, the amplification products were purified using the NZYGelpure kit (NZYTech), according to manufacturer’s instructions and sequenced by Sanger sequencing at STAB-Vida (Caparica, Portugal) using the 27f primer.

The sequences were then analyzed using the BioEdit Sequence Alignment Editor software (BioEdit v.7.2.5., Hall, 1999), where the quality of the sequences obtained was checked. Finally, once the sequence had been edited, the bacterial species was identified using the BLASTn tool from the National Center for Biotechnology Information (NCBI, Maryland, USA), which allowed access to the bacterial species with the highest percentage of identity with the query sequence, allowing the identification of the bacteria isolated from the midguts of mosquitoes.

#### **2.4. Evaluation of antibiotic susceptibility profiles of bacteria from the *Anopheles* midgut microbiota**

The antibiotic susceptibility profiles of bacteria isolated from the *Anopheles* midgut were determined using the Kirby-Bauer Disk Diffusion and E-test methods, according to the Clinical and Laboratory Standards Institute (CLSI) recommendations (CLSI, 2023). The antibiograms were performed for all isolates identified as *S. marcescens* or *Pseudomonas*

sp.. In addition, the tests were also applied to the quality control reference strains *Pseudomonas aeruginosa* ATCC® 27853™ and *Escherichia coli* ATCC® 25922™. Isolates were categorized as susceptible (S), intermediate (I) or resistant (R) following the CLSI recommendations (CLSI, 2023).

Briefly, four to five colonies from each pure culture were suspended and homogenized in physiological saline solution (Table 2) and the turbidity of the cellular suspension was adjusted to 0.5 McFarland standard. Using a sterile swab, the suspension was inoculated on the entire surface of a MHA plate. Next, the antibiotic-impregnated disks were placed on the surface of the agar. After 10 minutes, the plates were inverted and incubated at 37°C for 16 to 18 hours. After this, the plates were visualized, and inhibition zones diameters were measured. The antibiotics tested are listed in Table 6.

For the *Pseudomonas* isolate and for the reference strains *P. aeruginosa* ATCC 27853 and *E. coli* ATCC 25922, the E-test (LiofilChem) method was also applied to assess susceptibility profiles towards gentamicin, tetracycline, ciprofloxacin, and chloramphenicol (Table 7), with the same initial steps described for the disk diffusion method. After the suspension had been inoculated on the MHA plates, the E-test strip was placed. The minimum inhibitory concentrations (MICs) were registered after 16 to 18 hours of incubation at 37°C. The antibiotic susceptibility profiles were determined according to the CLSI recommendations (CLSI, 2023) (Table 7).

**Table 6 - Antibiotics tested, and respective class, for evaluation of antibiotic susceptibility profiles by the disk diffusion method.** The zone diameter breakpoints and the respective interpretative categories are also indicated. The interpretative categories are divided into susceptible (S), intermediate (I) and resistant (R), according to the Table 2A (Zone Diameter and MIC Breakpoints for *Enterobacterales*) of the CLSI M100 2023 recommendations (CLSI, 2023).

Antibiotic	Antibiotic class	Disk content (µg)	Interpretive Categories and Zone Diameter Breakpoints (mm)		
			S	I	R
<b>Ampicillin (AMP)</b>	Beta-lactams	10	≥ 17	14-16	≤ 13
<b>Ceftriaxone (CRO)</b>	Beta-lactams	30	≥ 23	20-22	≤ 19
<b>Gentamicin (CN)</b>	Aminoglycosides	10	≥ 18	15-17	≤ 14
<b>Tobramycin (TN)</b>		10	≥ 17	13-16	≤ 12
<b>Tetracycline (T)</b>	Tetracyclines	30	≥ 15	12-14	≤ 11
<b>Ciprofloxacin (CIP)</b>	Quinolones	5	≥ 26	22-25	≤ 21
<b>Trimethoprim-sulfamethoxazole (SXT)</b>	Sulfonamides	1.25/23.75	≥ 16	11-15	≤ 10
<b>Chloramphenicol (C)</b>	Phenicols	30	≥ 18	13-17	≤ 12

**Table 7 - Antibiotics tested, and respective class, for evaluation of antibiotic susceptibility profiles by the E-test method.** The MIC breakpoints ( $\mu\text{g/mL}$ ) and the respective interpretative categories are also indicated. The interpretative categories are divided into susceptible (S), intermediate (I) and resistant (R), according to the Table 2B-5 (MIC Breakpoints for Other Non-*Enterobacteriales*), for all antibiotics, and Table 2B-1 (Zone Diameter and MIC Breakpoints for *Pseudomonas aeruginosa*), for ciprofloxacin (marked by \*) of the CLSI M100 2023 recommendations (CLSI, 2023).

Antibiotic	Antibiotic class	Interpretive Categories and MIC Breakpoints ( $\mu\text{g/mL}$ )		
		S	I	R
<b>Gentamicin (CN)</b>	Aminoglycosides	$\leq 4$	8	$\geq 16$
<b>Tetracycline (T)</b>	Tetracyclines	$\leq 4$	8	$\geq 16$
<b>Ciprofloxacin (CIP)</b>	Quinolones	$\leq 0.5^*$	$1^*$	$\geq 2^*$
		$\leq 1$	2	$\geq 4$
<b>Chloramphenicol (C)</b>	Phenicol	$\leq 8$	16	$\geq 32$

### 2.5. Colonization assay of *Anopheles stephensi* midgut with *Pseudomonas* sp.

This experiment was conducted to evaluate the colonization of *Anopheles stephensi* by *Pseudomonas mendocina* and the reference strain *Pseudomonas aeruginosa* ATCC 27853.

A bacterial suspension of a pure culture was prepared in MHB with an optical density at 600 nm ( $\text{OD}_{600}$ ) corresponding to  $1 \times 10^6$  CFU/mL. After this step, an aliquot was taken and plated on MHA, which was incubated at  $37^\circ\text{C}$  for 24 hours for bacteria enumeration in colony forming units (CFU)/mL, for confirmation. From this suspension, three different bacterial inoculums were prepared: low ( $10^3$  CFU/mL), intermediate ( $10^5$  CFU/mL), and high ( $10^6$  CFU/mL). The inocula were centrifugated at 14000 rpm for 5 minutes, and the bacterial pellets were resuspended in blood from laboratory mice. Four groups of 30 mosquitoes each were fed with 500  $\mu\text{L}$  of blood inoculated with a different bacterial concentration. The fourth group, for control purposes, was fed with blood without the addition of any bacteria. The mosquitoes were allowed to feed for one hour, in a temperature-controlled room (at  $28^\circ\text{C}$ ). All mosquitoes were left in a temperature-controlled room for 72 hours (Ramirez *et al.*, 2014) at  $20^\circ\text{C}$ .

Pools of ten midguts of each group were dissected and macerated in 200  $\mu$ L of PBS (procedure described in subsection 2.2.2). Each suspension was added to 5 mL of MHB and incubated at 37°C, with 180 rpm of agitation, for 18-20 hours.

From the resulting overnight cultures, ten-fold serial dilutions were prepared in PBS and 100  $\mu$ L aliquots were plated on MHA, PIA and CHROMagar *Pseudomonas* (three replicates for each dilution for each media). Plates were incubated at 37°C for 18-20 hours. The CFU/mL counts were obtained for each morphologically distinct colony. Morphologically distinct colonies were characterized by Gram staining and oxidase test and identified by 16S rDNA Sanger sequencing (procedure described in subsection 2.3.). For each bacterium, this procedure was performed in two independent replicates.

## **2.6. Whole genome sequencing of bacteria isolated from the midgut**

Five bacterial isolates were selected for further study by whole genome sequencing (WGS): S1 – *Pseudomonas mendocina* isolated from *An. gambiae*; S2 - *Pseudomonas mendocina* isolate recovered after the colonization experiment on *An. stephensi* (see subsection 2.5.); S3 – *S. marcescens* An. steph A1-C1 isolated from *An. stephensi*; S4 – *S. marcescens* An. steph A7-A1 isolated from *An. stephensi*; S5 – *S. marcescens* An. col A9-C4 isolated from *An. coluzzii*.

For genomic DNA isolation, the bacterial isolates were grown in MHA at 37°C, and then liquid cultures were prepared in 5 mL of MHB at 37°C for 18 hours at 180 rpm. The genomic DNA was extracted with the NZY Tissue gDNA Isolation kit (NZYTech) from 1 mL of overnight culture, according to the manufacturer's instructions. The genomic DNA was analyzed by a 0.7% (p/v) agarose gel electrophoresis in TAE 1X buffer at 90V for 45 min to assess DNA degradation. To verify the concentration and quality of the isolated genomic DNA, 1-2  $\mu$ L aliquots were analyzed using the Qubit™ dsDNA HS Assay Kit (Invitrogen, Thermo Fisher Scientific) on a Qubit™ 4 Fluorometer (Invitrogen, Thermo Fisher Scientific) and NanoDrop 1000 (Thermo Fisher Scientific), respectively.

### 2.6.1. Bioinformatic analysis of sequences resulting from the WGS

Whole genome sequencing (WGS) was performed using Illumina technology by NovoGene Biotech Co., Ltd (Beijing, China), which included a bioinformatics analysis, ensuring data quality control. The subsequent analysis of the files received from the company was conducted in the Bacterial and Viral Bioinformatics Resource Center (BV-BRC v.3.31.12) information system. For each of the samples, the sequences were received in two FASTQ files (Clean Data). These files were uploaded to the BV-BRC platform, and the Genome Assembly tool was applied to obtain the best assembly and, at the same time, obtain only one file in FASTA format for each sample. The FASTA files resulting from this analysis were submitted to the Genome Annotation Service, which provides annotation of genomic features using the RAST tool kit (RASTtk). The FASTA files resulting from the assembly were also entered into the Comprehensive Genome Analysis Service, which performs a comprehensive analysis including annotation, identification of nearest neighbors, a basic comparative analysis that includes a subsystem summary, phylogenetic tree, and the features that distinguish the genome from its nearest neighbors. This tool allowed for a general analysis of these characteristics of the genomes analyzed. Although this last analysis already included a phylogenetic analysis and the identification of the bacterial species with the highest percentage of identity relative to the sequences under investigation, a direct analysis was also carried out in the BLAST tool, using the BLASTn program and the “Reference and representative genomes (bacteria, archaea)” database. Finally, the FASTA sequences were entered into the Genome Alignment Service, which aligns genomes using progressiveMauve (Darling *et al.*, 2010). An alignment was carried out between the sequences of the three *S. marcescens* isolates (S3, S4 and S5) and another between the sequences of *P. mendocina* (S1 and S2). All these analyses were carried out in a complementary and simplified approach.

In addition to this analysis, a prediction of the antimicrobial resistance phenotype was performed from the FASTA sequences after assembly. This analysis was carried out on the Center for Genomic Epidemiology online platform, using the ResFinder tool, which allows phenotype prediction, as well as identifying acquired antimicrobial resistance genes (AMR genes).

## **2.7. Determination of bacterial growth curves**

The growth curves were determined for the bacterial isolates used in the biofilm formation characterization assays: *P. mendocina*, *S. marcescens* An. steph A1-C1, *S. marcescens* An. steph A7-A1, *S. marcescens* An. col A9-C4 and the reference strain *P. aeruginosa* ATCC 27853. Bacterial suspensions were prepared in MHB at  $1 \times 10^6$  CFU/mL. In a 96-well U-bottom polystyrene plate (Orange Scientific, Braine-l'Alleud, Belgium), bacterial growth was monitored for 24 hours by measuring the optical density (OD) at ten minutes intervals, using a microplate reader SPECTROstar<sup>Nano</sup> (BMG Labtech, Ortenberg, Germany).

## **2.8. Analysis of biofilm formation potential**

### **2.8.1. Analysis of biofilm formation by confocal microscopy**

For these assays, the *P. mendocina* isolate, three isolates of *S. marcescens* (An. steph A1-C1, An. steph A7-A1 and An. col A9-C4) and the reference strain *P. aeruginosa* ATCC 27853 were selected. For biofilm incubation, from cultures in MHA, cellular suspensions were prepared (with OD<sub>600nm</sub> corresponding to  $1 \times 10^6$  CFU/mL) in six different culture media: MHB, LB, TSB, TSB supplemented with 0.25% glucose (TSBG), supplemented Roswell Park Memorial Institute medium (RPMI) and Schneider's *Drosophila* Medium. RPMI medium was supplemented with HEPES, albumax, hypoxanthine and NaHCO<sub>3</sub> (referred as RPMI\*) and Schneider's *Drosophila* Medium was supplemented with 20% (v/v) Fetal Bovine Serum (FBS) (referred as Schneider+FBS) (Table 1).

The liquid cultures were inoculated on uncoated plastic biofilm growth 8-well plates (200  $\mu$ L/well) (Ibidi GmbH, Munich, Germany). The CFU/mL of the initial inoculum was confirmed by plating and colony count in MHA medium. After 24h of incubation at 37°C, the media were carefully removed from each well, to wash out the non-adherent bacteria, and a solution of 1% SYTO 9 (Invitrogen, Thermo Fisher Scientific) was added. SYTO 9 is a membrane-permeable green-fluorescent nuclear and chromosome counterstain, which has a high affinity for DNA and exhibits enhanced fluorescence and quantum yield upon binding. By binding to DNA (both intracellular DNA and extracellular DNA from

the biofilm matrix), labeling with this probe allows the visualization of the biofilm's structure and biomass (McGoverin *et al.*, 2020; Tawakoli *et al.*, 2013).

The biofilms were stained in the dark at room temperature with 3  $\mu$ M SYTO 9 for 15 minutes, proceeded by a rinsing step with sterile PBS to remove the unbound dye. The plates were then observed under a Leica TCS SP5 inverted confocal microscope (Leica Microsystems CMS GmbH, Mannheim, Germany) to check for cell adhesion and biofilm formation. The microscope is equipped with a continuous Ar ion laser (Multi-line LASOS<sup>®</sup> LGK 7872 ML05). Images were collected at 512 by 512 pixels and using a scan rate of 100 Hz per frame. A 63x1.2 N.A. water immersion objective was used (HCX PL APO CS 63.0 x 1.20 WATER UV). SYTO 9 images were recorded using a 488 nm excitation line and emission was collected at 501–570 nm. Images were collected on the xyz plane view, using various digital zooms and on the xzy plane view. For each bacterium, this procedure was performed in at least two independent replicates.

This procedure was also performed for the bacteria *P. mendocina* and *S. marcescens* An. steph A1-C1 in the Schneider's *Drosophila* Medium supplemented with different percentages (v/v) of FBS (0%, 5%, 10% and 20%).

### **2.8.2. Quantitative analysis of adhesion and biofilm formation using the crystal violet assay**

The purpose of this assay was to investigate the differences in the adhesion step of biofilm formation between strains: the *P. mendocina* isolate and the *S. marcescens* An. steph A1-C1.

Briefly, in a 96-well clear flat-bottom polystyrene plate (VWR Life Science, Avantor), the two isolates ( $1 \times 10^6$  CFU/mL) were inoculated in different media: MHB, LB, TSB and TSBG, RPMI\* and Schneider+FBS (Table 1).

Six replicates were performed for each medium and a negative control containing only media was included in all assays. The plate was incubated at 37°C for three hours. After the three hours, a wash step was performed with sterile MHB to remove non-adhered cells. 200  $\mu$ L of a 0.25% crystal violet solution (Sigma-Aldrich) was added to each well

and left for 30 minutes. The 0.25% crystal violet solution was removed and three wash steps with sterile MHB were performed. 200  $\mu$ L of 95% ethanol was added to each well and left for five minutes under gentle agitation. The well volume was transferred to a new 96-well plate and absorbance readings at 590 nm were taken in the microplate reader SPECTROstar<sup>Nano</sup> (BMG Labtech). The experiment was performed in two independent assays, with six technical replicates each.

### **2.8.3. Evaluation of metabolic activity of biofilm-growing bacteria by a resazurin reduction fluorometric assay**

To discriminate the bacterial metabolic activity within the different biofilms, we used the PrestoBlue assay according to the description in Pinto *et al.*, (2019). Resazurin is the active compound in PrestoBlue and the assay takes into consideration the reduction by metabolic active cells of the oxidized blue dye resazurin into the pink fluorescent resorufin intermediate product.

Briefly, the five bacterial isolates were cultured in MHB, LB, TSB, TSBG, RPMI\* and Schneider+FBS at an initial inoculum of  $1 \times 10^6$  CFU/mL. Then, were incubated in 96-well microtiter flat-bottomed polystyrene plates (200  $\mu$ L/well) (VWR Life Science, Avantor) for 24 hours at 37°C, for biofilm formation. After 24 hours, the medium was carefully removed from each well, and fresh medium was added to wash out the non-adherent bacteria. The medium was removed again and a 5% (v/v) PrestoBlue (Invitrogen, Thermo Fisher Scientific) solution was added. The resazurin solution was prepared in MHB, and the washing step was also performed in MHB. As negative control, wells were prepared with MHB containing the same percentage of PrestoBlue (without bacteria), and the positive control was prepared according with the instructions of the manufacturer (i.e., a sample containing the fully reduced resazurin form obtained after autoclaving for 15 minutes MHB medium supplemented with 5% (v/v) PrestoBlue).

The reduction of resazurin by the bacteria was evaluated by the measured of the fluorescence intensity (excitation: 530 nm; emission: 590 nm) in a microplate reader POLARstar OPTIMA (BMG Labtech) every ten minutes for four hours, at 37°C.

#### **2.8.4. Evaluation of Colony Forming Units (CFU) of different biofilms**

This assay was only performed for the *P. mendocina* isolate and the *S. marcescens* An. steph A1-C1. In a 96-well clear flat-bottomed polystyrene plate, *P. mendocina* and *S. marcescens* An. steph A1-C1 were inoculated ( $1 \times 10^6$  CFU/mL) in three of the tested media: MHB, RPMI\* and Schneider+FBS (Table 1).

The plates were incubated at 37°C for 3 and for 24 hours. Then, the media were removed from the wells to remove the planktonic cells and a washing step was performed with PBS. PBS was added again, and the solution was homogenized by doing "up and down" steps with the pipette to loosen all the biofilm from the wells. The tip was also used to "scrape" the bottom and side of the well. After performing these steps repeatedly, ten-fold serial dilutions were prepared until  $10^{-8}$  in PBS in a 96-well plate and 5  $\mu$ l of each dilution were plated in spots in MHA. The plates were incubated at 37°C for 24 hours. The colonies on each plate were counted and the CFU/mL was calculated. Each experiment was performed in two independent assays, with six technical replicates each.

In an independent assay, this procedure was repeated only for the RPMI\*. In this assay, in half of the wells, a step was added before the attempt to release the biofilm, in which 50  $\mu$ L of TrypLE™ (Gibco, Thermo Fisher Scientific) was added, left for ten minutes, and then all wells were perfused with PBS, following the same steps described above. The purpose of this experiment was to see if the addition of TrypLE had an effect on the efficacy of the assay.

### 3. Results and Discussion

#### 3.1. Bacteria isolation from *Anopheles* mosquitoes midguts

The *Anopheles* species associated with malaria transmission have a wide geographical distribution. The *Anopheles* species covered in this work include African species (*An. gambiae* and *An. coluzzii*) (Sinka *et al.*, 2012; Wiebe *et al.*, 2017), Asian species (*An. stephensi*) (Kumar *et al.*, 2012; Sinka *et al.*, 2011, 2012), South American species, namely from Brazil, (*An. darlingi* and *An. aquasalis*) (Conn *et al.*, 2018; Laporta *et al.*, 2015; Sinka *et al.*, 2012; Torres *et al.*, 2022) and one species that was associated with malaria transmission in Europe before its eradication (*An. atroparvus*) (Bertola *et al.*, 2022; Hertig, 2019; Sinka *et al.*, 2012).

The representative microbiota of the various *Anopheles* species was also analyzed in different nutritional environments, as it is described that the ingestion of a blood meal by the mosquito results in drastic changes in the diversity/quantity of the colonizing bacteria of the midgut.

The bacterial species isolated and identified are shown in Table 8. In general, the majority of the bacteria isolated were Gram-negative and oxidase-negative, corroborating the available literature (Birnberg *et al.*, 2021; Das De *et al.*, 2022; Huang *et al.*, 2020). *Pseudomonas* species are Gram-negative, and although there are some species that do not produce the enzyme cytochrome oxidase, most are oxidase-positive. Thus, the oxidase test was also a criterion for the selection of bacteria for molecular identification through sequencing of a region of the 16S rDNA gene.

Contrary to what has been reported in the literature, an increase in the total CFU/mL counts was not observed in the experiments in which mosquitoes were fed 24 hours before dissection. In both experiments, where mosquitoes were fed, and those where they were not, the total CFU/mL counts of each pool of ten mosquitoes' midguts were in the order of  $10^7$  CFU/mL (Table 8). This observation may be related to the fact that there was no increase in the abundance of microorganisms in these particular mosquitoes, or to limitations regarding the isolation methods used. Regarding the diversity of the bacteria that were identified, it is also not possible to make a correlation between the feeding of the mosquitoes before dissection and the increase in bacterial diversity. On the other hand,

in the assays where an enrichment step in non-selective liquid medium was added, there was, as expected, a considerable increase of about 100-fold in the total amount of bacteria (Table 8).

Gram-staining and testing for the presence of the enzyme cytochrome oxidase were performed for all bacterial isolates as preliminary analyses. Based on these results, identification of some of the isolates was performed by Sanger sequencing of a region of the 16S rRNA coding gene. Due to the low rates of evolution of this region, accurate identification to species level is sometimes difficult. Consequently, for some of the isolates the identification using the NCBI BLAST database was not possible to the species level.

Although in the literature it is often mentioned that the genus *Pseudomonas* is one of the most abundant in the midgut microbiota of *Anopheles* mosquitoes, in this work we were only able to obtain one isolate, which was identified initially, by 16S rDNA sequencing, as either *P. mendocina* or *P. alcaliphila*. However, after analyzing the whole genome sequencing results, it was possible to identify this isolate as *P. mendocina*. Additionally, previous preliminary results from our laboratory group had already identified several species of *Pseudomonas* in mosquitoes from these laboratory colonies using sequence amplification methods. However, the bacteria were not isolated in culture media, so the colonization of these species in these mosquitoes was not confirmed at the time, nor was the possibility that these bacteria were unculturable.

The bacterial species most commonly identified were *Elizabethkingia meningoseptica/anophelis*, *S. marcescens* and *Aeromonas hydrophila*. All these species are also frequently identified in the literature as abundant components of the *Anopheles* midgut microbiota (Ganley *et al.*, 2020; Gendrin & Christophides, 2013; Wang *et al.*, 2017; Yordanova *et al.*, 2018).

The *Anopheles* species originating from Brazil were included because it is also known that the constitution of the midgut microbiota depends on the environment and geographical region of the mosquitoes and, although they are all laboratory reared mosquitoes, it was possible to associate some bacterial genera with each *Anopheles* species (Table 8). *Elizabethkingia* sp. were isolated from four of the six mosquito species considered, proving to be a frequent bacterial genus in *Anopheles* mosquitoes. The

*Klebsiella* genus was also isolated from *An. stephensi*, *An. gambiae* and *An. aquasalis*. These two genera were identified both in the species from Brazil and in the species from the IHMT laboratory colonies. Despite this, the *Klebsiella* species isolated were different between *An. aquasalis* [*Klebsiella ornithinolytica/planticola* (formerly known as *Raoultella ornithinolytica/planticola*)] and *An. stephensi/An. gambiae* (*Klebsiella michiganensis/Cedecea neteri*). *S. marcescens* was also isolated/identified from two different species (*An. stephensi* and *An. coluzzii*) (Table 8).

The other bacterial genera identified were isolated from only one of the *Anopheles* species. *Pantoea* sp. and *Acinetobacter* sp. were isolated from only one of the species originating from Brazil (*An. darlingi*). *Aeromonas* sp. and *Stenotrophomonas* sp. were isolated exclusively from *An. coluzzii*. *Staphylococcus* sp. was only identified in assays with *An. stephensi*. *Chryseobacterium* sp. was only isolated from *An. atroparvus*. Finally, the only *Pseudomonas* species isolated was recovered from *An. gambiae* (Table 8).

It is important to note that the isolation methods applied aimed at the isolation of *Pseudomonas* spp., thus not allowing a complete analysis of the composition of the mosquito midgut microbiota. However, from the results obtained, it is possible to make an association between some bacteria and some species of *Anopheles*. While different bacterial genera were identified in the case of *An. darlingi* (which is to be expected given the geographical differences), the bacteria isolated from *An. aquasalis* were relatively identical to those isolated from *An. stephensi* and *An. gambiae*.

For a deeper comparison and more detailed analysis, it would be necessary to identify the microbiota of the *Anopheles* midgut using more complete and complex methods, namely systematic metagenomic analysis, alongside with the cell culture methods.

**Table 8 – List of bacteria isolated from the midgut of *Anopheles* mosquitoes per assay.** Details are given on the respective *Anopheles* species and their nutritional conditions, as well as the use of the enrichment step for bacteria isolation and bacteria enumeration. The closest identification (NCBI BLAST matches) of the isolated bacterial species is also indicated, as well as their taxonomic classification (bacterial class, order and family).

Assay (#)	<i>Anopheles</i> species	Pre-blood-fed	Enrichment step**	Total CFU/mL counts	Closest database matches (NCBI BLAST)	Bacterial Class/Order/Family
1	<i>Anopheles stephensi</i> ♀	No	No	3.02x10 <sup>7</sup>	<i>Serratia marcescens</i>	<i>Gammaproteobacteria/Enterobacterales/Yersiniaceae</i>
2	<i>Anopheles atroparvus</i> ♀	No	No	1.36x10 <sup>7</sup>	<i>Chryseobacterium arthrospiraerae</i>	<i>Flavobacteriia/Flavobacterales/Weeksellaceae</i>
					<i>Elizabethkingia meningoseptica</i>	<i>Flavobacteriia/Flavobacterales/Weeksellaceae</i>
3	<i>Anopheles stephensi</i> ♀	Yes	No	5.39 x10 <sup>7</sup>	<i>Serratia marcescens</i>	<i>Gammaproteobacteria/Enterobacterales/Yersiniaceae</i>
4	<i>Anopheles stephensi</i> ♀	No	No	1.64 x10 <sup>7</sup>	<i>Serratia marcescens</i>	<i>Gammaproteobacteria/Enterobacterales/Yersiniaceae</i>
					<i>Elizabethkingia meningoseptica/anophelis</i>	<i>Flavobacteriia/Flavobacterales/Weeksellaceae</i>
					<i>Staphylococcus epidermidis</i>	<i>Bacilli/Caryophanales/Staphylococcaceae</i>
					<i>Klebsiella michiganensis/Cedecea neteri</i>	<i>Gammaproteobacteria/Enterobacterales/Enterobacteriaceae</i>

*Anopheles* species indicated with \* are mosquitoes from laboratory colonies in Brazil (preserved dry, so the dissection was of the entire abdomen and not just the midgut). The symbols ♀ (female) and ♂ (male) identify the gender of the mosquitoes used in each assay. The enrichment step (\*\*) was performed in non-selective liquid medium (MHB) for 24 hours after midgut dissection.

**Table 8 (continuation) – List of bacteria isolated from the midgut of *Anopheles* mosquitoes per assay.** Details are given on the respective *Anopheles* species and their nutritional conditions, as well as the use of the enrichment step for bacteria isolation and bacteria enumeration. The closest identification (NCBI BLAST matches) of the isolated bacterial species is also indicated, as well as their taxonomic classification (bacterial class, order and family).

Assay (#)	<i>Anopheles</i> species	Pre-blood-fed	Enrichment step**	Total CFU/mL counts	Closest database matches (NCBI BLAST)	Bacterial Class/Order/Family
5	<i>Anopheles stephensi</i> ♀	Yes (artificial diet)	No	6.3 x10 <sup>7</sup>	<i>Klebsiella michiganensis/Cedecea neteri</i>	<i>Gammaproteobacteria/Enterobacterales/Enterobacteriaceae</i>
					<i>Elizabethkingia meningoseptica/anophelis</i>	<i>Flavobacteriia/Flavobacteriales/Weeksellaceae</i>
6	<i>Anopheles stephensi</i> ♂	No	No	4.4 x10 <sup>6</sup>	<i>Klebsiella michiganensis/Cedecea neteri</i>	<i>Gammaproteobacteria/Enterobacterales/Enterobacteriaceae</i>
					<i>Elizabethkingia meningoseptica/anophelis</i>	<i>Flavobacteriia/Flavobacteriales/Weeksellaceae</i>
					<i>Staphylococcus epidermidis</i>	<i>Bacilli/Caryophanales/Staphylococcaceae</i>
7	<i>Anopheles stephensi</i> ♂	No	Yes	9.42 x10 <sup>9</sup>	<i>Serratia marcescens</i>	<i>Gammaproteobacteria/Enterobacterales/Yersiniaceae</i>
					<i>Elizabethkingia meningoseptica/anophelis</i>	<i>Flavobacteriia/Flavobacteriales/Weeksellaceae</i>
					<i>Aeromonas hydrophila</i>	<i>Gammaproteobacteria/Aeromonadales/Aeromonadaceae</i>

*Anopheles* species indicated with \* are mosquitoes from laboratory colonies in Brazil (preserved dry, so the dissection was of the entire abdomen and not just the midgut). The symbols ♀ (female) and ♂ (male) identify the gender of the mosquitoes used in each assay. The enrichment step (\*\*) was performed in non-selective liquid medium (MHB) for 24 hours after midgut dissection.

**Table 8 (continuation) – List of bacteria isolated from the midgut of *Anopheles* mosquitoes per assay.** Details are given on the respective *Anopheles* species and their nutritional conditions, as well as the use of the enrichment step for bacteria isolation and bacteria enumeration. The closest identification (NCBI BLAST matches) of the isolated bacterial species is also indicated, as well as their taxonomic classification (bacterial class, order and family).

Assay (#)	<i>Anopheles</i> species	Pre-blood-fed	Enrichment step**	Total CFU/mL counts	Closest database matches (NCBI BLAST)	Bacterial Class/Order/Family
8	<i>Anopheles stephensi</i> ♀	Yes	Yes	5.82 x10 <sup>9</sup>	<i>Serratia marcescens</i>	<i>Gammaproteobacteria/Enterobacterales/Yersiniaceae</i>
					<i>Elizabethkingia meningoseptica/anophelis</i>	<i>Flavobacteriia/ Flavobacterales/Weeksellaceae</i>
9	<i>Anopheles coluzzii</i> ♀	Yes	Yes	4.61 x10 <sup>9</sup>	<i>Serratia marcescens</i>	<i>Gammaproteobacteria/Enterobacterales/Yersiniaceae</i>
					<i>Aeromonas hydrophila</i>	<i>Gammaproteobacteria/ Aeromonadales/Aeromonadaceae</i>
					<i>Stenotrophomonas maltophilia</i>	<i>Gammaproteobacteria/Lysobacterales/Lysobacteraceae</i>
10	<i>Anopheles darlingi</i> ♂*	No	Yes	2.1 x10 <sup>9</sup>	<i>Acinetobacter baylyi / baumannii</i>	<i>Gammaproteobacteria/Pseudomonadales/Moraxellaceae</i>
11	<i>Anopheles darlingi</i> ♀*	No	Yes	6.05 x10 <sup>9</sup>	<i>Pantoea dispersa</i>	<i>Gammaproteobacteria/Enterobacterales/Erwiniaceae</i>

*Anopheles* species indicated with \* are mosquitoes from laboratory colonies in Brazil (preserved dry, so the dissection was of the entire abdomen and not just the midgut). The symbols ♀ (female) and ♂ (male) identify the gender of the mosquitoes used in each assay. The enrichment step (\*\*) was performed in non-selective liquid medium (MHB) for 24 hours after midgut dissection.

**Table 8 (continuation) – List of bacteria isolated from the midgut of *Anopheles* mosquitoes per assay.** Details are given on the respective *Anopheles* species and their nutritional conditions, as well as the use of the enrichment step for bacteria isolation and bacteria enumeration. The closest identification (NCBI BLAST matches) of the isolated bacterial species is also indicated, as well as their taxonomic classification (bacterial class, order and family).

Assay (#)	<i>Anopheles</i> species	Pre-blood-fed	Enrichment step**	Total CFU/mL counts	Closest database matches (NCBI BLAST)	Bacterial Class/Order/Family
12	<i>Anopheles gambiae</i> ♀	Yes	Yes	6.91 x10 <sup>9</sup>	<i>Pseudomonas alcaliphila/mendocina</i>	<i>Gammaproteobacteria/Pseudomonadales/Pseudomonadaceae</i>
					<i>Klebsiella michiganensis/Cedecea neteri</i>	<i>Gammaproteobacteria/Enterobacterales/Enterobacteriaceae</i>
					<i>Elizabethkingia meningoseptica/anophelis</i>	<i>Flavobacteriia/Flavobacteriales/Weeksellaceae</i>
13	<i>Anopheles aquasalis</i> ♂*	No	Yes	6.83 x10 <sup>9</sup>	<i>Klebsiella ornithinolytica/planticola</i>	<i>Gammaproteobacteria/Enterobacterales/Enterobacteriaceae</i>
					<i>Elizabethkingia meningoseptica/anophelis</i>	<i>Flavobacteriia/Flavobacteriales/Weeksellaceae</i>
14	<i>Anopheles aquasalis</i> ♀*	No	Yes	4.91 x10 <sup>9</sup>	<i>Klebsiella ornithinolytica/planticola</i>	<i>Gammaproteobacteria/Enterobacterales/Enterobacteriaceae</i>

*Anopheles* species indicated with \* are mosquitoes from laboratory colonies in Brazil (preserved dry, so the dissection was of the entire abdomen and not just the midgut). The symbols ♀ (female) and ♂ (male) identify the gender of the mosquitoes used in each assay. The enrichment step (\*\*) was performed in non-selective liquid medium (MHB) for 24 hours after midgut dissection.

### **3.2. Antibiotic susceptibility profiles of bacteria isolated from mosquito midgut**

The potential of different bacteria as candidates for paratransgenesis is already described in the literature (Bahia *et al.*, 2014; Bai *et al.*, 2019; Cirimotich *et al.*, 2011; Ramirez *et al.*, 2014; Wang *et al.*, 2012, 2017; Wilke & Marrelli, 2015). In the context of this work, eight *S. marcescens* isolates and one *P. mendocina* isolate were identified in different *Anopheles* species. Both, *S. marcescens* and *Pseudomonas* spp. are commonly found in the *Anopheles* midgut microbiota (Birnberg *et al.*, 2021; Das De *et al.*, 2022; Gendrin & Christophides, 2013; Yordanova *et al.*, 2018) and thus we carried out this experiment with the isolates from both genera. The antibiotic susceptibility profiles observed for all isolates are shown in Table 9 and 10. The antibiograms allowed access to the resistance profile of the bacteria to some antibiotics of different classes. The goals here were: i) to easily differentiate phenotypically the various *S. marcescens* isolates; ii) by studying the antibiotic susceptibility profile of the bacteria isolated, we could possibly obtain relevant information to later develop a paratransgenesis strategy. This control strategy genetically modifies bacteria to be introduced and disseminated throughout the mosquito population in the environment (Wilke & Marrelli, 2015).

The antibiotic susceptibility profiles allowed the identification of two groups within the *S. marcescens* isolates with distinct antibiotic susceptibility profiles. The differences were observed for the antibiotics tobramycin (an aminoglycoside) and chloramphenicol (a phenicol). In general, all *S. marcescens* isolates show a resistance phenotype to the beta-lactam (subclass penicillins) ampicillin, while showing a susceptibility profile to ceftriaxone (a beta-lactam from the subclass cephalosporins), gentamicin (an aminoglycoside), tetracycline (a tetracycline), ciprofloxacin (a fluoroquinolone) and trimethoprim-sulfamethoxazole (a sulfonamide). From a clinical point of view, *S. marcescens* is an opportunistic pathogen of growing concern in terms of antibiotic resistance. This bacterium often shows intrinsic resistance to several classes of antibiotics, namely ampicillins, first and second generation cephalosporins and macrolides (Tavares-Carreón *et al.*, 2023). Some recent studies have also emphasized the increase in resistance to gentamicin and tobramycin in clinical strains (Bertrand & Dowzicky, 2012; Sader *et al.*, 2014). With specific regard to *S. marcescens* isolates from

mosquitoes, the antibiotic susceptibility profiles of strains isolated from *An. stephensi* (Chen *et al.*, 2017) have also been investigated, and it was concluded that those strains were multidrug resistant, displaying a resistance phenotype for most of the antibiotics tested from the several classes, including ampicillin, tetracycline and chloramphenicol (Chen *et al.*, 2017). Comparatively, our results indicate a lower rate of antibiotic resistance, with a susceptibility profile for most of the antibiotics tested. These differences may be related to differences in the origin of the colonizing strain and its previous contact with antimicrobials. These lower levels of resistance may represent an advantage in the possibility of genetically modifying these bacteria and releasing them into wild mosquito populations, as part of a paratransgenesis approach.

In addition, based on the antibiotic susceptibility profiles, the *S. marcescens* isolates were then divided into two major groups. This division also reveals different patterns of antibiotic resistance between the *S. marcescens* isolated from *An. stephensi* and *An. coluzzii*. For the next stages of the work, we selected for further study two isolates from the first group (*S. marcescens* An. steph A1-C1 and *S. marcescens* An. steph A7-A1) and the only isolate from the second group (*S. marcescens* An. col A9-C4).

For *Pseudomonas* species, the CLSI recommendations only establish breakpoints derived from MIC data. So, for *P. mendocina*, E-tests were performed for the antibiotics gentamicin (an aminoglycoside), tetracycline (a tetracycline), ciprofloxacin (a fluoroquinolone) and chloramphenicol (a phenicol). The isolate *P. mendocina* only showed a resistance phenotype for chloramphenicol (Table 10).

Regarding the bacterium *P. mendocina*, no information was found in literature on the antibiotic susceptibility profile of mosquito isolates. However, studies with *P. mendocina* environmental strains showed that they were susceptible to all the antibiotics normally used against *Pseudomonas* spp., including tobramycin, gentamicin and ciprofloxacin (Ruiz-Roldán *et al.*, 2021). In the same study, genetic approaches concluded that one of the environmental isolates did not encode antimicrobial resistance genes, while another encoded only one gene that confers resistance to chloramphenicol, but it was mutated (Ruiz-Roldán *et al.*, 2021). These data appear to be consistent with our results, since the *P. mendocina* isolate from *An. gambiae* showed a susceptibility phenotype to all the antibiotics tested, except for chloramphenicol.

**Table 9 – Antibiotic susceptibility profiles of *S. marcescens* isolates tested by the disk diffusion method.** The Inhibition Zone Diameters (IZD) were determined in triplicate and are presented as the range of values obtained. S/I/R represents the corresponding interpretative category according to the Table 2A of the CLSI M100 2023 recommendations (CLSI, 2023), classified as: susceptible (S), intermediate (I) and resistant (R).

Isolate	AMP		CRO		CN		TN		T		CIP		SXT		C		
	IZD (mm)	S/I/R	IZD (mm)	S/I/R	IZD (mm)	S/I/R	IZD (mm)	S/I/R	IZD (mm)	S/I/R	IZD (mm)	S/I/R	IZD (mm)	S/I/R	IZD (mm)	S/I/R	
<i>E. coli</i> ATCC 25922	19	S	31	S	18	S	17	S	22	S	36	S	29	S	22	S	
<i>S. marcescens</i> isolates																<b>Groups</b>	
An. steph A1-C1	6	R	30-32	S	19-20	S	18	S	14	I	35	S	34-35	S	15	I	<b>1</b>
An. steph A3-C1	6	R	30-32	S	21-22	S	19-20	S	15-16	S	34-36	S	33-35	S	16	I	
An. steph A7-C1	6	R	32-34	S	19-26	S	19	S	15-16	S	34-38	S	35	S	16-17	I	
An. steph A7-C4	6	R	32-33	S	20-22	S	18-19	S	15	S	31-33	S	31-35	S	15-16	I	
An. steph A8-C1	6	R	31-32	S	20-28	S	18-22	S	15-16	S	34-36	S	35-36	S	15-17	I	
An. steph A7-A1	6	R	30-33	S	20-22	S	18-19	S	14-16	S/I	33	S	32-34	S	17-19	S/I	
An. steph A7-A2	6	R	30-33	S	20-26	S	18-19	S	14-16	S/I	31-36	S	20-32	S	14-20	S/I	
An. col A9-C4	6	R	31-32	S	18-20	S	10-12	R	20-22	S	36-38	S	40	S	32-34	S	

AMP- Ampicillin (10 µg); CRO - Ceftriaxon (30 µg); CN- Gentamicin (10 µg); TN- Tobramycin (10 µg); T-Tetracycline (30 µg); CIP- Ciprofloxacin (5 µg); SXT - Trimethoprim- sulfamethoxazole (1.25/23.75 µg); C- Chloramphenicol (30 µg).

**Table 10 – Antibiotic susceptibility profiles of *Pseudomonas* isolate tested by the E-test method.** MICs ( $\mu\text{g/mL}$ ) were determined in triplicate and are presented as the range of values obtained. S/I/R represents the corresponding interpretative category according to the Table 2A (for *E. coli* ATCC 25922), Table 2B-1 (for *P. aeruginosa* ATCC 27853) and Table 2B-5 (for *P. mendocina*) of the CLSI M100 2023 recommendations (CLSI, 2023), classified as: susceptible (S), intermediate (I) and resistant (R).

Isolate	CN		T		CIP		C	
	MIC ( $\mu\text{g/mL}$ )	S/I/R	MIC ( $\mu\text{g/mL}$ )	S/I/R	MIC ( $\mu\text{g/mL}$ )	S/I/R	MIC ( $\mu\text{g/mL}$ )	S/I/R
<i>P. mendocina</i>	2	S	0.75	S	0.032	S	32-96	R
<i>P. aeruginosa</i> ATCC 27853	2	-	12	-	0.38	S	>256	-
<i>E. coli</i> ATCC 25922	-	-	0.5	S	-	-	6	S

CN – Gentamicin (10  $\mu\text{g}$ ); T – Tetracycline (30  $\mu\text{g}$ ); CIP – Ciprofloxacin (5  $\mu\text{g}$ ); C – Chloramphenicol (30  $\mu\text{g}$ ).

### 3.3. Colonization of the midgut of *Anopheles stephensi* with *Pseudomonas* sp.

*Pseudomonas* is one of the most common bacterial genera in the midgut microbiota of *Anopheles* as evidence by the existing literature (Birnberg *et al.*, 2021; Das De *et al.*, 2022; Gendrin & Christophides, 2013). However, in this work it was only possible to isolate/identify one isolate belonging to the species *P. mendocina.*, from the laboratory colony of *An. gambiae*. This raised three major questions. First, we hypothesized whether there might be some sort of competition between *Pseudomonas* species and the midgut microbiota of the other species of *Anopheles*. On the other hand, we considered whether the isolation and identification methods used were the most appropriate and whether they allowed for the isolation/identification of *Pseudomonas* species, particularly those that are environmental and not clinically relevant. Finally, we also considered differences in the background of the mosquitoes used, as well as their conditions of maintenance in laboratory colonies, as a possible justification for the clear differences between our results and what is highlighted in the literature. For example, in some of the studies that mention *Pseudomonas* as one of the most frequently isolated genus in *Anopheles* mosquitoes (Chavshin *et al.*, 2012; Lindh *et al.*, 2005), the mosquitoes considered are field-caught. The study by Boissière *et al.*, (2012) also reports *Pseudomonas* spp. as frequent members of the midgut microbiota of lab-reared adult *An. gambiae*, however, in this study the

larvae were field-caught and kept in laboratory colonies in their original habitat water, until the emergence of the adult mosquito. The mosquitoes used in our study developed their entire life cycle in the laboratory colony, so this could also influence the composition of the *Anopheles* gut microbiota. Accordingly, we also hypothesize that the laboratory maintenance and origin of the mosquitoes used have a significant impact on the midgut microbiota of *Anopheles* mosquitoes. On the other hand, preliminary data from our group had already identified sequences of several *Pseudomonas* species in the mosquitoes from these laboratory colonies (only by sequencing methods).

In this sense, experiments were carried out in which *An. stephensi* mosquitoes were fed with *P. mendocina* and the reference strain *P. aeruginosa* ATCC 27853 (separately) at three different concentrations to see if colonization of these bacteria occurred (Figure 5).

Following the colonization assay, the procedure for dissection, isolation and identification of the bacteria was the same as for the initial assays (see subsections 2.2.2., 2.2.3. and 2.3.). *P. aeruginosa* ATCC 27853 was used as reference strain to optimize the method. This bacterium produces a green color pigment in MHA and PIA media, which facilitated the identification of the bacterium in the procedure of the culture methods used.

For *P. aeruginosa* ATCC 27853, the CFU/mL count showed identical results for all groups, regardless of the initial bacterial inoculum (Figure 5A). This indicates that there is indeed colonization of the *An. stephensi* used by the *P. aeruginosa* ATCC 27853. However, the bacterial concentration used at low concentration may already be limiting, as no increase in colonization is observed with increasing of initial inoculum.

For *P. mendocina*, an increase in colonization is observed with an increase in the initial inoculum (Figure 5B). There is an increase of about 100-fold comparing the low inoculum ( $3.9 \times 10^3$  CFU/mL) with the medium inoculum ( $3.9 \times 10^5$  CFU/mL), however, between the medium inoculum and the high inoculum ( $3.9 \times 10^6$  CFU/mL) the difference is no longer so pronounced, which may indicate that the amount of bacteria begins to be limiting for colonization.

These experiments allow us to conclude that both the reference strain *P. aeruginosa* ATCC 27853 and *P. mendocina* can colonize the midgut of these *An. stephensi* mosquitoes with their natural microbiota intact. These also demonstrate the higher colonization potential of the *P. mendocina* isolate compared to the *P. aeruginosa* reference strain. It was also confirmed that the dissection, isolation and identification

methods used allow the isolation/identification of *Pseudomonas* spp. so we can conclude that the methods used did not interfere with the differences observed between our results and the findings described in the literature. As such, the reason for the difficulty in isolating *Pseudomonas* species throughout all assays is probably due to the low quantity of these species in the microbiota of these particular mosquitoes. As mentioned above, in contrast with our data, the studies by Chavshin *et al.*, (2012) and Rani *et al.*, (2009) have demonstrated that bacteria of the genus *Pseudomonas* are significant representatives of the midgut microbiota of *An. stephensi* in both wild and lab-reared mosquitoes. However, these studies focus on mosquitoes from Asian countries. As such, the geographical region and conditions in which mosquitoes are reared has a major influence on the composition of their microbiota, which may explain the differences observed between our results and those of the aforementioned studies.

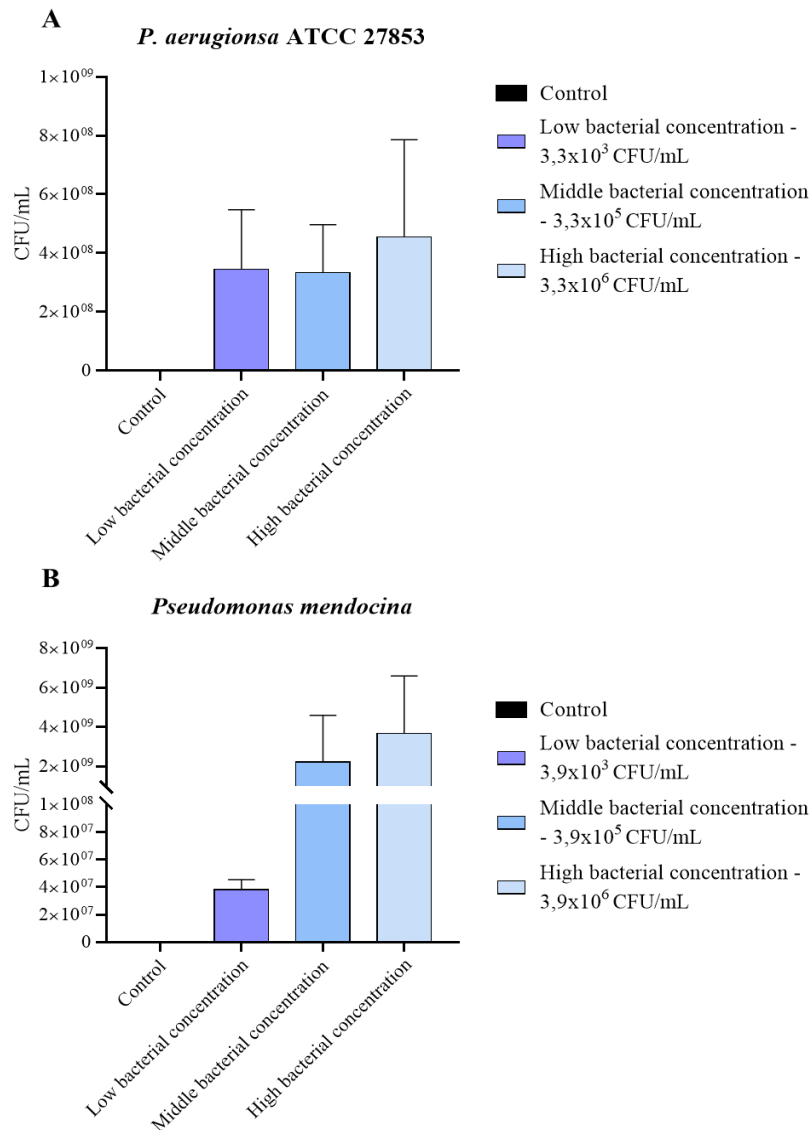


**Figure 5 - Colonization of *Anopheles stephensi* midguts by *Pseudomonas* sp.** CFU/mL counts after colonization of *An. stephensi* by (A) *P. aeruginosa* ATCC 27853 and (B) *P. mendocina* for 72 hours, by feeding the respective bacteria to the mosquitoes with three different initial inocula, in addition to the control group, which was fed with blood but without inoculum of the bacteria. The values presented represent the mean of two independent replicates.

### 3.4. Analysis of whole genome sequencing results

Whole genome sequencing was performed using Illumina technology by NovoGene Biotech Co., Ltd. The received data were analyzed and processed using the online analysis platform BV-BRC (v. 3.31.12). The initial purpose of this analysis was to confirm the species of *Pseudomonas* that had been isolated from *An. gambiae*, as Sanger sequencing of a region of the 16S rDNA did not allow for differentiation between *P. mendocina* and *P. alcaliphila*. Furthermore, the BLASTn analysis (in BV-BRC) of the

sequences resulting from WGS allowed us to assess the bacterial species with the highest percentage of identity relative to the sequences of the isolates, and it was concluded that the isolated species corresponds to *P. mendocina*, a species that had previously been identified as a component of the midgut microbiota of *An. stephensi* (Rani *et al.*, 2009). As can be seen in Table 11, the closest database match for S1/S2 was the genome of the environmental strain *Pseudomonas mendocina* ymp, which was originally isolated from the Yucca Mountain Site for long-term nuclear waste storage (GenBank accession number NC\_009439) (Annex, Figure S1).

Whole genome sequencing was also performed for the selected *S. marcescens* isolates chosen for the analysis of biofilm formation potential (An. steph A1-C1, An. steph A7-A1 and An. col A9-C4). In this case, the objective was to determine whether the three isolates corresponded to the same *S. marcescens* strain, as previous differences in antibiotic susceptibility profiles were observed (subsection 3.2.). The analysis showed that all the three isolates of *S. marcescens* have the highest percentage of identity with the strain *Serratia marcescens* subsp. *marcescens* Db11, which was originally isolated and identified from the insect *Drosophila melanogaster* (Flyg *et al.*, 1980) (Annex, Figure S2), however, deeper analyses of the sequences would be necessary to actually typify these isolates at the strain level. The alignment between the three sequences (using the BV-BRC Genome Alignment Service tool) allowed a visual analysis of the differences in the annotation of the three genomes. It can be noted that there are clear differences between isolate S5 (*S. marcescens* An. col A9-C4) and isolates S3 and S4 (*S. marcescens* An. steph A1-C1 and An. steph A7-A1, respectively) (Annex, Figure S3). Differences between these isolates had already been observed in the phenotypic profile of antibiotic susceptibility (see subsection 3.2.). Thus, based on the alignment of the genomes, there appear to be genotypic differences between the *An. stephensi* isolates and the *An. coluzzii* isolate, indicating that the two isolates of *An. stephensi* probably belong to the same strain. The analysis of the alignment of the *P. mendocina* sequences (S1 and S2) is a process that is still ongoing (data not shown).

Annotation of the genomes and Comprehensive Genome Analysis allowed access to the genes encoded in these genomes and also the identification of genes associated with virulence factors. Given the context and objective of this work, in this category we searched for genes involved in the process of biofilm formation (Table 11).

The process of biofilm formation involves several steps, which are highly regulated and controlled by various complex systems, such as quorum sensing, which is a process of chemical communication between cells, based on the production, detection, and reception of signaling molecules (autoinducers) (Miller & Bassler, 2001; Mukherjee & Bassler, 2019). Each bacterial genus/species has specific particularities in the biofilm formation process, which can make the process easier and more common or, on the other hand, highly dependent on specific conditions. In the adhesion step to surfaces, the mobility of the bacteria is very important for the stabilization of the bacteria and also to guarantee the constant expansion of the microcolonies along the surface, so that they evolve into a mature and well-structured biofilm. Swarming motility is often adopted by bacterial communities in the adhesion phase, as it allows for rapid and coordinated translocation of the bacterial population in a defined pattern across the surface (Fraser & Hughes, 1999).

Swarming motility is normally involved in the expansion of microcolonies in biofilm formation by *S. marcescens* bacteria. This motility is associated with the activity of the flagellum and the production of surfactants (Lindum *et al.*, 1998; Rice *et al.*, 2005). In *S. marcescens*, flagellum expression is controlled by the *flhDC* operon and surfactant production is dependent on the expression of *swr* genes, which are controlled by two quorum sensing regulatory systems (Givskov *et al.*, 1998; Li *et al.*, 2005; Lindum *et al.*, 1998; Rice *et al.*, 2005). The analysis of the genes associated with the virulence factors in the BV-BRC allowed us to conclude that the genes responsible for the production and control of the flagellum are present in the *S. marcescens* isolates analyzed (Table 11). However, it seems that the *swr* genes are absent. Thus, these bacteria appear to have only one of these essential systems for swarming motility, which may indicate that the transition from the microcolony phase to a mature, well-structured biofilm is hampered. Additionally, no matches were found with genes involved in the major quorum sensing systems in *S. marcescens* (Jiang *et al.*, 2023). Despite this, these isolates also encode genes involved in the production of fimbriae and genes involved in two-component regulatory systems, which may be involved in the process of biofilm formation.

There is no doubt that the process of biofilm formation in *Pseudomonas* species has been extensively studied. However, these studies are mostly focused on the type species *P. aeruginosa*, given its clinical relevance. In a general and simplistic way, the process of biofilm formation by *P. aeruginosa* can be divided into the following phases: reversible

adhesion, irreversible adhesion, microcolony formation, biofilm maturation and biofilm dispersion. Flagella and type IV pili are essential structures for the reversible attachment of the bacteria to a surface, and mutants for genes involved in the synthesis/regulation of these structures exhibit a deficiency in biofilm development (Karygianni *et al.*, 2020). Alginate is a major component of *P. aeruginosa* mucoid biofilms. This exopolysaccharide also contributes to the surface adhesion due to being mucous. In addition, during the stage of microcolony formation and biofilm maturation, alginate is very important, guaranteeing the structural integrity of the biofilm (Ghafoor *et al.*, 2011), and contributing to the retention of water and nutrients within the structure (Lee & Yoon, 2017). The exopolysaccharides Psl and Pel are also major components of the extracellular matrix of the *P. aeruginosa* biofilm. However, the production of alginate gives a more structured architecture and results in so-called mushroom-like structures. All these components of the biofilm, particularly the extracellular matrix, provide important protection against the immune system, environmental stress and antibiotics (from a clinical perspective) (Moradali & Rehm, 2019).

Analysis of the genes encoding virulence factors annotated in the genome of the *P. mendocina* isolate (S1/S2) in the BV-BRC software revealed correspondence with various genes involved in biofilm formation (Table 11). The presence of genes involved in alginate biosynthesis and its regulation was verified. In addition, it was possible to identify genes involved in the biosynthesis of flagella and type IV pili, which are essential in the initial adhesion process. It was not possible to verify matches with the genes involved in the production of the other exopolysaccharides (Pel and Psl), nor the genes involved in the production and regulation of fimbriae, which are also very important structures in the process of reversible and irreversible adhesion, as well as in the formation of microcolonies and maturation of the biofilm (Sultan *et al.*, 2021). However, the fact that these genes have not been annotated in these genomes does not necessarily mean that this bacterium does not produce these components, as this analysis is based on comparing similarities with other genes that have already been studied and annotated in other bacterial genomes, so confirmation would require a more in-depth analysis. Nevertheless, the presence in the *P. mendocina* genome of several genes involved and essential in biofilm formation in *P. aeruginosa* is a good indicator of the natural potential of this bacterium to form biofilms.

The antimicrobial resistance phenotype was predicted using the ResFinder tool from the Center for Genomic Epidemiology online software (Table 12). In the case of *P. mendocina*, no antimicrobial resistance was predicted based on the genome, although the antibiograms showed a resistance phenotype for chloramphenicol (see subsection 3.2.). No acquired resistance genes were identified either. On the other hand, in the case of the three *S. marcescens* isolates, resistance to various aminoglycosides, beta-lactams and two tetracyclines was predicted (Table 12). In the antibiograms, a resistance phenotype to ampicillin had been observed for all the isolates and to tobramycin for the *S. marcescens* An. col A9-C4 isolate (see subsection 3.2.). Acquired resistance genes have also been identified for the aforementioned classes of antibiotics (Table 12).

The lack of association between resistance phenotypes and AMR genes may be due to different factors, such as possible mutations occurring in their promoter regions or in the coding sequence that may impair their expression or the activity of the proteins they encode, respectively.

**Table 11 - *In silico* analysis of the sequences resulting from whole genome sequencing.** Information was obtained through the BLASTn tool and the Comprehensive Genome Analysis Service, using the BV-BRC platform. The samples are identified by the nomenclature used in the whole genome sequencing analysis: S1 – *Pseudomonas* sp. isolated from *An. gambiae*; S2 – *Pseudomonas* sp. isolate recovered after the colonization experiment on *An. stephensi* (marked by \*); S3 – *S. marcescens* An. steph A1-C1 isolated from *An. stephensi*; S4 – *S. marcescens* An. steph A7-A1 isolated from *An. stephensi*; S5 – *S. marcescens* An. col A9-C4 isolated from *An. coluzzii*. The accession numbers correspond to the identification numbers of the sequences in NCBI/GenBank identified as Closest database matches. Identity (%) corresponds to the percentage of similarity between the analyzed sequence and the database sequence identified as closest match. Hits with genes related to biofilm production corresponds to the genes identified in the Comprehensive Genome Analysis Service (BV-BRC) analysis as coding for virulence factors and which are identified in the literature as being involved in the different phases of biofilm formation. The genes are grouped according to the component of the biofilm or bacterium with which they are related (either in biosynthesis or regulation).

Sample	Isolate	Closest database matches (BLASTn BV-BRC)	Accession number	Identity (%)	Genome Length (bp)	Contigs	Protein coding sequences (CDS)	Hits with genes related to biofilm production
S1	<i>Pseudomonas</i> sp.	<i>Pseudomonas mendocina</i> ymp	NC009439	99	5,420,819	16	5,089	<ul style="list-style-type: none"> <li>• Alginate - <i>alg8</i>, <i>algD</i>, <i>algC</i>, <i>algA</i>, <i>algB</i>, <i>algZ</i>, <i>algW</i>, <i>algR</i></li> <li>• Type IV pili - <i>pilI</i>, <i>pilJ</i>, <i>pilM</i>, <i>pilN</i>, <i>pilT</i>, <i>pilH</i>, <i>pilU</i>, <i>pilC</i>, <i>pilR</i>, <i>pilG</i></li> </ul>
S2	<i>Pseudomonas</i> sp.*	<i>Pseudomonas mendocina</i> ymp	NC009439	99	5,419,391	27	5,090	<ul style="list-style-type: none"> <li>• Flagella - <i>fliP</i>, <i>fliM</i>, <i>fliA</i>, <i>fliI</i>, <i>fliQ</i>, <i>fliG</i>, <i>fleQ</i>, <i>fleN</i>, <i>fleS</i>, <i>fleR</i>, <i>motC</i>, <i>flgC</i>, <i>flgG</i></li> <li>• Two-component regulatory system – <i>ompR</i></li> </ul>
S3	<i>S. marcescens</i> An. steph A1-C1	<i>Serratia marcescens</i> subsp. <i>marcescens</i> Db11	HG326223	94	5,545,631	79	5,521	<ul style="list-style-type: none"> <li>• Fimbriae - <i>ecpA</i>, <i>yagZ</i></li> <li>• Flagella - <i>fliQ</i>, <i>fliP</i>, <i>fliM</i>, <i>fliR</i>, <i>fliI</i>, <i>fliS</i>, <i>fliN</i>, <i>fliG</i>, <i>fliA</i>, <i>fliZ</i>, <i>flhA</i>, <i>flhC</i>, <i>flhD</i>, <i>flgF</i>, <i>flgI</i>, <i>flgH</i>, <i>flgB</i>, <i>flgG</i>, <i>flgC</i>, <i>motA</i></li> <li>• Two-component regulatory system – <i>ompR</i>, <i>cpxR</i>, <i>luxS</i></li> </ul>
S4	<i>S. marcescens</i> An. steph A7-A1	<i>Serratia marcescens</i> subsp. <i>marcescens</i> Db11	HG326223	94	5,545,721	79	5,522	
S5	<i>S. marcescens</i> An. col A9-C4	<i>Serratia marcescens</i> subsp. <i>marcescens</i> Db11	HG326223	99.984	5,484,339	72	5,445	

**Table 12 - Prediction of antimicrobial susceptibility phenotype based on whole genome sequencing.** For these analyses was used the ResFinder tool from the Center for Genomic Epidemiology platform. Acquired AMR gene hits identified the correspondence to acquired antimicrobial resistance genes, based on whole genome sequencing. It is also indicated the antibiotics for which a resistance phenotype was found in the susceptibility tests carried out using the disk diffusion and E-tests methods (subsection 3.2.). The samples are identified by the nomenclature used in the whole genome sequencing analysis: S1 - *Pseudomonas* sp. isolated from *An. gambiae*; S2 - *Pseudomonas* sp. isolate recovered after the colonization experiment on *An. stephensi*; S3 – *S. marcescens* An. steph A1-C1 isolated from *An. stephensi*; S4 – *S. marcescens* An. steph A7-A1 isolated from *An. stephensi*; S5 – *S. marcescens* An. col A9-C4 isolated from *An. coluzzii*.

Samples	WGS-predicted phenotype of antimicrobial resistance		Acquired AMR gene hits	Resistance profiles resulting from the antibiograms
	Antimicrobial class	Antimicrobial		
S1, S2	-	-	-	chloramphenicol
	Aminoglycoside	tobramycin, amikacin, dibekacin, netilmicin, sisomicin	<i>aac(6')-Ic</i>	-
S3, S4	Beta-lactam	amoxicillin, amoxicillin+clavulanic acid, ampicillin, ampicillin+clavulanic acid, cefotaxime, ceftazidime, piperacillin, piperacillin+tazobactam, ticarcillin, ticarcillin+clavulanic acid	<i>blaSRT-2</i>	ampicillin
	Tetracycline	tetracycline, doxycycline	<i>tet(41)</i>	-
	Aminoglycoside	tobramycin, amikacin, dibekacin, netilmicin, sisomicin	<i>aac(6')-Ic</i>	tobramycin
S5	Beta-lactam	amoxicillin, amoxicillin+clavulanic acid, ampicillin, ampicillin+clavulanic acid, cefotaxime, ceftazidime, piperacillin, piperacillin+tazobactam, ticarcillin, ticarcillin+clavulanic acid	<i>blaSRT-2</i>	ampicillin
	Tetracycline	tetracycline, doxycycline	<i>tet(41)</i>	-

### 3.5. Determination of bacterial growth curves

In order to determine the cell growth behavior of the different isolates, the optical density at 600 nm was followed over time (Figure 6). From the analysis of the results, it is noticeable that there is a difference in the behavior of the cell growth curve between the *Pseudomonas* species (*P. mendocina* and *P. aeruginosa* ATCC 27853) and the *S. marcescens* strains (An. steph A1-C1, An. steph A7-A1 and An. col A9-C4). For the *S. marcescens* isolates, the An. col A9-C4 isolate shows a slightly different curve from the other two isolates, which may be an indication that it belongs to a different strain.

*S. marcescens* isolates reach exponential phase earlier (approximately after three hours) than *Pseudomonas* species (approximately after six hours). On the other hand, *P. mendocina* and *P. aeruginosa* ATCC 27853 reach the stationary phase earlier. Also, in the curves for *P. mendocina* and *P. aeruginosa* ATCC 27853, following the decrease observed after the maximum of the curves, we observed an additional increase in the optical density values. These observations may be due the agitation carried out by the plate reader not being sufficient, resulting for instance in the formation of biofilm-like structures. *Pseudomonas* spp. form more viscous biofilms as biomass increases, due to the enhanced release and accumulation of metabolic bioproducts by the bacterial cells (Greener *et al.*, 2016; Lau *et al.*, 2009; Paquet-Mercier *et al.*, 2016).

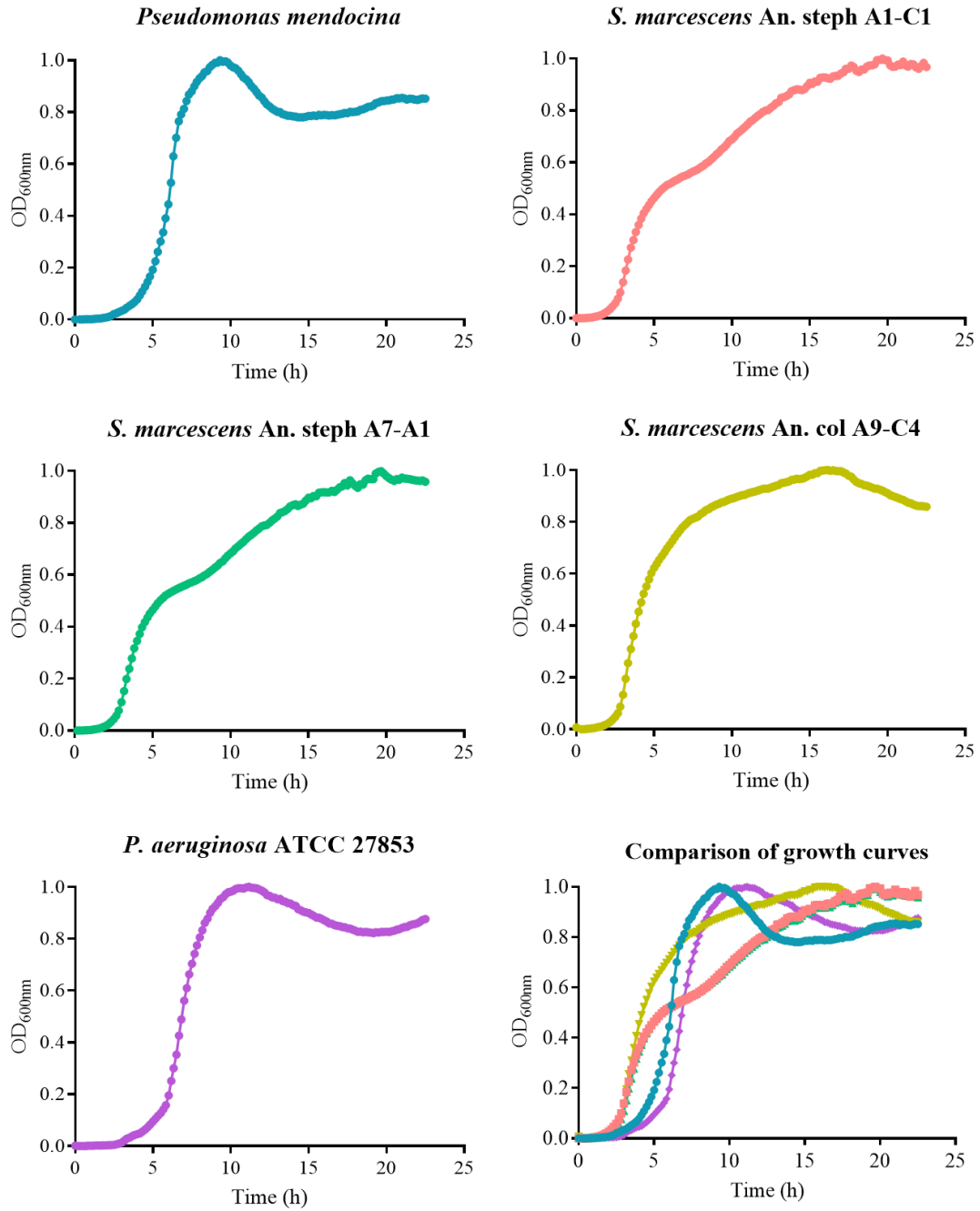


**Figure 6 – Representative growth curves of the selected bacteria isolated from *Anopheles* midguts.** Optical density values at 600 nm were monitored every ten minutes over a period of 22.5 hours at 37°C on a microplate reader. The OD<sub>600nm</sub> values were normalized to the maximum of each set of values. The values presented represent the mean of eight replicates for each bacterial species.

### **3.6. Potential of biofilm production by bacteria isolated from the midgut of *Anopheles***

#### **3.6.1. Analysis of biofilm formation by confocal microscopy**

Biofilm formation potential can be assessed using different methodologies (Azeredo *et al.*, 2017), with studies often focusing on metabolic assays and indirect measurements of biomass formed. Analysis of biofilm formation using confocal microscopy allows us to obtain a representation of the 3-D architecture and spatial structure of the biofilm, permitting us to obtain quantitative structural parameters such as biofilm thickness (by visualization of the orthogonal xzy plane) (Azeredo *et al.*, 2017). In our work, biofilm formation and structure were assessed by labeling them with the fluorescent probe SYTO 9, which binds with high affinity to nucleic acids (both intra- and extracellular) (McGoverin *et al.*, 2020; Tawakoli *et al.*, 2013).

This technique allows a real-time visualization of the biofilms and it is possible, for instance, to understand if the bacterial cells are really adherent to the surface and to identify differences in biofilm thickness.

The media used to study biofilm formation were MHB, LB, TSB and TSB + glucose (0.25%) as they are commonly used culture media for bacterial study (simple and with the basic nutrients for bacterial growth). These are also routinely used to study biofilm formation, although these studies are usually in the context of clinically relevant bacteria, rather than bacterial species isolated from mosquitoes (Chen *et al.*, 2020; Fekrirad *et al.*, 2020; Fu *et al.*, 2021; Luo *et al.*, 2021; Rodrigues Perez *et al.*, 2011). In addition to these, media that attempted to more closely mimic the environment which bacteria would encounter in the midgut of mosquitoes were also tested. This was done by testing RPMI supplemented with HEPES, albumax, hypoxanthine and NaHCO<sub>3</sub>, which is often used as culture medium for eukaryotic cells including *Plasmodium* parasite (Duffy & Avery, 2018). Schneider medium, a medium used for insect cell lines (Hendricks & Wright, 1979; Marango *et al.*, 2017), supplemented with 20% FBS, was also tested because we believe that it would be useful to mimic the surrounding environment of mosquito cells *in vivo*, where the bacteria that constitute the midgut microbiota of the mosquitoes develop. Similar with literature observations (Wijesinghe *et al.*, 2019), we expected with these assays that the inclusion of more complex media will form more well-structured biofilms. Thus, the inclusion of several media allowed us to observe the influence of

culture media and nutrients on biofilm growth. Beside this, a medium used in *in vitro* oocyst cultures and an artificial diet, used as a substitute for blood meal in the maintenance of a laboratory colony of *Anopheles*, were also preliminarily tested (data not shown). However, the results for these media were not promising, namely because some components of the media bonded to the probe (or acted as a quencher for the probe), not allowing the real visualization of the structures formed, so these media did not proceed to the remaining stages of the work.

A crucial process in the formation of a biofilm is the initial adhesion of cells to a surface (Brindhadevi *et al.*, 2020; Cendra & Torrents, 2021; Sauer *et al.*, 2022). It is only after this initial adhesion step that the formation of more complex biofilm structures starts to occur. As such, the adhesion step was studied by following the behavior of the various bacteria after three hours of incubation.

Therefore, the bacteria were inoculated for only three hours on the microscopy plates, in all the previously mentioned media.

Images in Figure 7 refer to the xyz plane of the bacteria *P. mendocina* and *S. marcescens* An. steph A1-C1 after three hours of incubation. As shown in this Figure, there is a clear difference between the two bacteria, with a considerably higher cell density of adhered cells in the case of *P. mendocina*.

Apart from Schneider+FBS, for *P. mendocina* all media allowed for the observation of a "carpet" of adherent cells covering nearly the whole well. Additionally, the development of microcolonies, which generally occurs after cell adhesion in biofilm formation, was observed in the TSB, TSBG, and supplemented RPMI medium (RPMI\*). In the Schneider+FBS medium, the cell density throughout the well is lower, but larger and more numerous microcolonies are observed (Figure 7), suggesting that the biofilm formation process is faster in this medium.

Regarding *S. marcescens* An. steph A1-C1, although in smaller quantities, some adherent cells are also observed in most media at this incubation time, but we were not able to observe the formation of microcolonies at this time point (Figure 7).

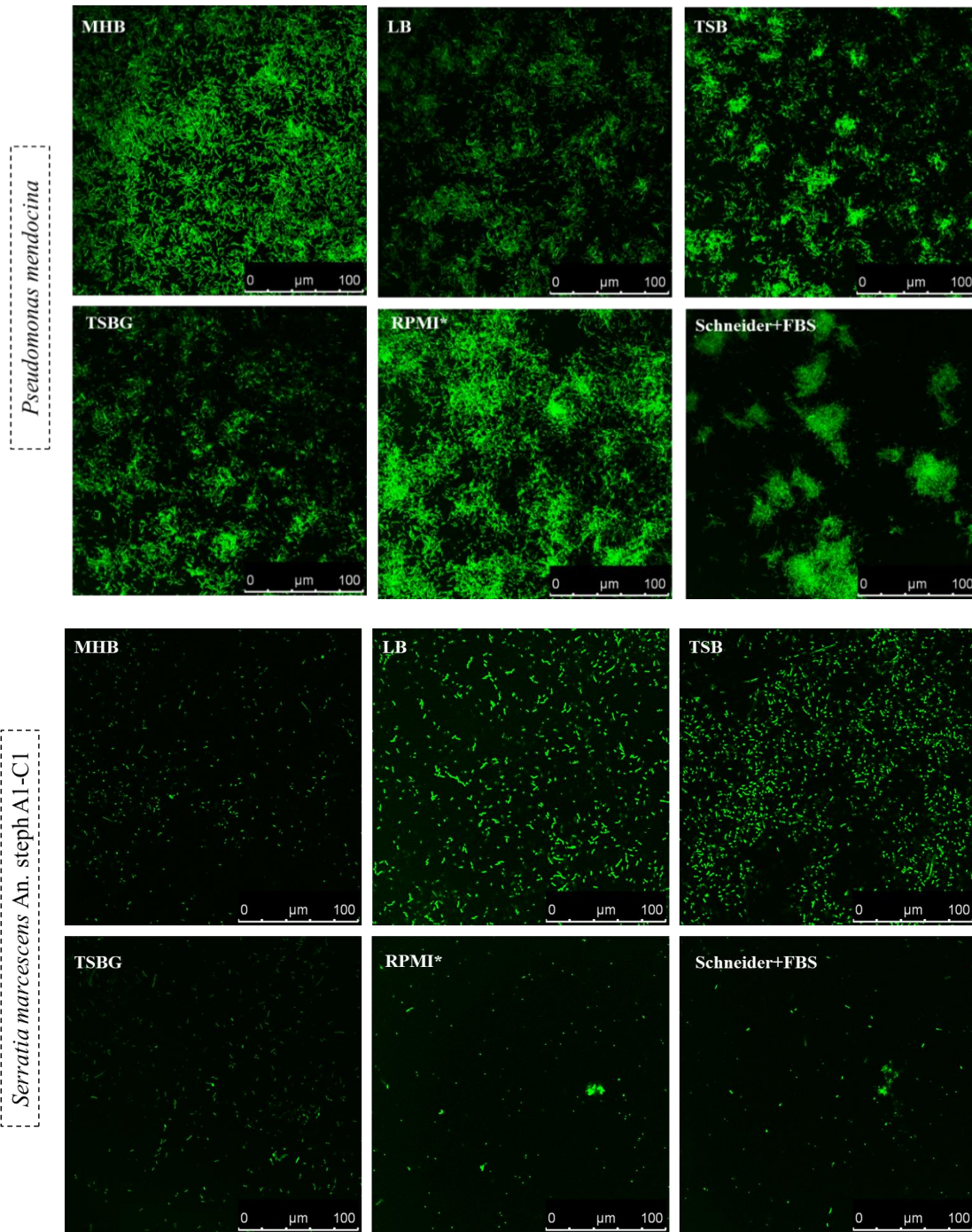


**Figure 7 – Representative confocal microscopy images of biofilms formed during 3 hours in different culture conditions.** The biofilms were labeled with the probe SYTO 9 and then imaged. The images depicted in the Figure correspond to the xyz plane view. The images correspond to a 1x digital zoom. Each image corresponds to different biofilm culture conditions. The first panel of six images corresponds to biofilms formed by *Pseudomonas mendocina* and the second panel to biofilms formed by *Serratia marcescens* An. steph A1-C1.

Biofilm formation was also observed 24 hours after inoculation. The biofilms visualized all showed heterogeneity along the well of the microscopy plate, which is probably related to the washing steps inherent to the incubation of the probe, which results in the loosening of some part of the biofilm (Figure 8).

Also, we evaluated here the biofilm height (Figure 10), for that we acquired two images in two different channels (x-z – vertical slice): one that corresponds to the surface of the coverslip, and in the other channel the fluorescence signal of the probe is recorded. The position corresponding to the biofilm surface is then used to quantify biofilm height.

In the 24h assays, the Schneider medium was supplemented with different amounts of FBS (0%, 5%, 10% and 20%), allowing us to detect the impact of serum dose in biofilm formation for both *P. mendocina* and *S. marcescens* An. steph A1-C1 (Figure 9), at 24h of incubation. The results showed that for both bacteria, the supplementation of Schneider's medium with 0% and 5% FBS did not allow the formation of significant microcolonies, with very similar observations. Supplementation with 10% FBS allowed the formation of some microcolonies with significant height, in a very heterogeneous way in the case of *P. mendocina*, but very poor biofilm production was still observed by *S. marcescens* An. steph A1-C1. On the other hand, when the Schneider medium was supplemented with 20% FBS, the formation of a slightly more homogeneous biofilm was observed, with a significant height for *P. mendocina*. The formation of some relevant microcolonies was also observed in the case of *S. marcescens* An. steph A1-C1 (Figure 9).

In view of these results, the supplementation of Schneider medium with 20% FBS (referred as Schneider+FBS) was selected for the remaining experiments performed following the analysis of biofilm formation by bacteria isolated from the midgut of *Anopheles* mosquitoes (metabolic assay, crystal violet assay and colony counting assay).

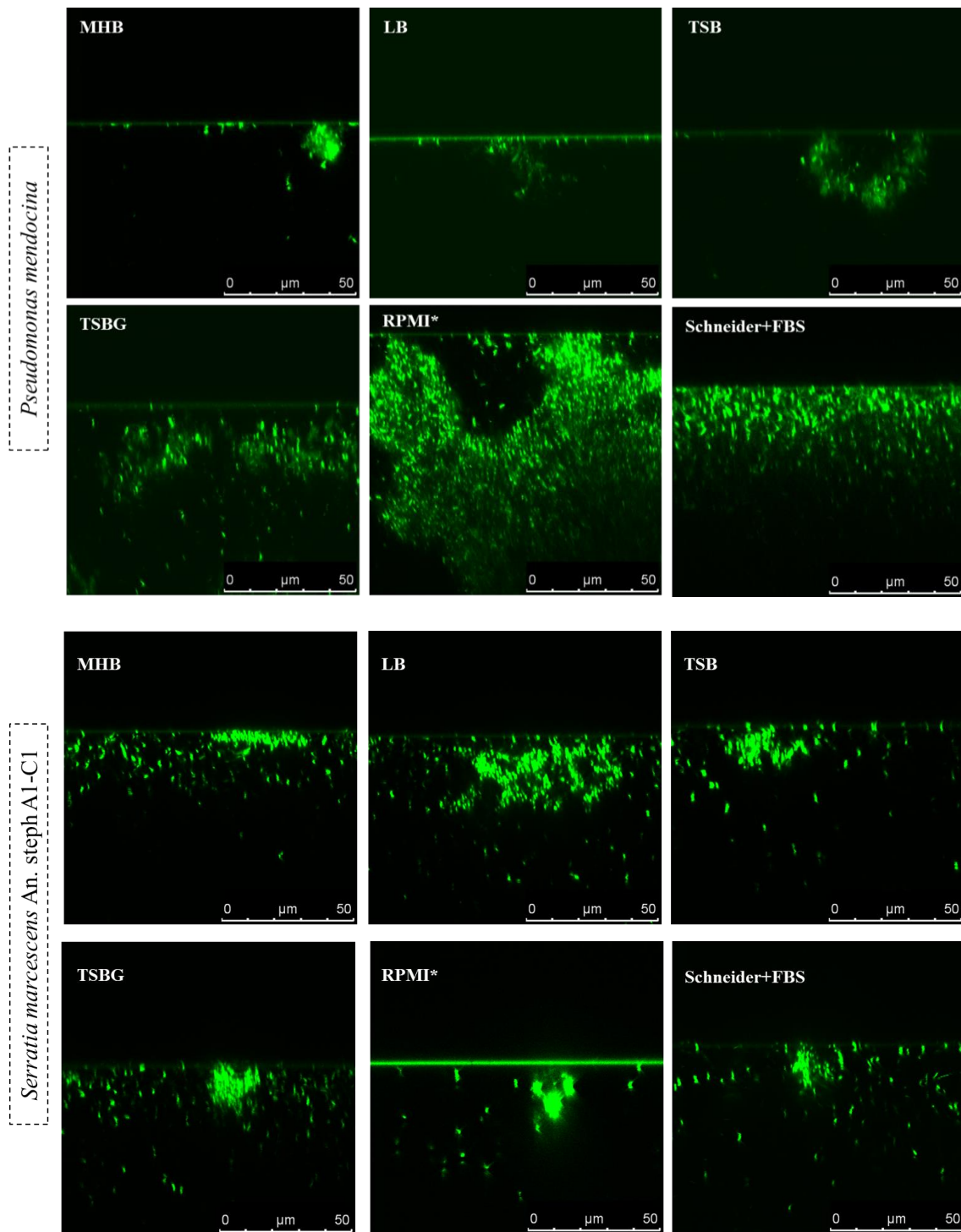


**Figure 8 – Representative confocal microscopy images of biofilms formed during 24 hours in different culture conditions.** The biofilms were labeled with the probe SYTO 9 and then imaged. The images depicted in the Figure correspond to the xzy plane view. Each image corresponds to different biofilm culture conditions. The first panel of six images corresponds to biofilms formed by *Pseudomonas mendocina* and the second panel to biofilms formed by *Serratia marcescens* An. steph A1-C1.

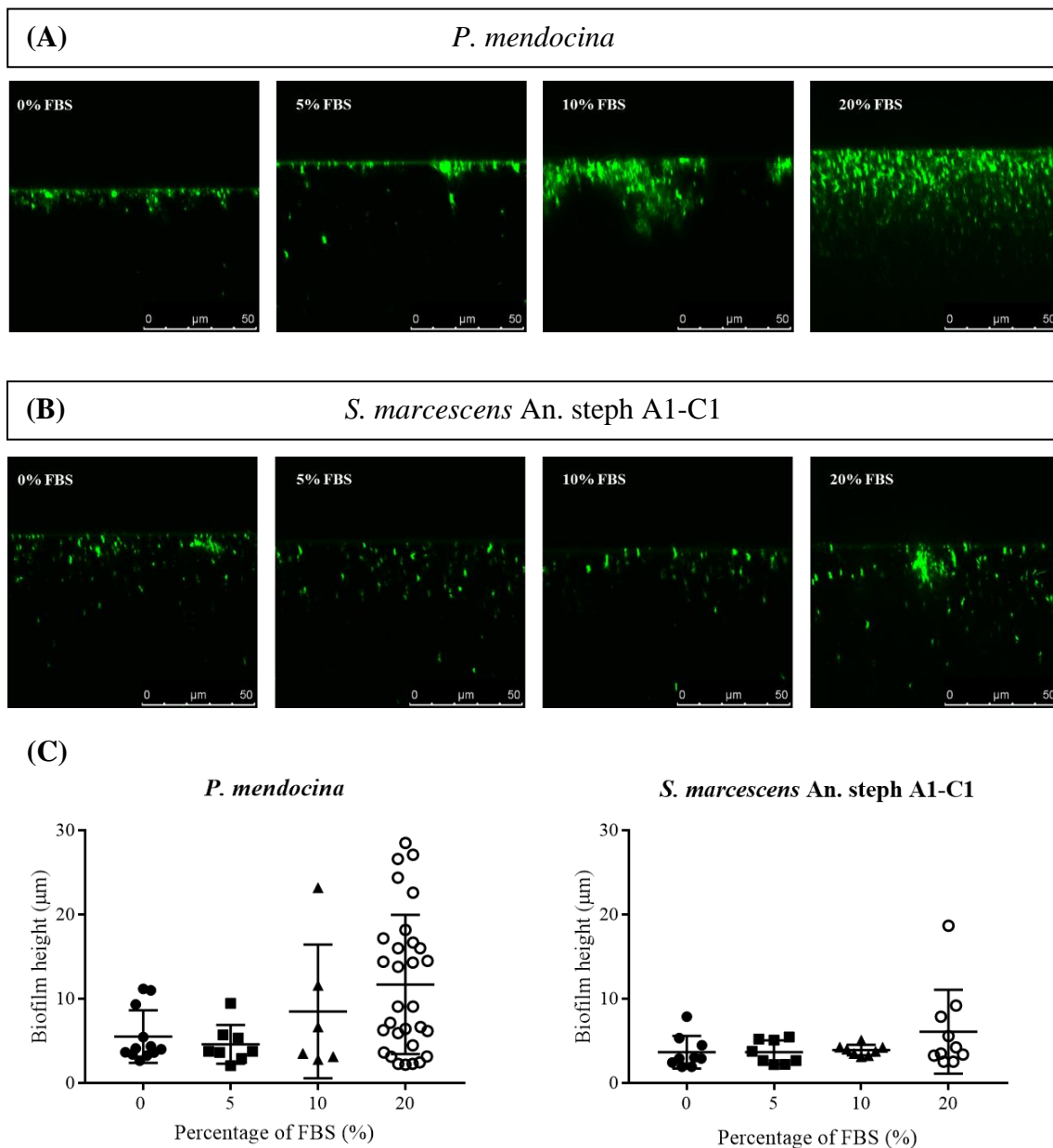


**Figure 9 - Influence of FBS in Schneider medium on biofilm formation.** Representative confocal microscopy images of biofilms formed during 24h in different culture conditions by (A) *P. mendocina* and (B) *S. marcescens* An. steph A1-C1. The biofilms were labeled with the probe SYTO 9 and then imaged. The images depicted in the Figure correspond to the xzy plane view. Each image corresponds to different biofilm culture conditions (percentage of FBS used to supplement the Schneider medium where the biofilm was grown). (C) Graphical representation of the values of heights (in  $\mu\text{m}$ ) recorded in the visualizations of the biofilms under the confocal microscope for *P. mendocina* and *S. marcescens* An. steph A1-C1. Measurements were taken at various sites along the wells, considering both areas with significant biofilm formation and areas with less biofilm formation to reflect a real representation of the heterogeneity observed.

Overall, a higher biofilm formation was observed for *P. mendocina* compared to the other tested bacteria. For this bacterium, biofilms with significant heights were observed in TSBG and supplemented RPMI, and in Schneider+FBS media, with a slightly lower height but a more homogeneous structure (Figure 8). In the case of *P. aeruginosa* ATCC 27853, significant bacterial colonies were observed in TSBG medium, and a low but highly homogeneous biofilm layer was observed in supplemented RPMI medium (Annex, Figure S6). In the other media, these bacteria did not form well-structured biofilms, showing only the presence of some microcolonies along the well.

For *S. marcescens* isolates, biofilm production was generally lower compared to *Pseudomonas* species. The isolate An. steph A1-C1 presented in all media several microcolonies with some height, but overall, a well-structured biofilm was not observed (Figure 8). The isolate An. steph A7-A1 was the one that presented the weakest biofilm production, with only a few microcolonies with minimal height (Annex, Figure S4). As for the An. col A9-C4 isolate, it was observed larger microcolonies in TSB, TSBG and supplemented RPMI media, however, it was also not possible to observe a well-structured biofilm (Annex, Figure S5).

Comparing these results with the adhesion assay at 3h incubation (Figure 7), it is evident that, for most of the media, there is a regression in cell adhesion. At 3 hours of observation, adhered cells were seen in a continuous layer along the well, and it would be expected that at 24 hours, a biofilm would also be observed throughout the well. However, this is not the case, as considerably heterogeneous biofilms are observed in most media. It is likely that as the biofilm formation process progresses, the forces of adhesion to the surface become more unstable, resulting in the loss of some parts of the biofilm during the washing steps at 24 hours. As the adhered structures are larger in size at 24 hours, they are more easily washed away during the washing steps compared to the layer of adhered cells at 3 hours.

Overall, all biofilms were quite heterogeneous, justifying the variation of results seen in the biofilm heights (Figure 10). Despite this, based on the analysis of the results, it can be stated that *P. mendocina* is the bacterium with the highest potential for biofilm formation, particularly notable in the supplemented RPMI medium. This information leads us to believe that similar events may occur within the midgut of the *Anopheles* mosquito, which could have some influence on the course of infection of the *Plasmodium* parasite in the mosquito.

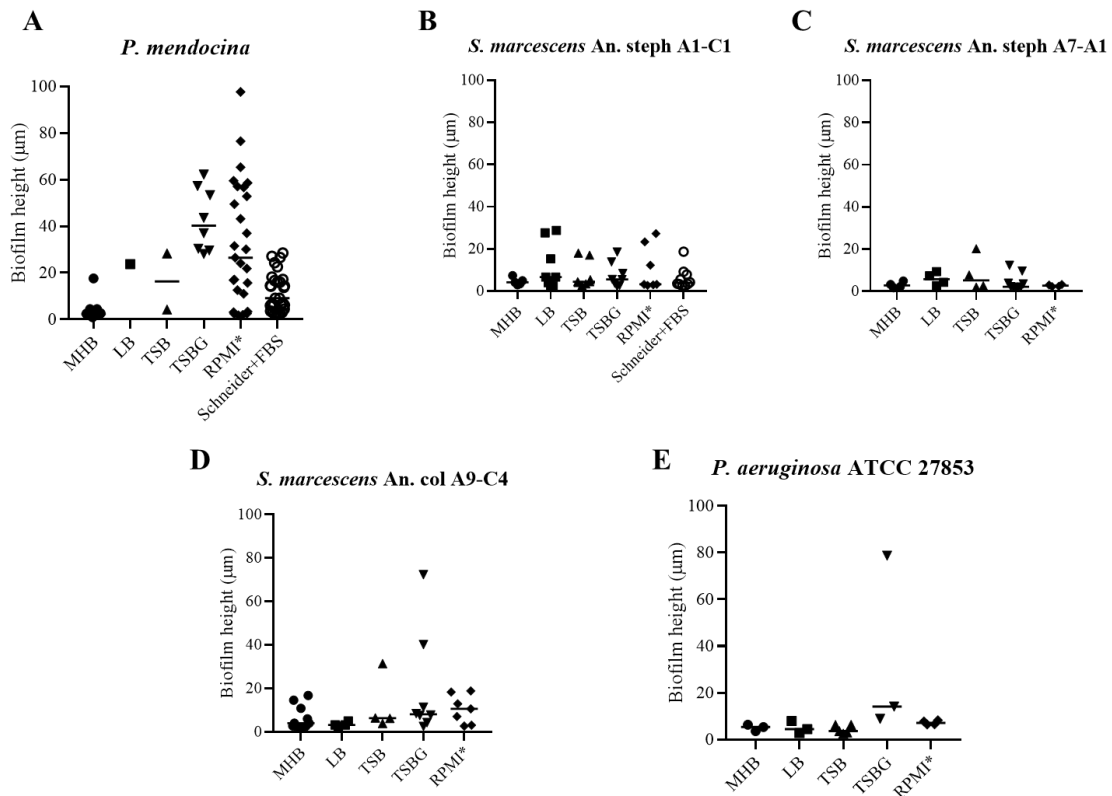


**Figure 10 – Biofilm height captured by confocal microscopy.** Graphical representation of the values of heights (in  $\mu\text{m}$ ) recorded in the visualizations of the biofilms under the confocal microscope. Measurements were taken at various points along the wells, considering both areas with significant biofilm formation and areas with less biofilm formation to reflect a real representation of the heterogeneity observed. These data rely on measurements from the various independent tests performed (at least duplicates per bacterium per medium). **A-** *P. mendocina*; **B-** *S. marcescens* An. steph A1-C1; **C-** *S. marcescens* An. steph A7-A1; **D-** *S. marcescens* An. col A9-C4; **E-** *P. aeruginosa* ATCC 27853.

It is essential to note that the probe used to label the biofilms in these assays has an affinity for nucleic acids only, including the extracellular DNA often found in biofilm matrices. However, it does not allow visualization of the complete structure of the extracellular matrix, which also prevents us from getting a real understanding of the appearance of all biofilm components. To achieve this, the study would need to be complemented with confocal microscopy assays using probes that label the various components of the extracellular matrix.

Nevertheless, the models described on the frequent composition of *Pseudomonas* biofilms are limited to *P. aeruginosa*. Therefore, it would be crucial to first investigate the metabolism and molecular mechanisms inherent in biofilm formation concerning environmental species of this bacterial genus.

Mosquitoes do not control their body temperature, so it coincides with the environmental temperature (Barr *et al.*, 2023). In this sense, an assay was also performed to adapt the biofilm growth temperature in supplemented RPMI to values closer to what naturally occurs in the natural environment (about 20°C). As shown in Figure 11, this temperature adjustment resulted in a decrease in biofilm formation by the *P. mendocina*. At 37°C slightly more consistent biofilms are observed.

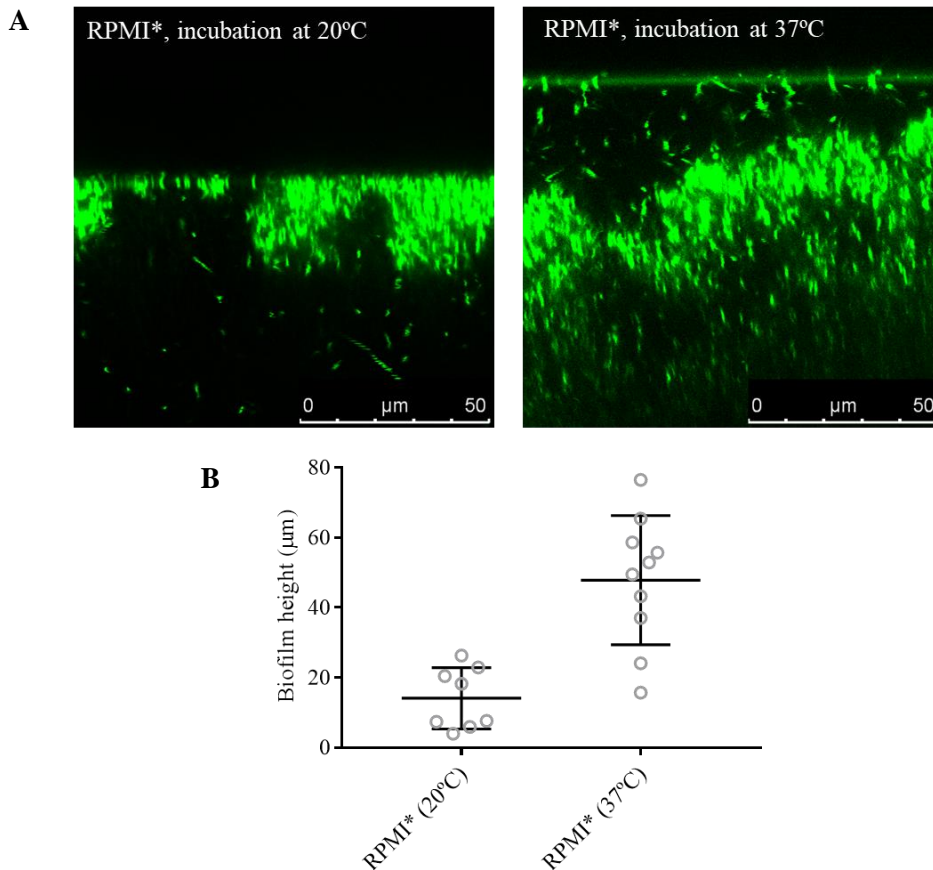


**Figure 11 – Influence of the incubation temperature on biofilm formation by *P. mendocina*.** (A) Representative confocal microscopy images of biofilms formed during 24h in supplemented RPMI medium (RPMI\*) by *P. mendocina*. The biofilms were labeled with the probe SYTO 9 and then imaged. The images depicted in the Figure correspond to the xzy plane view. Each image corresponds to different biofilm culture conditions. (B) Graphical representation of the values of heights (in µm) recorded in the visualizations of the biofilms under the confocal microscope. Measurements were taken at various points along the wells, considering both areas with significant biofilm formation and areas with less biofilm formation to reflect a real representation of the heterogeneity observed.

### 3.6.2. Quantitative analysis of adhesion and biofilm formation using the crystal violet assay

The initial adhesion step was also detected through biofilm biomass quantification using the crystal violet assay. Crystal violet is a cationic dye that binds to negatively charged molecules. As a result, this dye will attach to the bacterial surface and the extracellular matrix components of the biofilm, which are predominantly negatively charged, providing an indirect measurement of the formed biofilm biomass by measuring the absorbance at 590 nm (Peeters *et al.*, 2008; Stepanovic *et al.*, 2000). It is important to note that this assay only gives us information about the biomass of biofilm formed and does not allow the evaluation of other parameters such as cell viability, since crystal violet stains both living and dead cells (Peeters *et al.*, 2008; Skogman *et al.*, 2012), by binding to the negative components of the bacterial surface.

This assay was performed only for *P. mendocina* and *S. marcescens* An. steph A1-C1 in the six different media. Despite relying on indirect measurements of the biofilm biomass, this assay allowed us to complement the information obtained with the confocal microscopy at three hours of biofilm incubation. This assay gives quantitative information about the total components of the extracellular matrix (those that are negatively charged) and bacterial cells, and an indirect quantification of the total amount of biofilm.

In agreement with the confocal microscopy data (Figure 7), we observe that *P. mendocina* shows tendentially higher absorbance values compared to *S. marcescens* An. steph A1-C1, indicating a higher quantity of the total biofilm biomass (Figure 12).

For *P. mendocina*, absorbance values are relatively close for the various media, except for Schneider+FBS (Figure 12). In the confocal microscopy assays, it was noted that, despite observing more microcolonies in supplemented RPMI and Schneider+FBS, there was also a significant density of adherent cells in the other media (Figure 7), which could justify the relatively close values for all media in this assay. Also for the Schneider+FBS medium, it was observed through confocal microscopy that some microcolonies of considerable size were forming. However, lower cell density was observed throughout the well compared to the other media, which probably led to the lower absorbance values for this medium.

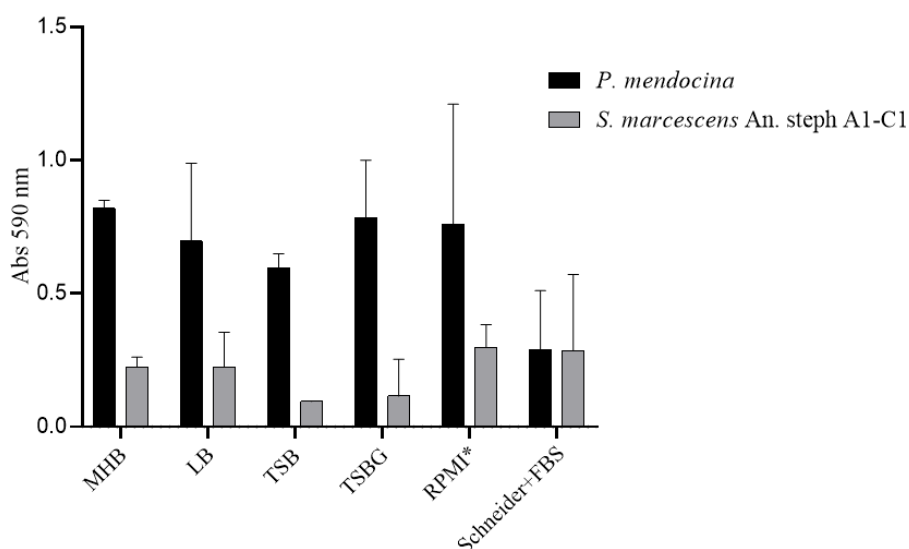


**Figure 12 – Adhesion assay at 3 hours of biofilm incubation.** Results of the adhesion assay at 3 hours of biofilm incubation, for *P. mendocina* and *S. marcescens* An. steph A1-C1 bacteria, by the crystal violet method. The biomass of biofilm formed was indirectly measured by measuring the absorbance at 590 nm on a microplate reader. The values presented represent the mean of at least two independent assays, with six technical replicates each.

### 3.6.3. Evaluation of metabolic activity of biofilm-growing bacteria by a resazurin reduction fluorometric assay

To further characterize biofilms, it is also important to quantify the cells that are metabolically active. Within the structure of a biofilm there are several populations of cells, where the metabolisms activated depend on the population. Normally, there is a group of metabolically dormant cells that are maintained in a state of dormancy within the biofilm, with drastically reduced metabolic activity (Donlan, 2001). These cells have very low metabolic activity and are more resistant to antimicrobial agents, oxidative stress and the adverse conditions to which the biofilm may be subjected. Therefore, these metabolically dormant cells populations are not detected in viability assays, being detected, on the other hand, in colony-forming units assays (Cordeiro *et al.*, 2021).

It was performed a metabolic assay based on the reduction of resazurin (blue color, oxidized form) into resorufin (pink color, reduced form), which unlike the former, is a highly fluorescent compound (Figure 13A).

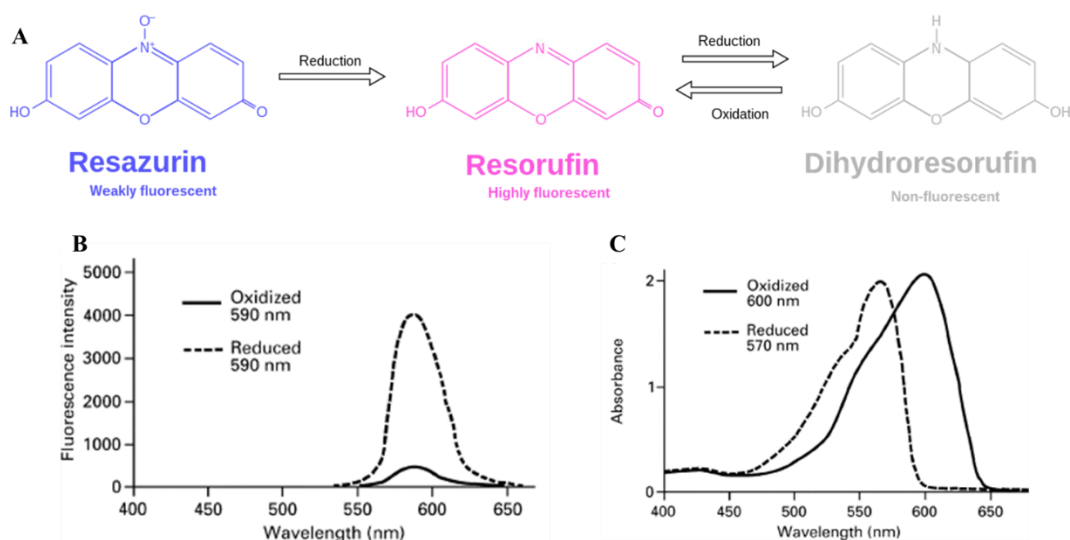


**Figure 13 – Chemical reaction and emission/absorption spectra on which the metabolic assay is based.** (A) Schematic of the chemical reaction on which the PrestoBlue metabolic assay is based. Reproduced from Wikipedia Contributors, 2019. Graphical representation of the (B) emission and (C) absorption spectra of the oxidized species in the reaction (resazurin), represented by the continuous line in the graphs, and of the semi-reduced species in the reaction (resorufin), represented by the dashed line in the graphs. Reproduced from Braut-Boucher & Aubery, 2016.

Considering the same amount of CFU/mL initially inoculated, metabolic assays are usually slower in biofilm contexts when compared to planktonic cells. This is due to the fact that microorganisms in biofilm mode have slower growth rates (so they are less affected by antimicrobial agents) and also to the fact that the components of the extracellular matrix act as a physical and chemical barrier to the entry of the chemical compound (in this case, resazurin) into the biofilm (as it happens with antimicrobial agents) (Donlan, 2001; Sandberg *et al.*, 2009).

The analysis of cellular metabolic activity using the resazurin-based assays can be carried out by measuring absorbance or via fluorescence detection. However, as we can see in Figure 13B and 13C, the assay is much sensitive when using fluorescence detection. This is because, resazurin is weakly fluorescent when compared to its derivative resorufin (7-hydroxy-3H-phenoxazin-3-one) (Costa *et al.*, 2021).

In these metabolic assays, it is important to take into account that the presence of specific components in the culture media may have an influence. For example, ascorbic acid causes a large fluorescence background if it is present in the culture medium, as it has the

ability to reduce resazurin without the presence of cells, due to its redox potential (Natto *et al.*, 2012). It has also been found that components of yeast extract and cysteine also have this ability (Natto *et al.*, 2012). Thus, the cell culture medium can interfere strongly on the outcome of this metabolic assay. In addition to the contribution that the components of the culture medium can have on the fluorescence signal, if the cell density or incubation time is too high, the fluorescent compound (resorufin) can subsequently be reduced to the final product of the reaction, dihydroresorufin, which in contrast is a non-fluorescent compound (Costa *et al.*, 2021) (Figure 13A). Therefore, when a decrease in fluorescence is observed after a certain incubation time, this does not necessarily mean cell death, but may indicate a reduction in the metabolic activity of the cells or, on the other hand, an increase in the reduction of resorufin to dihydroresorufin.

In this assay, the metabolization of resazurin was evaluated for the several bacteria and for the various media that had been used in the confocal microscopy assays.

In the process of optimizing this assay, we verified that components of the TSB and TSBG media contributed (although slightly) to the reduction of resazurin, with an increase in the fluorescence signal in the negative controls (without bacterial cells), and the conversion of resorufin to dihydroresorufin after a short incubation time. On the other hand, components of the supplemented RPMI medium prevented the reduction reaction to occur, as there was no significant increase in the fluorescence signal over time in the wells with pre-formed biofilms. Consequently, biofilms were grown in the different media, and only the resazurin incubation step was performed for all metabolic assays in MHB (endpoint of the assay), which had shown to have practically no influence on the metabolization of the compound (Pinto *et al.*, 2019).

We observed that *P. mendocina* is the bacterial species for which resazurin conversion is slowest for all media tested (Figure 14 and 15). This is probably associated with the fact that there is a greater amount of bacteria in biofilm form, and therefore the amount of cells that may be metabolically inactive, in a state of metabolic dormancy will be higher. Additionally, resazurin might not be able to penetrate certain sections of the biofilm where there are structures with significant heights (as shown in the confocal microscopy data), preventing it from reaching several of the metabolically active cells within the biofilm.

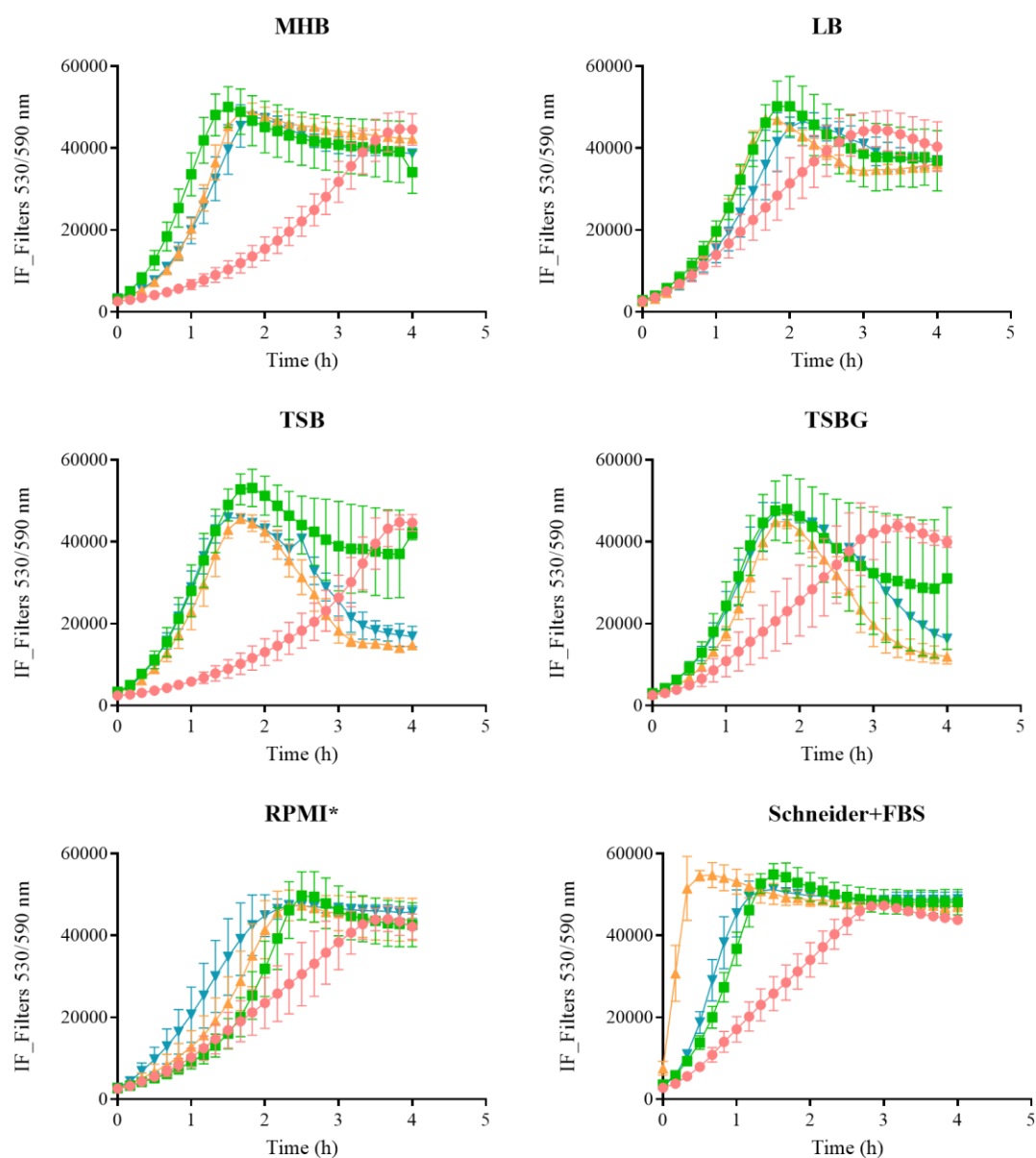


**Figure 14 – Metabolic assay in relation to the medium.** Graphical representation of the fluorescence kinetic over time resulting from the reduction of resazurin by the various bacterial species in the various media in which the biofilms were grown for 24 hours. The reduction of resazurin by the bacteria was evaluated by the measured of the fluorescence intensity (excitation: 530 nm; emission: 590 nm) on a microplate reader every ten minutes for four hours, at 37°C. The red curve corresponds to *P. mendocina*. The green curve corresponds to *S. marcescens* An. steph A1-C1. The orange curve corresponds to *S. marcescens* An. steph A7-A1. The blue curve corresponds to *S. marcescens* An. col A9-C4. The values presented represent the mean of at least two independent assays, with six technical replicates each.

*S. marcescens* isolates showed a similar behavior for the majority of media, presenting a faster kinetics than that observed for *P. mendocina* (Figure 14 and 15). This is probably related to the growth curves of the various bacteria. We had already observed that *S. marcescens* isolates reach the exponential phase faster than *Pseudomonas* species, i.e. a larger amount of bacterial cells also results in faster compound conversion kinetics. Bacteria in biofilm tend to have lower growth rates than planktonic cells, so the fact that *S. marcescens* isolates form less biofilm than *P. mendocina* also justifies the slower kinetics for the latter.

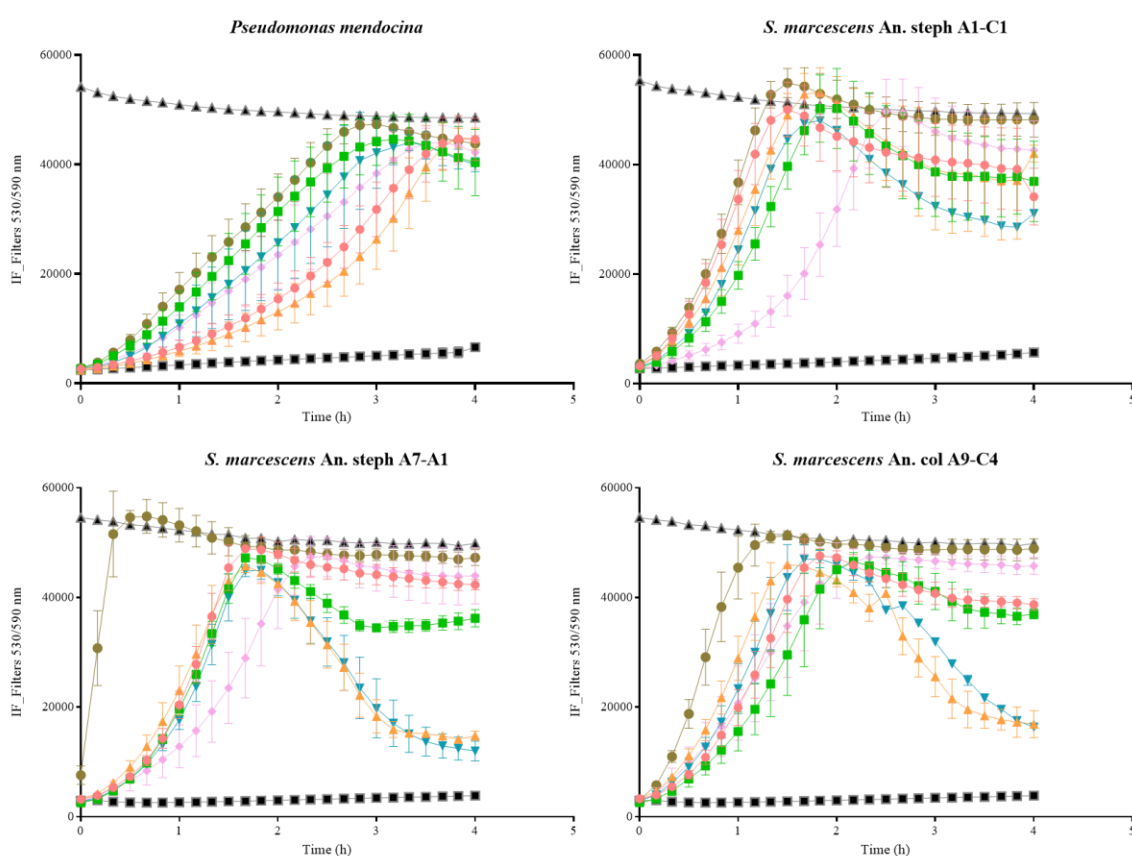


**Figure 15 – Metabolic assay in relation to the bacterial isolate.** Graphical representation of the fluorescence kinetic over time resulting from the reduction of resazurin by the various bacterial species in the various media in which the biofilms were grown for 24 hours. The reduction of resazurin by the bacteria was evaluated by the measured of the fluorescence intensity (excitation: 530 nm; emission: 590 nm) on a microplate reader every ten minutes for four hours, at 37°C. The red curve corresponds to growth in MHB medium. The green curve corresponds to growth in LB medium. The orange curve corresponds to growth in TSB medium. The blue curve corresponds to growth in TSBG medium. The pink curve corresponds to growth in supplemented RPMI (RPMI\*). The brown curve corresponds to growth in Schneider+FBS. The black curve (square symbols) corresponds to the negative control. The black curve (triangle symbols) corresponds to the positive control. The values presented represent the mean of at least two independent assays, with six technical replicates each.

### 3.6.4. Evaluation of Colony Forming Units (CFU) of different biofilms

The characterization of the biofilm-forming potential was further analyzed with the colony counting assay, which involve counting the colony-forming units (CFU) of the biofilms. The biofilms were inoculated in 96-well plates, and subsequently, at 3 and 24 hours of biofilm formation, the adhered cells were mechanically detached and plated on MHA (Mueller-Hinton Agar), according to Pinto *et al.*, (2019). Unlike the metabolic assay, this method allows the detection of the metabolically dormant cells present in the biofilm (those that are metabolically inactive). Due to time and resource management, the colony counting assay was conducted only for *P. mendocina* and *S. marcescens* An. steph A1-C1, and for the media MHB, supplemented RPMI, and Schneider supplemented with 20% FBS. The initial inoculum was approximately  $10^6$  CFU/mL.

As shown in Figure 16, at 3 hours of incubation, *S. marcescens* An. steph A1-C1 showed CFU/mL in the order of  $10^6$  (Figure 16B), while *P. mendocina* exhibited CFU/mL in the order of  $10^7$  (Figure 16A), corroborating the information obtained from the microscopy and crystal violet assays, where a higher cell density of adhered cells was visible for *P. mendocina* (Figure 7 and Figure 12).

The results at 24 hours of incubation are more intriguing. In the case of *P. mendocina*, the lowest CFU/mL value is recorded for RPMI\* (Figure 16C), while the microscopy assays show that a larger quantity of well-structured biofilm is formed in this medium. Additionally, it is observed that for supplemented RPMI and Schneider+FBS media, *S. marcescens* An. steph A1-C1 presents higher CFU counts than *P. mendocina* (Figure 16C and D), which does not correspond to the confocal microscopy observations.

It has already been described that the type of plates used to grow biofilms has an impact on the structures formed and observed/detected (Azeredo *et al.*, 2017). It is important to note that the plates used in this CFU counting assay and the microscopy assays are different. This could lead to variations in the biofilm formation process because the microscopy plates have a larger surface area and a square shape, whereas the 96-well plates have smaller round wells.

Another possible explanation is that, as observed in microscopy, *P. mendocina* forms larger biofilms with stronger adhesion forces at 24 hours of incubation than *S. marcescens* An. steph A1-C1. Therefore, this discrepancy may be due to insufficient mechanical forces to disaggregate the thicker biofilms formed by *P. mendocina*, while they may be

sufficient for *S. marcescens*, as they are less adhered as illustrated by the crystal violet assay (Figure 12).

There are some alternatives to the dispersing biofilms method used in this study. Ultrasonication is a recurrently used method (Haney *et al.*, 2018; Monsen *et al.*, 2009; Moraes *et al.*, 2021; Taff *et al.*, 2012), which disrupts the extracellular matrix, allowing the biofilm cells to be released. Another method that has already been used is the application of electrical pulses, which interfere with the adhesion forces between the biofilm and the surface, allowing water to enter the structure, and biofilm cells release (Khan *et al.*, 2016). Both methods are based on the mechanical dispersion of the biofilm. However, these methods can result in the damage of some cells, thus affecting the assessment of the viability of the biofilm cells. In addition to mechanical methods, biofilm dispersion can also be promoted by chemical methods (Liu *et al.*, 2020). An example of this is the use of surfactants, such as rhamnolipids, to degrade the extracellular matrix (Wood *et al.*, 2018). However, as the bacterial surface is also made up of these constituents (mainly because in this case they are gram-negative bacteria), these strategies can also result in damage to cells that would otherwise be viable in the biofilm.

In the context of this work, the influence of the addition of Tryple (a trypsin substitute used in cell cultures) was evaluated, prior to the disaggregation of the biofilm using the method already described (see subsection 2.8.4.). This strategy was tested in the colony counting assay for *P. mendocina* biofilm at 24 hours of incubation in the supplemented RPMI medium. The addition of this compound appeared to have no significant influence on the disruption of the biofilms, since the results obtained were similar to those obtained in the assays without the Tryple addition step.

The highest CFU/mL count was observed when Schneider+FBS medium was used (Figure 16). Although confocal microscopy did not showed biofilms as significant in height as in supplemented RPMI, it was Schneider+FBS that promoted the formation of the most homogeneous biofilms. As such, the forces established between the components of the biofilm itself are, in theory, greater, also due to the supplementation with FBS. As the biofilm structure is more cohesive it may facilitate the detachment of a greater quantity of biofilm by the dispersal mechanical method. On the other hand, in the supplemented RPMI medium the biofilm formed is much more heterogeneous, which may lead smaller portions of the biofilm being detached, making it more difficult to detach the entire structure.

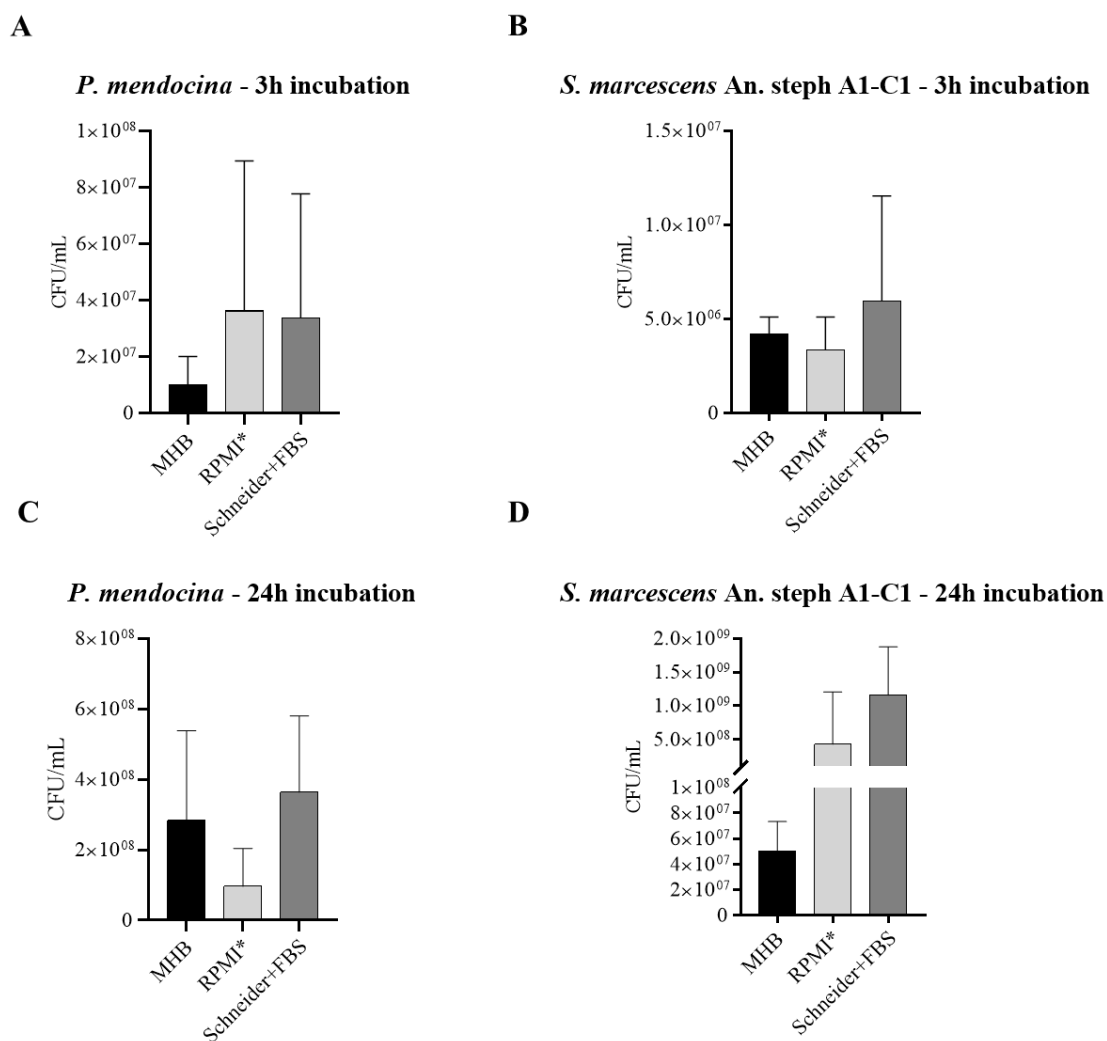


**Figure 16 – Counting of CFU/mL of the different bacterial biofilms.** The results show the CFU/mL counts from colony counting assay after disaggregation of biofilms formed by *P. mendocina* at (A) 3 and (C) 24 hours of incubation and *S. marcescens* An. steph A1-C1 at (B) 3 and (D) 24 hours of incubation. Biofilms were detached by mechanical forces and serial dilutions of this homogenate were plated on MHA. The values presented represent the mean of at least two independent assays, with six technical replicates each.

## 4. Conclusions

Malaria continues to be the vector-borne disease with the highest prevalence and the highest number of deaths each year (CDC, 2023; Milner, 2018). Although this disease is no longer an imminent problem in most developed countries, a large part of the tropical and sub-tropical regions of Africa, Asia and Central/South America are still extremely affected by *Plasmodium* infection (World Health Organization, 2022). As such, it is essential that the prevention of parasite transmission, as well as the treatment of the infection, remain central focuses of scientific research. The *Plasmodium* parasite is transmitted to humans through the bite of female mosquitoes of the *Anopheles* genus, and there is a cycle of infection in the mosquito (Cowman *et al.*, 2016; Garcia, 2010). Due to the recurrent use of insecticides and anti-malarial drugs, these are no longer completely effective to prevent transmission and treating the infected host (Hemingway *et al.*, 2016; Zoure *et al.*, 2020). An imminent and innovative strategy is the genetic manipulation of components of the microbiota of *Anopheles* mosquitoes, with the purpose of making the mosquito refractory (or at least less susceptible) to infection by the parasite, significantly reducing the circulation of *Plasmodium* in the environment and, consequently, reducing the impact of the disease (Abraham & Jacobs-Lorena, 2004; Wang & Jacobs-Lorena, 2013).

The purpose of this research project was to evaluate the biofilm-forming capacity of bacteria isolated from the midguts of various *Anopheles* species. Although the study of the composition of the *Anopheles* microbiota is a frequent focus of scientific research, the capacity for biofilm formation is not often studied in this context. To the best of our knowledge, there are still no concrete conclusions about the formation of biofilms by these bacteria and their impact on *Plasmodium* infection in mosquitoes.

Contrary to what is frequently reported in the literature (Birnberg *et al.*, 2021; Das De *et al.*, 2022; Zoure *et al.*, 2020), the bacterial diversity identified in the isolation assays was not significantly high. This may have been due to the mosquitoes used in this work being from laboratory colonies rather than wild. The fact that they were reared in a controlled environment leads to less contact with environmental microorganisms, so the diversity of their microbiota is lower. Additionally, the isolation methods were based on cell culture, which also does not allow the identification of all the existing diversity (Rani *et al.*, 2009). Therefore, a more complex and complementary approach would be needed to provide a

real picture of the diversity of these mosquitoes' microbiota. Contrary to what would be expected, feeding the mosquitoes with blood 24 hours before dissection also did not result in an increase in bacterial diversity and abundance.

The composition of the mosquito midgut microbiota depends on numerous factors, including environmental and nutritional factors. Despite this, there is always some inter-individual variability (Birnberg *et al.*, 2021). The study covered several *Anopheles* species, and bacterial genera common to various *Anopheles* species were identified, while others were only isolated from specific *Anopheles* species. These results seem to indicate the presence of a core microbiota, complemented by some species-dependent bacterial genera. As some authors have already pointed out (Gendrin & Christophides, 2013), there were no bacterial species isolated and identified in all the studies carried out, which seems to strengthen the idea that *Anopheles* mosquitoes probably do not have an obligatory symbiont for their survival, at least colonizing the midgut.

Therefore, paratransgenesis strategies focus on altering the mosquito's vectorial capacity by genetically manipulating its symbionts to heighten their anti-*Plasmodium* effect (Wilke & Marrelli, 2015; Zoure *et al.*, 2020). The success of this type of strategy depends on the introduction and dissemination of the bacteria by wild mosquito populations. Therefore, it is also important to consider certain factors that may have unintended repercussions, such as the large-scale introduction into the environment of bacteria with resistance phenotypes to antibiotics commonly used in clinical and agronomic practice. Accordingly, the antibiotic susceptibility profiles of the *S. marcescens* isolates and the *P. mendocina* isolate were also evaluated. These results made it possible to divide the *S. marcescens* isolates into two groups (those isolated from *An. stephensi* and one isolated from *An. coluzzii*) with different susceptibility profiles. Analysis of the sequences from whole genome sequencing allowed us to conclude that there are genotypic differences between the *An. coluzzii* isolate (An. col A9-C4) and the *An. stephensi* isolates (An. steph A1-C1 and An. steph A7-A1), justifying the differences observed in the antibiogram results. Although BLASTn analysis of the three isolates revealed that the closest database match was the same strain (*S. marcescens* subsp. *marcescens* Db11), deeper analysis of the genome sequences would be necessary to conclude whether An. col A9-C4 isolate belongs to the same strain as the *An. stephensi* isolates.

The resulting WGS sequences also led to the identification of the *Pseudomonas* species that had been isolated from *An. gambiae* as *P. mendocina*, since the sequencing of the 16S rDNA gene region alone had not allowed for species-level identification. One of the most interesting results of the genome sequences analysis was the identification of hits with gene sequences involved in the various stages of biofilm formation. For both *P. mendocina* and the various isolates of *S. marcescens*, genes involved in the biosynthesis and regulation of structures involved in mobility (flagella, pili, fimbriae), essential for the steps of adhesion to surfaces, were identified. In the case of *P. mendocina*, it was also possible to identify genes involved in the biosynthesis and regulation of alginate, a very relevant exopolysaccharide in *P. aeruginosa* mucoid biofilms. Overall, this genotypic analysis allowed the identification of some genes that are essential for biofilm formation, which supports the results of characterizing the potential for biofilm formation *in vitro* and being a good indicator of *P. mendocina* natural capacity for biofilm formation.

The colonization assays of the midgut of *An. stephensi* with *Pseudomonas* sp. was important to confirm that the isolation methods used allowed for the efficient isolation of species from the *Pseudomonas* genus. In addition, it allowed us to conclude that *P. mendocina* isolated from *An. gambiae* can efficiently colonize the midgut of another *Anopheles* species, which would be an important factor to implement paratransgenesis candidates.

After isolating bacteria from the midgut of the *Anopheles* mosquito, the second major objective of this work was to characterize the biofilm-forming capacity of *P. mendocina* and three of the *S. marcescens* isolates (An. steph A1-C1, An. steph A7-A1 and An. col A9-C4). It is thought that the presence of bacterial biofilms in the midgut epithelium of *Anopheles* mosquitoes contributes to blocking the *Plasmodium* development cycle in the mosquito, acting as a physical and chemical barrier to the passage of ookinetes through the midgut epithelium (Jiang *et al.*, 2023). Therefore, biofilm production could be a bacterial feature to be studied for application in the context of paratransgenesis. This ability was assessed using metabolic assays, confocal microscopy, indirect measurement of biofilm biomass (crystal violet assay) and colony counting. In particular, supplemented RPMI medium (RPMI\*) and Schneider medium supplemented with 20% FBS were included as an attempt to mimic the conditions bacteria encounter inside the mosquito.

As would be expected given the context of each of the bacterial genera (*Pseudomonas* and *Serratia*) in biofilm formation, there were clear differences between *P. mendocina*

and the *S. marcescens* isolates, with the *Pseudomonas* species being more successful in forming more structured biofilms. Despite this, *P. mendocina* did not achieve the same success in biofilm formation in all media, with TSBG and supplemented RPMI standing out as the media where larger structures were obtained, however, the biofilm formed was always quite heterogeneous. The most homogeneous biofilm was achieved in the Schneider+FBS medium, probably due to the presence of serum, which was intended to mimic the blood ingested by mosquitoes (where the parasite could be found). Therefore, it can be concluded that biofilm formation by this isolate of *P. mendocina* is highly dependent on growth conditions.

Adhesion tests carried out at 3 hours of incubation also showed a higher bacterial density and microcolony formation in the case of *P. mendocina*, when compared to *S. marcescens* An. steph A1-C1. This indicates that even the initial steps of the biofilm formation process are more efficient and faster in *P. mendocina*. On the other hand, in the colony counting assay, the observations were different and, in some cases, inconsistent with the other assays. After 24 hours of incubating the biofilm, *S. marcescens* An. steph A1-C1 has formed a greater number of CFU/mL than *P. mendocina*. In addition, for *P. mendocina* the lowest value was observed for supplemented RPMI medium, the medium in which the greatest biofilm formation had been observed in the confocal microscopy tests. This may be due to the easiness biofilms are detached from the microplate surface, which the results indicate being easier for the *S. marcescens* isolate, justifying the higher CFU/mL values. On the other hand, supplementing the Schneider medium with 20% FBS allows for more cohesive and homogeneous biofilms, which results in easier detachment of the adhered cells. Also in the experiments to characterize the potential for biofilm formation, metabolic assays showed that, in general, *P. mendocina* had slower kinetics than the *S. marcescens* isolates, regardless of the biofilm growth medium. This seems to be consistent with the idea that in structures such as biofilms, there is a sharing of resources between the bacterial cells, allowing some to enter a state of metabolic dormancy, and also that the cell viability biomarker has greater difficulty in penetrating the structure. Thus, *P. mendocina* showed slower kinetics, which in theory means greater biofilm formation.

As referred in literature (Anju *et al.*, 2022; Kulshrestha & Gupta, 2022), the majority of biofilms that occur in nature are polymicrobial. Considering the great diversity of microorganisms that constitute the mosquito microbiota (some of which is demonstrated

in our results), it is thought that biofilms within the mosquito midgut are also polymicrobial (Chattopadhyay *et al.*, 2022). However, inter-species relationships and communication are highly relevant in this context, as some bacteria may have an inhibitory effect on the biofilm development of another species, or vice versa. Therefore, this hypothesis would have to be further investigated and studied with different and complementary approaches to those described here.

In general, this work shows the potential of *P. mendocina* isolated from *An. gambiae* as a target for the development of strategies to control malaria, since its biofilm production can be advantageous when formed on the mosquito epithelium, acting as a physical and chemical barrier to the passage of ookinetes, in the life cycle of the *Plasmodium* parasite within the *Anopheles* mosquito. In the context of continuing this project, it would be interesting and important to conduct biofilm formation experiments using mosquito cell cultures as the adhesion surface. In addition, *in vivo* studies on live mosquitoes would also be one of the following steps. Besides this, further research is needed to understand the mechanisms underlying the biofilm formation by these species and its impact on malaria transmission, and more specifically, on the *Plasmodium* development cycle in the mosquito. As previously noted in the course of this report, there are several imminent challenges in the research of this malaria control strategy, which need to be overcome in order to allow for more cross-sectional studies and conclusions that can be more generalized. Nonetheless, paratransgenesis strategies have enormous potential to overcome the problems currently encountered in the use of insecticides and anti-malarial drugs to fight malaria. Therefore, studies such as this one are important for bringing this type of strategy closer to viable and real alternatives that can be applied in the context of countries where malaria continues to be one of the main public health problems.

## 5. Bibliographic References

- Abraham, E. G., & Jacobs-Lorena, M. (2004). Mosquito midgut barriers to malaria parasite development. *Insect Biochemistry and Molecular Biology*, *34*(7), 667–671. <https://doi.org/10.1016/j.ibmb.2004.03.019>
- Anju, V. T., Busi, S., Imchen, M., Kumavath, R., Mohan, M. S., Salim, S. A., Subhaswaraj, P., & Dyavaiah, M. (2022). Polymicrobial Infections and Biofilms: Clinical Significance and Eradication Strategies. *Antibiotics*, *11*(12):1731. <https://doi.org/10.3390/antibiotics11121731>
- Azeredo, J., Azevedo, N. F., Briandet, R., Cerca, N., Coenye, T., Costa, A. R., Desvaux, M., Di Bonaventura, G., Hébraud, M., Jaglic, Z., Kačániová, M., Knøchel, S., Lourenço, A., Mergulhão, F., Meyer, R. L., Nychas, G., Simões, M., Tresse, O., & Sternberg, C. (2017). Critical review on biofilm methods. *Critical Reviews in Microbiology*, *43*(3), 313–351. <https://doi.org/10.1080/1040841X.2016.1208146>
- Bahia, A. C., Dong, Y., Blumberg, B. J., Mlambo, G., Tripathi, A., Benmarzouk-Hidalgo, O. J., Chandra, R., & Dimopoulos, G. (2014). Exploring *Anopheles* gut bacteria for *Plasmodium* blocking activity. *Environmental Microbiology*, *16*(9), 2980–2994. <https://doi.org/10.1111/1462-2920.12381>
- Bai, L., Wang, L., Vega-Rodríguez, J., Wang, G., & Wang, S. (2019). A Gut Symbiotic Bacterium *Serratia marcescens* Renders Mosquito Resistance to *Plasmodium* Infection Through Activation of Mosquito Immune Responses. *Frontiers in Microbiology*, *10*:1580. <https://doi.org/10.3389/fmicb.2019.01580>
- Barr, J. S., Estevez-Lao, T. Y., Khalif, M., Saksena, S., Yarlagadda, S., Farah, O., Shivere, Y., & Hillyer, J. F. (2023). Temperature and age, individually and interactively, shape the size, weight, and body composition of adult female mosquitoes. *Journal of Insect Physiology*, *148*:104525. <https://doi.org/10.1016/j.jinsphys.2023.104525>
- Belda, E., Coulibaly, B., Fofana, A., Beavogui, A. H., Traore, S. F., Gohl, D. M., Vernick, K. D., & Riehle, M. M. (2017). Preferential suppression of *Anopheles gambiae* host sequences allows detection of the mosquito eukaryotic microbiome. *Scientific Reports*, *7*(1):3241. <https://doi.org/10.1038/s41598-017-03487-1>

- Bertola, M., Mazzucato, M., Pombi, M., & Montarsi, F. (2022). Updated occurrence and bionomics of potential malaria vectors in Europe: a systematic review (2000–2021). *Parasites and Vectors*, *15*(1):88. <https://doi.org/10.1186/s13071-022-05204-y>
- Bertrand, X., & Dowzicky, M. J. (2012). Antimicrobial susceptibility among gram-negative isolates collected from intensive care units in North America, Europe, the Asia-Pacific Rim, Latin America, the Middle East, and Africa between 2004 and 2009 as part of the Tigecycline Evaluation and Surveillance Trial. *Clinical Therapeutics*, *34*(1), 124–137. <https://doi.org/10.1016/J.CLINTHERA.2011.11.023>
- Birnberg, L., Climent-Sanz, E., Codoñer, F. M., & Busquets, N. (2021). Microbiota Variation Across Life Stages of European Field-Caught *Anopheles atroparvus* and During Laboratory Colonization: New Insights for Malaria Research. *Frontiers in Microbiology*, *12*:775078. <https://doi.org/10.3389/fmicb.2021.775078>
- Blumberg, B. J., Trop, S., Das, S., & Dimopoulos, G. (2013). Bacteria- and IMD Pathway-Independent Immune Defenses against *Plasmodium falciparum* in *Anopheles gambiae*. *PLoS ONE*, *8*(9):e72130. <https://doi.org/10.1371/journal.pone.0072130>
- Boissière, A., Tchioffo, M. T., Bachar, D., Abate, L., Marie, A., Nsango, S. E., Shahbazkia, H. R., Awono-Ambene, P. H., Levashina, E. A., Christen, R., & Morlais, I. (2012). Midgut microbiota of the malaria mosquito vector *Anopheles gambiae* and interactions with *Plasmodium falciparum* infection. *PLoS Pathogens*, *8*(5):e1002742. <https://doi.org/10.1371/journal.ppat.1002742>
- Braut-Boucher, F., & Aubery, M. (2016). Fluorescent molecular probes. In *Encyclopedia of Spectroscopy and Spectrometry* (pp. 661–669). Elsevier. <https://doi.org/10.1016/B978-0-12-803224-4.00072-8>
- Brindhadevi, K., LewisOscar, F., Mylonakis, E., Shanmugam, S., Verma, T. N., & Pugazhendhi, A. (2020). Biofilm and Quorum sensing mediated pathogenicity in *Pseudomonas aeruginosa*. *Process Biochemistry*, *96*, 49–57. <https://doi.org/10.1016/j.procbio.2020.06.001>
- Buck, M., Nilsson, L. K. J., Brunius, C., Dabiré, R. K., Hopkins, R., & Terenius, O. (2016). Bacterial associations reveal spatial population dynamics in *Anopheles*

*gambiae* mosquitoes. *Scientific Reports*, 6(1):22806.  
<https://doi.org/10.1038/srep22806>

- Capone, A., Ricci, I., Damiani, C., Mosca, M., Rossi, P., Scuppa, P., Crotti, E., Epis, S., Angeletti, M., Valzano, M., Sacchi, L., Bandi, C., Daffonchio, D., Mandrioli, M., & Favia, G. (2013). Interactions between *Asaia*, *Plasmodium* and *Anopheles*: New insights into mosquito symbiosis and implications in Malaria Symbiotic Control. *Parasites and Vectors*, 6(1):182. <https://doi.org/10.1186/1756-3305-6-182>
- CDC. (2020a). *CDC - Malaria - about Malaria - Where Malaria Occurs*. <https://www.cdc.gov/malaria/about/distribution.html>. Date of access: 29/06/2023
- CDC. (2020b, July 16). *CDC - Malaria - About Malaria - Biology*. <https://www.cdc.gov/malaria/about/biology/index.html>. Date of access: 29/06/2023
- CDC. (2023). *Malaria*. <https://www.cdc.gov/parasites/malaria/index.html>. Date of access: 29/06/2023
- Cendra, M. del M., & Torrents, E. (2021). *Pseudomonas aeruginosa* biofilms and their partners in crime. *Biotechnology Advances*, 49:107734. <https://doi.org/10.1016/j.biotechadv.2021.107734>
- Chattopadhyay, A., Ghosh, S., & Banerjee, P. K. (2022). Role of gut microbial biofilm of *anopheline* mosquitoes to control its vectorial attribute: A study in some areas of West Bengal. *Biocatalysis and Agricultural Biotechnology*, 40:102305. <https://doi.org/10.1016/j.bcab.2022.102305>
- Chavshin, A. R., Oshaghi, M. A., Vatandoost, H., Pourmand, M. R., Raeisi, A., Enayati, A. A., Mardani, N., & Ghoorchian, S. (2012). Identification of bacterial microflora in the midgut of the larvae and adult of wild caught *Anopheles stephensi*: A step toward finding suitable paratransgenesis candidates. *Acta Tropica*, 121(2), 129–134. <https://doi.org/10.1016/j.actatropica.2011.10.015>
- Cheeseman, I. H., Miller, B. A., Nair, S., Nkhoma, S., Tan, A., Tan, J. C., Al Saai, S., Phyto, A. P., Ler Moo, C., Lwin, K. M., McGready, R., Ashley, E., Imwong, M., Stepniewska, K., Yi, P., Dondorp, A. M., Mayxay, M., Newton, P. N., White, N. J., ... Anderson, T. J. C. (2012). A major genome region underlying artemisinin resistance in malaria. *Science*, 335(6077), 79–82. <https://doi.org/10.1126/science.1215966>

- Chen, S., Blom, J., & Walker, E. D. (2017). Genomic, physiologic, and symbiotic characterization of *Serratia marcescens* strains isolated from the mosquito *Anopheles stephensi*. *Frontiers in Microbiology*, 8:1483. <https://doi.org/10.3389/fmicb.2017.01483>
- Chen, X., Thomsen, T. R., Winkler, H., & Xu, Y. (2020). Influence of biofilm growth age, media, antibiotic concentration and exposure time on *Staphylococcus aureus* and *Pseudomonas aeruginosa* biofilm removal *in vitro*. *BMC Microbiology*, 20(1):264. <https://doi.org/10.1186/s12866-020-01947-9>
- Cirimotich, C. M., Dong, Y., Clayton, A. M., Sandiford, S. L., Souza-Neto, J. A., Mulenga, M., & Dimopoulos, G. (2011). Natural microbe-mediated refractoriness to *Plasmodium* infection in *Anopheles gambiae*. *Science*, 332(6031), 855–858. <https://doi.org/10.1126/science.1201618>
- CLSI. (2023). *CLSI M100-ED33:2023 Performance Standards for Antimicrobial Susceptibility Testing, 33rd Edition*.
- Cohuet, A., Harris, C., Robert, V., & Fontenille, D. (2010). Evolutionary forces on *Anopheles*: what makes a malaria vector? *Trends in Parasitology*, 26(3), 130–136. <https://doi.org/10.1016/j.pt.2009.12.001>
- Conn, J. E., Grillet, M. E., Correa, M., Sallum, M. A. M., Conn, J. E., Grillet, M. E., Correa, M., & Sallum, M. A. M. (2018). Malaria Transmission in South America—Present Status and Prospects for Elimination. In *Towards Malaria Elimination - A Leap Forward* (Vol. 12). IntechOpen. <https://doi.org/10.5772/INTECHOPEN.76964>
- Coon, K. L., Vogel, K. J., Brown, M. R., & Strand, M. R. (2014). Mosquitoes rely on their gut microbiota for development. *Molecular Ecology*, 23(11), 2727–2739. <https://doi.org/10.5061/dryad.s6223>
- Cordeiro, R. de A., Aguiar, A. L. R., da Silva, B. N., Pereira, L. M. G., Portela, F. V. M., de Camargo, Z. P., de Lima-Neto, R. G., Castelo-Branco, D. de S. C. M., Rocha, M. F. G., & Sidrim, J. J. C. (2021). *Trichosporon asahii* and *Trichosporon inkin* Biofilms Produce Antifungal-Tolerant Persister Cells. *Frontiers in Cellular and Infection Microbiology*, 11:645812. <https://doi.org/10.3389/fcimb.2021.645812>

- Costa, P., Gomes, A. T. P. C., Braz, M., Pereira, C., & Almeida, A. (2021). Application of the resazurin cell viability assay to monitor *Escherichia coli* and *Salmonella typhimurium* inactivation mediated by phages. *Antibiotics*, 10(8):974. <https://doi.org/10.3390/antibiotics10080974>
- Cowman, A. F., Healer, J., Marapana, D., & Marsh, K. (2016). Malaria: Biology and Disease. *Cell*, 167(3), 610–624. <https://doi.org/10.1016/j.cell.2016.07.055>
- Darling, A. E., Mau, B., & Perna, N. T. (2010). Progressivemauve: Multiple genome alignment with gene gain, loss and rearrangement. *PLoS ONE*, 5(6):e11147. <https://doi.org/10.1371/journal.pone.0011147>
- Das De, T., Sharma, P., Tevatiya, S., Chauhan, C., Kumari, S., Yadav, P., Singla, D., Srivastava, V., Rani, J., Hasija, Y., Pandey, K. C., Kajla, M., & Dixit, R. (2022). Bidirectional Microbiome-Gut-Brain-Axis Communication Influences Metabolic Switch-Associated Responses in the Mosquito *Anopheles culicifacies*. *Cells*, 11(11):1798. <https://doi.org/10.3390/cells11111798>
- Dennison, N. J., Jupatanakul, N., & Dimopoulos, G. (2014). The mosquito microbiota influences vector competence for human pathogens. *Current Opinion in Insect Science*, 3, 6–13. <https://doi.org/10.1016/j.cois.2014.07.004>
- Djadid, N. D., Jazayeri, H., Raz, A., Favia, G., Ricci, I., & Zakeri, S. (2011). Identification of the midgut microbiota of *An. stephensi* and *An. maculipennis* for their application as a paratransgenic tool against malaria. *PLoS ONE*, 6(12):e28484. <https://doi.org/10.1371/journal.pone.0028484>
- Dondorp, A. M., Yeung, S., White, L., Nguon, C., Day, N. P. J., Socheat, D., & Von Seidlein, L. (2010). Artemisinin resistance: Current status and scenarios for containment. *Nature Reviews Microbiology*, 8(4), 272–280. <https://doi.org/10.1038/nrmicro2331>
- Dong, Y., Manfredini, F., & Dimopoulos, G. (2009). Implication of the mosquito midgut microbiota in the defense against malaria parasites. *PLoS Pathogens*, 5(5):e1000423. <https://doi.org/10.1371/journal.ppat.1000423>
- Donlan, R. M. (2001). Biofilm Formation: A Clinically Relevant Microbiological Process. *Clinical Infectious Diseases*, 33, 1387–1392. <https://academic.oup.com/cid/article/33/8/1387/347551>

- Drenkard, E. (2003). Antimicrobial resistance of *Pseudomonas aeruginosa* biofilms. *Microbes and Infection*, 5(13), 1213–1219. <https://doi.org/10.1016/j.micinf.2003.08.009>
- Duffy, S., & Avery, V. M. (2018). Routine *In vitro* Culture of *Plasmodium falciparum*: Experimental Consequences? *Trends in Parasitology*, 34(7), 564–575. <https://doi.org/10.1016/j.pt.2018.04.005>
- Fekrirad, Z., Gattali, B., & Kashef, N. (2020). Quorum sensing-regulated functions of *Serratia marcescens* are reduced by eugenol. *Iranian Journal of Microbiology*, 12(5), 451–459. <https://doi.org/10.18502/ijm.v12i5.4607>
- Flyg, C., Kenne, K., & Boman, H. G. (1980). Insect pathogenic properties of *Serratia marcescens*: phage-resistant mutants with a decreased resistance to *Cecropia* immunity and a decreased virulence to *Drosophila*. *Journal of General Microbiology*, 120(1), 173–181. <https://doi.org/10.1099/00221287-120-1-173>
- Fraser, G. M., & Hughes, C. (1999). Swarming motility. *Current Opinion in Microbiology*, 2(6), 630–635. [https://doi.org/10.1016/S1369-5274\(99\)00033-8](https://doi.org/10.1016/S1369-5274(99)00033-8)
- Fu, Y., Liu, W., Liu, M., Zhang, J., Yang, M., Wang, T., & Qian, W. (2021). *In vitro* anti-biofilm efficacy of sanguinarine against carbapenem-resistant *Serratia marcescens*. *Biofouling*, 37(3), 341–351. <https://doi.org/10.1080/08927014.2021.1919649>
- Ganley, J. G., D'Ambrosio, H. K., Shieh, M., & Derbyshire, E. R. (2020). Coculturing of Mosquito-Microbiome Bacteria Promotes Heme Degradation in *Elizabethkingia anophelis*. *ChemBioChem*, 21(9), 1279–1284. <https://doi.org/10.1002/cbic.201900675>
- Gao, H., Cui, C., Wang, L., Jacobs-Lorena, M., & Wang, S. (2020). Mosquito Microbiota and Implications for Disease Control. *Trends in Parasitology*, 36(2), 98–111. <https://doi.org/10.1016/j.pt.2019.12.001>
- Garcia, L. S. (2010). Malaria. *Clinics in Laboratory Medicine*, 30(1), 93–129. <https://doi.org/10.1016/j.cll.2009.10.001>
- Gendrin, M., & Christophides, G. K. (2013). The *Anopheles* Mosquito Microbiota and Their Impact on Pathogen Transmission. In *Anopheles mosquitoes - New insights into malaria vectors* (pp. 525–548). InTech. <https://doi.org/10.5772/55107>

- Gething, P. W., Elyazar, I. R. F., Moyes, C. L., Smith, D. L., Battle, K. E., Guerra, C. A., Patil, A. P., Tatem, A. J., Howes, R. E., Myers, M. F., George, D. B., Horby, P., Wertheim, H. F. L., Price, R. N., Müller, I., Baird, J. K., & Hay, S. I. (2012). A Long Neglected World Malaria Map: *Plasmodium vivax* Endemicity in 2010. *PLoS Neglected Tropical Diseases*, 6(9):e1814. <https://doi.org/10.1371/journal.pntd.0001814>
- Ghafoor, A., Hay, I. D., & Rehm, B. H. A. (2011). Role of exopolysaccharides in *Pseudomonas aeruginosa* biofilm formation and architecture. *Applied and Environmental Microbiology*, 77(15), 5238–5246. <https://doi.org/10.1128/AEM.00637-11>
- Gimonneau, G., Tchioffo, M. T., Abate, L., Boissière, A., Awono-Ambéné, P. H., Nsango, S. E., Christen, R., & Morlais, I. (2014). Composition of *Anopheles coluzzii* and *Anopheles gambiae* microbiota from larval to adult stages. *Infection, Genetics and Evolution*, 28, 715–724. <https://doi.org/10.1016/j.meegid.2014.09.029>
- Givskov, M., Ostling, J., Eberl, L., Lindum, P. W., Christensen, A. B., Christiansen, G., Molin, S., & Kjelleberg, S. (1998). Two separate regulatory systems participate in control of swarming motility of *Serratia liquefaciens* MG1. *Journal of Bacteriology*, 180(3), 742–745. <https://doi.org/10.1128/jb.180.3.742-745.1998>
- Greener, J., Gashti, M. P., Eslami, A., Zarabadi, M. P., & Taghavi, S. M. (2016). A microfluidic method and custom model for continuous, non-intrusive biofilm viscosity measurements under different nutrient conditions. *Biomicrofluidics*, 10(6):064107. <https://doi.org/10.1063/1.4968522>
- Greenwood, B. M., Fidock, D. A., Kyle, D. E., Kappe, S. H. I., Alonso, P. L., Collins, F. H., & Duffy, P. E. (2008). Malaria: Progress, perils, and prospects for eradication. *Journal of Clinical Investigation*, 118(4), 1266–1276. <https://doi.org/10.1172/JCI33996>
- Hall, T. A. (1999). BioEdit: a user-friendly biological sequence alignment editor and analysis program for Windows 95/98/ NT. *Oxford University Press - Nucleic Acids Symposium Series*, 41(2), 95–98. <https://doi.org/10.14601/Phytopathol Mediterr-14998u1.29>

- Haney, E. F., Trimble, M. J., Cheng, J. T., Vallé, Q., & Hancock, R. E. W. (2018). Critical assessment of methods to quantify biofilm growth and evaluate antibiofilm activity of host defense peptides. *Biomolecules*, 8(2):29. <https://doi.org/10.3390/biom8020029>
- Harmsen, M., Yang, L., Pamp, S. J., & Tolker-Nielsen, T. (2010). An update on *Pseudomonas aeruginosa* biofilm formation, tolerance, and dispersal. *FEMS Immunology and Medical Microbiology*, 59(3), 253–268. <https://doi.org/10.1111/j.1574-695X.2010.00690.x>
- Hegde, S., Khanipov, K., Albayrak, L., Golovko, G., Pimenova, M., Saldaña, M. A., Rojas, M. M., Hornett, E. A., Motl, G. C., Fredregill, C. L., Dennett, J. A., Debboun, M., Fofanov, Y., & Hughes, G. L. (2018). Microbiome interaction networks and community structure from laboratory-reared and field-collected *Aedes aegypti*, *Aedes albopictus*, and *Culex quinquefasciatus* mosquito vectors. *Frontiers in Microbiology*, 9:2160. <https://doi.org/10.3389/fmicb.2018.02160>
- Hemingway, J., Ranson, H., Magill, A., Kolaczinski, J., Fornadel, C., Gimnig, J., Coetzee, M., Simard, F., Roch, D. K., Hinzoumbe, C. K., Pickett, J., Schellenberg, D., Gething, P., Hoppé, M., & Hamon, N. (2016). Averting a malaria disaster: Will insecticide resistance derail malaria control? *The Lancet*, 387(10029), 1785–1788. [https://doi.org/10.1016/S0140-6736\(15\)00417-1](https://doi.org/10.1016/S0140-6736(15)00417-1)
- Hendricks, L., & Wright, N. (1979). Diagnosis of cutaneous leishmaniasis by *in vitro* cultivation of saline aspirates in Schneider's *Drosophila* Medium. *The American Journal of Tropical Medicine and Hygiene*, 28(6), 962–964. <https://doi.org/10.4269/ajtmh.1979.28.962>
- Hertig, E. (2019). Distribution of *Anopheles* vectors and potential malaria transmission stability in Europe and the Mediterranean area under future climate change. *Parasites and Vectors*, 12(1):18. <https://doi.org/10.1186/s13071-018-3278-6>
- Huang, W., Wang, S., & Jacobs-Lorena, M. (2020). Use of Microbiota to Fight Mosquito-Borne Disease. *Frontiers in Genetics*, 11:196. <https://doi.org/10.3389/fgene.2020.00196>
- Hugo, R. L. E., & Birrell, G. W. (2018). Proteomics of *Anopheles* Vectors of Malaria. *Trends in Parasitology*, 34(11), 961–981. <https://doi.org/10.1016/j.pt.2018.08.009>

- Jenkins, T. A., Nguyen, J. C. D., Polglaze, K. E., & Bertrand, P. P. (2016). Influence of tryptophan and serotonin on mood and cognition with a possible role of the gut-brain axis. *Nutrients*, 8(1):56. <https://doi.org/10.3390/nu8010056>
- Jiang, Y., Gao, H., Wang, L., Hu, W., Wang, G., & Wang, S. (2023). Quorum sensing-activated phenylalanine metabolism drives OMV biogenesis to enhance mosquito commensal colonization resistance to *Plasmodium*. *Cell Host & Microbe*, 31, 1–13. <https://doi.org/10.1016/J.CHOM.2023.08.017>
- Kalappa, D. M., Subramani, P. A., Basavanna, S. K., Ghosh, S. K., Sundaramurthy, V., Uragayala, S., Tiwari, S., Anvikar, A. R., & Valecha, N. (2018). Influence of midgut microbiota in *Anopheles stephensi* on *Plasmodium berghei* infections. *Malaria Journal*, 17(1):385. <https://doi.org/10.1186/s12936-018-2535-7>
- Karygianni, L., Ren, Z., Koo, H., & Thurnheer, T. (2020). Biofilm Matrixome: Extracellular Components in Structured Microbial Communities. *Trends in Microbiology*, 28(8), 668–681. <https://doi.org/10.1016/J.TIM.2020.03.016>
- Khan, S. I., Blumrosen, G., Vecchio, D., Golberg, A., McCormack, M. C., Yarmush, M. L., Hamblin, M. R., & Austen, W. G. (2016). Eradication of multidrug-resistant *Pseudomonas* biofilm with pulsed electric fields. *Biotechnology and Bioengineering*, 113(3), 643–650. <https://doi.org/10.1002/bit.25818>
- Kulshrestha, A., & Gupta, P. (2022). Polymicrobial interaction in biofilm: mechanistic insights. *Pathogens and Disease*, 80(1), 1–10. <https://doi.org/10.1093/femspd/ftac010>
- Kumar, A., Chery, L., Biswas, C., Dubhashi, N., Dutta, P., Dua, V. K., Kacchap, M., Kakati, S., Khandeparkar, A., Kour, D., Mahajan, S. N., Maji, A., Majumder, P., Mohanta, J., Mohapatra, P. K., Narayanasamy, K., Roy, K., Shastri, J., Valecha, N., ... Rathod, P. K. (2012). Malaria in South Asia: Prevalence and control. *Acta Tropica*, 121(3), 246–255. <https://doi.org/10.1016/j.actatropica.2012.01.004>
- Lane, D. J. (1991). 16S/23S rRNA Sequencing. In *Stackebrandt, E. and Goodfellow, M., Eds., Nucleic Acid Techniques in Bacterial Systematic*, John Wiley and Sons, New York (pp. 115–175).
- Lane, D. J., Pace, B., Olsen, G. J., Stahl, D. A., Sogin, M. L., & Pace, N. R. (1985). Rapid determination of 16S ribosomal RNA sequences for phylogenetic analyses.

*Proceedings of the National Academy of Sciences of the United States of America*, 82(20), 6955. <https://doi.org/10.1073/PNAS.82.20.6955>

- Laporta, G. Z., Linton, Y. M., Wilkerson, R. C., Bergo, E. S., Nagaki, S. S., Sant'Ana, D. C., & Sallum, M. A. M. (2015). Malaria vectors in South America: Current and future scenarios. *Parasites and Vectors*, 8(1):426. <https://doi.org/10.1186/s13071-015-1038-4>
- Lau, P. C. Y., Dutcher, J. R., Beveridge, T. J., & Lam, J. S. (2009). Absolute Quantitation of Bacterial Biofilm Adhesion and Viscoelasticity by Microbead Force Spectroscopy. *Biophysical Journal*, 96(7), 2935–2948. <https://doi.org/10.1016/J.BPJ.2008.12.3943>
- Lee, K., & Yoon, S. S. (2017). *Pseudomonas aeruginosa* Biofilm, a Programmed Bacterial Life for Fitness. *Journal of Microbiology and Biotechnology*, 27(6), 1053–1064. <https://doi.org/10.4014/JMB.1611.11056>
- Lewis, K. (2008). Multidrug Tolerance of Biofilms and Persister Cells. *Current Topics in Microbiology and Immunology*, 322, 107–131. [https://doi.org/10.1007/978-3-540-75418-3\\_6](https://doi.org/10.1007/978-3-540-75418-3_6)
- Li, H., Tanikawa, T., Sato, Y., Nakagawa, Y., & Matsuyama, T. (2005). *Serratia marcescens* Gene Required for Surfactant Serrawettin W1 Production Encodes Putative Aminolipid Synthetase Belonging to Nonribosomal Peptide Synthetase Family. *Microbiology and Immunology*, 49(4), 303–310. <https://doi.org/10.1111/J.1348-0421.2005.TB03734.X>
- Lindh, J. M., Kännaste, A., Kännaste, K., Knols, B. G. J., Faye, I., & Borg-Karlson, A.-K. (2008). Oviposition Responses of *Anopheles gambiae* s.s. (Diptera: Culicidae) and Identification of Volatiles from Bacteria-Containing Solutions. *J. Med. Entomol.*, 45(6), 1039–1049. <https://doi.org/https://doi.org/10.1093/jmedent/45.6.1039>
- Lindh, J. M., Terenius, O., & Faye, I. (2005). 16S rRNA gene-based identification of midgut bacteria from field-caught *Anopheles gambiae* sensu lato and *An. funestus* mosquitoes reveals new species related to known insect symbionts. *Applied and Environmental Microbiology*, 71(11), 7217–7223. <https://doi.org/10.1128/AEM.71.11.7217-7223.2005>

- Lindum, P. W., Anthoni, U., Christophersen, C., Eberl, L., Molin, S., & Givskov, A. M. (1998). N-Acyl-L-Homoserine Lactone Autoinducers Control Production of an Extracellular Lipopeptide Biosurfactant Required for Swarming Motility of *Serratia liquefaciens* MG1. *Journal of Bacteriology*, 180(23), 6384–6388. <https://doi.org/10.1128/JB.180.23.6384-6388.1998>
- Liu, Z., Hong, C. J., Yang, Y., Dai, L., & Ho, C. L. (2020). Advances in Bacterial Biofilm Management for Maintaining Microbiome Homeostasis. *Biotechnology Journal*, 15(10):e1900320. <https://doi.org/10.1002/biot.201900320>
- Luo, H. Z., Zhou, J. W., Sun, B., Jiang, H., Tang, S., & Jia, A. Q. (2021). Inhibitory effect of norharmane on *Serratia marcescens* NJ01 quorum sensing-mediated virulence factors and biofilm formation. *Biofouling*, 37(2), 145–160. <https://doi.org/10.1080/08927014.2021.1874942>
- Ma, L., Conover, M., Lu, H., Parsek, M. R., Bayles, K., & Wozniak, D. J. (2009). Assembly and development of the *Pseudomonas aeruginosa* biofilm matrix. *PLoS Pathogens*, 5(3):e1000354. <https://doi.org/10.1371/journal.ppat.1000354>
- Manda, H., Gouagna, L. C., Foster, W. A., Jackson, R. R., Beier, J. C., Githure, J. I., & Hassanali, A. (2007). Effect of discriminative plant-sugar feeding on the survival and fecundity of *Anopheles gambiae*. *Malaria Journal*, 6(1):113. <https://doi.org/10.1186/1475-2875-6-113>
- Manguin, S., Ngo, C. T., Tainchum, K., Juntarajumnong, W., Chareonviriyaphap, T., Michon, A.-L., & Jumas-Bilak, E. (2013). Bacterial Biodiversity in Midguts of *Anopheles* Mosquitoes, Malaria Vectors in Southeast Asia. In *Anopheles mosquitoes - New insights into malaria vectors* (pp. 549–576). InTech. <https://doi.org/10.5772/55610>
- Marango, S. N., Khayeka-Wandabwa, C., Makwali, J. A., Jumba, B. N., Choge, J. K., Adino, E. O., & Anjili, C. O. (2017). Experimental therapeutic assays of *Tephrosia vogelii* against *Leishmania major* infection in murine model: *In vitro* and *in vivo*. *BMC Research Notes*, 10(1):698. <https://doi.org/10.1186/s13104-017-3022-x>
- McGoverin, C., Robertson, J., Jonmohamadi, Y., Swift, S., & Vanholsbeeck, F. (2020). Species Dependence of SYTO 9 Staining of Bacteria. *Frontiers in Microbiology*, 11:545419. <https://doi.org/10.3389/fmicb.2020.545419>

- Meibalan, E., & Marti, M. (2017). Biology of malaria transmission. *Cold Spring Harbor Perspectives in Medicine*, 7(3):a025452. <https://doi.org/10.1101/cshperspect.a025452>
- Meister, S., Agianian, B., Turlure, F., Relógio, A., Morlais, I., Kafatos, F. C., & Christophides, G. K. (2009). *Anopheles gambiae* PGRPLC-mediated defense against bacteria modulates infections with malaria parasites. *PLoS Pathogens*, 5(8):e1000542. <https://doi.org/10.1371/journal.ppat.1000542>
- Miller, M. B., & Bassler, B. L. (2001). Quorum sensing in bacteria. *Annual Review of Microbiology*, 55(1), 165–199. <https://doi.org/https://doi.org/10.1146/annurev.micro.55.1.165>
- Milner, D. A. (2018). Malaria pathogenesis. *Cold Spring Harbor Perspectives in Medicine*, 8(1):a025569. <https://doi.org/10.1101/cshperspect.a025569>
- Molina-Cruz, A., DeJong, R. J., Charles, B., Gupta, L., Kumar, S., Jaramillo-Gutierrez, G., & Barillas-Mury, C. (2008). Reactive oxygen species modulate *Anopheles gambiae* immunity against bacteria and *Plasmodium*. *Journal of Biological Chemistry*, 283(6), 3217–3223. <https://doi.org/10.1074/jbc.M705873200>
- Moll, R. M., Romoser, W. S., Modrzakowski, M. C., Moncayo, A. C., & Lerdthusnee, K. (2001). Meconial peritrophic membranes and the fate of midgut bacteria during mosquito (Diptera: *Culicidae*) metamorphosis. *Journal of Medical Entomology*, 38(1), 29–32. <https://doi.org/10.1603/0022-2585-38.1.29>
- Monsen, T., Lövgren, E., Widerström, M., & Wallinder, L. (2009). *In vitro* effect of ultrasound on bacteria and suggested protocol for sonication and diagnosis of prosthetic infections. *Journal of Clinical Microbiology*, 47(8), 2496–2501. <https://doi.org/10.1128/JCM.02316-08>
- Moradali, M. F., & Rehm, B. H. A. (2019). The Role of Alginate in Bacterial Biofilm Formation. In *Extracellular Sugar-Based Biopolymers Matrices* (pp. 517–537). [https://doi.org/10.1007/978-3-030-12919-4\\_13](https://doi.org/10.1007/978-3-030-12919-4_13)
- Moraes, G. S., Cachoeira, V. S., Alves, F. M. C., Kiratcz, F., Albach, T., Bueno, M. G., Neppelenbroek, K. H., & Urban, V. M. (2021). Is there an optimal method to detach *Candida albicans* biofilm from dental materials? *Journal of Medical Microbiology*, 70(10), 001436. <https://doi.org/10.1099/JMM.0.001436/CITE/REFWORKS>

- Mukherjee, S., & Bassler, B. L. (2019). Bacterial quorum sensing in complex and dynamically changing environments. *Nature Reviews Microbiology*, *17*(6), 371–382. <https://doi.org/10.1038/s41579-019-0186-5>
- Nájera, J. A., González-Silva, M., & Alonso, P. L. (2011). Some lessons for the future from the global malaria eradication programme (1955-1969). *PLoS Medicine*, *8*(1):e1000412. <https://doi.org/10.1371/journal.pmed.1000412>
- Natto, M. J., Savioli, F., Quashie, N. B., Dardonville, C., Rodenko, B., & de Koning, H. P. (2012). Validation of novel fluorescence assays for the routine screening of drug susceptibilities of *Trichomonas vaginalis*. *Journal of Antimicrobial Chemotherapy*, *67*(4), 933–943. <https://doi.org/10.1093/jac/dkr572>
- Oliveira, G. D. A., Lieberman, J., & Barillas-Mury, C. (2012). Epithelial nitration by a peroxidase/NOX5 system mediates mosquito antiplasmodial immunity. *Science*, *335*(6070), 856–859. <https://doi.org/10.1126/science.1209678>
- O’neill, S. L., Kittayapong, P., Braig, H. R., Andreadis, J. T. G., Gonzalez, J. P., & Tesh, R. B. (1995). Insect densovirus may be widespread in mosquito cell lines. *Journal of General Virology*, *76*, 2067–2074. <https://doi.org/10.1099/0022-1317-76-8-2067>
- Osei-Poku, J., Mbogo, C. M., Palmer, W. J., & Jiggins, F. M. (2012). Deep sequencing reveals extensive variation in the gut microbiota of wild mosquitoes from Kenya. *Molecular Ecology*, *21*(20), 5138–5150. <https://doi.org/10.1111/j.1365-294X.2012.05759.x>
- Palleroni, N. J. (2015). *Pseudomonas*. In *Bergey’s Manual of Systematics of Archaea and Bacteria* (pp. 1–1). Wiley. <https://doi.org/10.1002/9781118960608.gbm01210>
- Paquet-Mercier, F., Parvinezadeh Gashti, M., Bellavance, J., Taghavi, S. M., & Greener, J. (2016). Through thick and thin: a microfluidic approach for continuous measurements of biofilm viscosity and the effect of ionic strength. *Lab on a Chip*, *16*(24), 4710–4717. <https://doi.org/10.1039/C6LC01101B>
- Peeters, E., Nelis, H. J., & Coenye, T. (2008). Comparison of multiple methods for quantification of microbial biofilms grown in microtiter plates. *Journal of Microbiological Methods*, *72*(2), 157–165. <https://doi.org/10.1016/j.mimet.2007.11.010>

- Pereira, M. H., Kumar Mohanty, A., Garg, S., Tyagi, S., & Kumar, A. (2021). Characterization of midgut microbiome of *Anopheles stephensi* Liston. *Journal of Vector Borne Diseases*, 58(1), 74–84. <https://doi.org/10.4103/0972-9062.289392>
- Pinto, S. N., Dias, S. A., Cruz, A. F., Mil-Homens, D., Fernandes, F., Valle, J., Andreu, D., Prieto, M., Castanho, M. A. R. B., Coutinho, A., & Veiga, A. S. (2019). The mechanism of action of pepR, a viral-derived peptide, against *Staphylococcus aureus* biofilms. *Journal of Antimicrobial Chemotherapy*, 74(9), 2617–2625. <https://doi.org/10.1093/jac/dkz223>
- Radovanovic, R. S., Savic, N. R., Ranin, L., Smitran, A., Opavski, N. V., Tepavcevic, A. M., Ranin, J., & Gajic, I. (2020). Biofilm Production and Antimicrobial Resistance of Clinical and Food Isolates of *Pseudomonas* spp. *Current Microbiology*, 77(12), 4045–4052. <https://doi.org/10.1007/s00284-020-02236-4>
- Ramirez, J. L., Short, S. M., Bahia, A. C., Saraiva, R. G., Dong, Y., Kang, S., Tripathi, A., Mlambo, G., & Dimopoulos, G. (2014). *Chromobacterium* Csp\_P reduces Malaria and Dengue infection in vector mosquitoes and has entomopathogenic and *in vitro* anti-pathogen activities. *PLoS Pathogens*, 10(10):e1004398. <https://doi.org/10.1371/journal.ppat.1004398>
- Rani, A., Sharma, A., Rajagopal, R., Adak, T., & Bhatnagar, R. K. (2009). Bacterial diversity analysis of larvae and adult midgut microflora using culture-dependent and culture-independent methods in lab-reared and field-collected *Anopheles stephensi*-an Asian malarial vector. *BMC Microbiology*, 9(1):96. <https://doi.org/10.1186/1471-2180-9-96>
- Ranson, H., & Lissenden, N. (2016). Insecticide Resistance in African *Anopheles* Mosquitoes: A Worsening Situation that Needs Urgent Action to Maintain Malaria Control. *Trends in Parasitology*, 32(3), 187–196. <https://doi.org/10.1016/j.pt.2015.11.010>
- Ricci, I., Damiani, C., Scuppa, P., Mosca, M., Crotti, E., Rossi, P., Rizzi, A., Capone, A., Gonella, E., Ballarini, P., Chouaia, B., Sagnon, N. F., Esposito, F., Alma, A., Mandrioli, M., Sacchi, L., Bandi, C., Daffonchio, D., & Favia, G. (2011). The yeast *Wickerhamomyces anomalus* (*Pichia anomala*) inhabits the midgut and reproductive

- system of the Asian malaria vector *Anopheles stephensi*. *Environmental Microbiology*, 13(4), 911–921. <https://doi.org/10.1111/j.1462-2920.2010.02395.x>
- Ricci, I., Mosca, M., Valzano, M., Damiani, C., Scuppa, P., Rossi, P., Crotti, E., Cappelli, A., Ulissi, U., Capone, A., Esposito, F., Alma, A., Mandrioli, M., Sacchi, L., Bandi, C., Daffonchio, D., & Favia, G. (2011). Different mosquito species host *Wickerhamomyces anomalus* (*Pichia anomala*): Perspectives on vector-borne diseases symbiotic control. *Antonie van Leeuwenhoek, International Journal of General and Molecular Microbiology*, 99(1), 43–50. <https://doi.org/10.1007/s10482-010-9532-3>
- Rice, S. A., Koh, K. S., Queck, S. Y., Labbate, M., Lam, K. W., & Kjelleberg, S. (2005). Biofilm formation and sloughing in *Serratia marcescens* are controlled by quorum sensing and nutrient cues. *Journal of Bacteriology*, 187(10), 3477–3485. <https://doi.org/10.1128/JB.187.10.3477-3485.2005>
- Riehle, M. A., Moreira, C. K., Lampe, D., Lauzon, C., & Jacobs-Lorena, M. (2007). Using bacteria to express and display anti-*Plasmodium* molecules in the mosquito midgut. *International Journal for Parasitology*, 37(6), 595–603. <https://doi.org/10.1016/j.ijpara.2006.12.002>
- Rodgers, F. H., Gendrin, M., Wyer, C. A. S., & Christophides, G. K. (2017). Microbiota-induced peritrophic matrix regulates midgut homeostasis and prevents systemic infection of malaria vector mosquitoes. *PLoS Pathogens*, 13(5):e1006391. <https://doi.org/10.1371/journal.ppat.1006391>
- Rodrigues Perez, L. R., Luís Barth, A., & Rodrigues, L. R. (2011). Biofilm production using distinct media and antimicrobial susceptibility profile of *Pseudomonas aeruginosa*. *The Brazilian Journal of Infectious Diseases*, 15(4), 301–304. [https://doi.org/10.1016/s1413-8670\(11\)70196-9](https://doi.org/10.1016/s1413-8670(11)70196-9)
- Romoli, O., & Gendrin, M. (2018). The tripartite interactions between the mosquito, its microbiota and *Plasmodium*. *Parasites and Vectors*, 11(1):200. <https://doi.org/10.1186/s13071-018-2784-x>
- Ruiz-Roldán, L., de Toro, M., & Sáenz, Y. (2021). Whole genome analysis of environmental *Pseudomonas mendocina* strains: Virulence mechanisms and phylogeny. *Genes*, 12(1), 1–14. <https://doi.org/10.3390/genes12010115>

- Sader, H. S., Farrell, D. J., Flamm, R. K., & Jones, R. N. (2014). Antimicrobial susceptibility of Gram-negative organisms isolated from patients hospitalised with pneumonia in US and European hospitals: Results from the SENTRY Antimicrobial Surveillance Program, 2009-2012. *International Journal of Antimicrobial Agents*, 43(4), 328–334. <https://doi.org/10.1016/j.ijantimicag.2014.01.007>
- Sandberg, M. E., Schellmann, D., Brunhofer, G., Erker, T., Busygin, I., Leino, R., Vuorela, P. M., & Fallarero, A. (2009). Pros and cons of using resazurin staining for quantification of viable *Staphylococcus aureus* biofilms in a screening assay. *Journal of Microbiological Methods*, 78(1), 104–106. <https://doi.org/10.1016/j.mimet.2009.04.014>
- Sauer, K., Stoodley, P., Goeres, D. M., Hall-Stoodley, L., Burmølle, M., Stewart, P. S., & Bjarnsholt, T. (2022). The biofilm life cycle: expanding the conceptual model of biofilm formation. *Nature Reviews Microbiology*, 20(10), 608–620. <https://doi.org/10.1038/s41579-022-00767-0>
- Segata, N., Baldini, F., Pompon, J., Garrett, W. S., Truong, D. T., Dabiré, R. K., Diabaté, A., Levashina, E. A., & Catteruccia, F. (2016). The reproductive tracts of two malaria vectors are populated by a core microbiome and by gender-and swarm-enriched microbial biomarkers. *Scientific Reports*, 6(1):24207. <https://doi.org/10.1038/srep24207>
- Sharma, P., Rani, J., Chauhan, C., Kumari, S., Tevatiya, S., Das De, T., Savargaonkar, D., Pandey, K. C., & Dixit, R. (2020). Altered Gut Microbiota and Immunity Defines *Plasmodium vivax* Survival in *Anopheles stephensi*. *Frontiers in Immunology*, 11:609. <https://doi.org/10.3389/fimmu.2020.00609>
- Sharma, P., Sharma, S., Kumar Maurya, R., Das De, T., Thomas, T., Lata, S., Singh, N., Pandey, K. C., Valecha, N., & Dixit, R. (2014). Salivary glands harbor more diverse microbial communities than gut in *Anopheles culicifacies*. *Parasites & Vectors*, 7(1):235. <https://doi.org/10.1186/1756-3305-7-235>
- Silva, B. E., Matsena Zingoni, Z., Koekemoer, L. L., & Dahan-Moss, Y. L. (2021). Microbiota identified from preserved *Anopheles*. *Malaria Journal*, 20(1):230. <https://doi.org/10.1186/s12936-021-03754-7>

- Silverio, M. P., Kraychete, G. B., Rosado, A. S., & Bonelli, R. R. (2022). *Pseudomonas fluorescens* Complex and its intrinsic, adaptive, and acquired antimicrobial resistance mechanisms in pristine and human-impacted sites. *Antibiotics*, *11*(8):985. <https://doi.org/10.3390/antibiotics11080985>
- Sinka, M. E., Bangs, M. J., Manguin, S., Chareonviriyaphap, T., Patil, A. P., Temperley, W. H., Gething, P. W., Elyazar, I. R., Kabaria, C. W., Harbach, R. E., & Hay, S. I. (2011). The dominant *Anopheles* vectors of human malaria in the Asia-Pacific region: Occurrence data, distribution maps and bionomic précis. *Parasites and Vectors*, *4*(1):89. <https://doi.org/10.1186/1756-3305-4-89>
- Sinka, M. E., Bangs, M. J., Manguin, S., Rubio-Palis, Y., Chareonviriyaphap, T., Coetzee, M., Mbogo, C. M., Hemingway, J., Patil, A. P., Temperley, W. H., Gething, P. W., Kabaria, C. W., Burkot, T. R., Harbach, R. E., & Hay, S. I. (2012). A global map of dominant malaria vectors. *Parasites and Vectors*, *5*(1):69. <https://doi.org/10.1186/1756-3305-5-69>
- Skogman, M. E., Vuorela, P. M., & Fallarero, A. (2012). Combining biofilm matrix measurements with biomass and viability assays in susceptibility assessments of antimicrobials against *Staphylococcus aureus* biofilms. *Journal of Antibiotics*, *65*(9), 453–459. <https://doi.org/10.1038/ja.2012.49>
- Smith, D. L., & McKenzie, F. E. (2004). Statics and dynamics of malaria infection in *Anopheles* mosquitoes. *Malaria Journal*, *3*(1), 13. <https://doi.org/10.1186/1475-2875-3-13>
- Stepanovic, S., Vukovic, D., Dakic, I., Savic, B., & Svabic-Vlahovic, M. (2000). A modified microtiter-plate test for quantification of *Staphylococcal* biofilm formation. *Journal of Microbiological Methods*, *40*, 175–179. [https://doi.org/10.1016/s0167-7012\(00\)00122-6](https://doi.org/10.1016/s0167-7012(00)00122-6)
- Stoodley, P., Sauer, K., Davies, D. G., & Costerton, J. W. (2002). Biofilms as complex differentiated communities. *Annual Review of Microbiology*, *56*(1), 187–209. <https://doi.org/10.1146/annurev.micro.56.012302.160705>
- Sultan, M., Arya, R., & Kim, K. K. (2021). Roles of two-component systems in *Pseudomonas aeruginosa* virulence. *International Journal of Molecular Sciences*, *22*(22):12152. <https://doi.org/10.3390/ijms222212152>

- Taff, H. T., Nett, J. E., & Andes, D. R. (2012). Comparative analysis of *Candida* biofilm quantitation assays. *Medical Mycology*, 50(2), 214–218. <https://doi.org/10.3109/13693786.2011.580016>
- Tavares-Carreón, F., de Anda-Mora, K., Rojas-Barrera, I. C., & Andrade, A. (2023). *Serratia marcescens* antibiotic resistance mechanisms of an opportunistic pathogen: a literature review. *PeerJ*, 11:e14399. <https://doi.org/10.7717/peerj.14399>
- Tawakoli, P. N., Al-Ahmad, A., Hoth-Hannig, W., Hannig, M., & Hannig, C. (2013). Comparison of different live/dead stainings for detection and quantification of adherent microorganisms in the initial oral biofilm. *Clinical Oral Investigations*, 17(3), 841–850. <https://doi.org/10.1007/s00784-012-0792-3>
- Taylor, L. H. (1999). Infection rates in, and the number of *Plasmodium falciparum* genotypes carried by *Anopheles* mosquitoes in Tanzania. *Annals of Tropical Medicine & Parasitology*, 93(6), 659–662. <https://doi.org/10.1080/00034989958168>
- Tchioffo, M. T., Boissière, A., Abate, L., Nsango, S. E., Bayibéki, A. N., Awono-Ambéné, P. H., Christen, R., Gimonneau, G., & Morlais, I. (2016). Dynamics of Bacterial community composition in the malaria mosquito's epithelia. *Frontiers in Microbiology*, 6:1500. <https://doi.org/10.3389/fmicb.2015.01500>
- Terenius, O., De Oliveira, C. D., Pinheiro, W. D., Tadei, W. P., James, A. A., & Marinotti, O. (2008). 16S rRNA gene sequences from bacteria associated with adult *Anopheles darlingi* (Diptera: Culicidae) mosquitoes. *Journal of Medical Entomology*, 45(1), 172–175. [https://doi.org/10.1603/0022-2585\(2008\)45\[172:SRGSFB\]2.0.CO;2](https://doi.org/10.1603/0022-2585(2008)45[172:SRGSFB]2.0.CO;2)
- Torres, K., Ferreira, M. U., Castro, M. C., Escalante, A. A., Conn, J. E., Villasis, E., Da Silva Araujo, M., Almeida, G., Rodrigues, P. T., Corder, R. M., Fernandes, A. R. J., Calil, P. R., Ladeia, W. A., Garcia-Castillo, S. S., Gomez, J., Do Valle Antonelli, L. R., Gazzinelli, R. T., Golenbock, D. T., Llanos-Cuentas, A., ... Vinetz, J. M. (2022). Malaria Resilience in South America: Epidemiology, Vector Biology, and Immunology Insights from the Amazonian International Center of Excellence in Malaria Research Network in Peru and Brazil. *American Journal of Tropical Medicine and Hygiene*, 107(4\_Suppl), 168–181. <https://doi.org/10.4269/ajtmh.22-0127>

- Tremblay, Y. D. N., Hathroubi, S., & Jacques, M. (2014). Les biofilms bactériens : leur importance en santé animale et en santé publique [Bacterial biofilms: their importance in animal health and public health]. *Canadian Journal of Veterinary Research = Revue Canadienne de Recherche Veterinaire*, 78(2), 110–116. <https://www.ncbi.nlm.nih.gov/pmc/articles/PMC3962273/>
- Wang, S., Dos-Santos, A. L. A., Huang, W., Liu, K. C., Oshaghi, M. A., Wei, G., Agre, P., & Jacobs-Lorena, M. (2017). Driving mosquito refractoriness to *Plasmodium falciparum* with engineered symbiotic bacteria. *Science*, 357(6358), 1399–1402. <https://doi.org/10.1126/science.aan5478>
- Wang, S., Ghosh, A. K., Bongio, N., Stebbings, K. A., Lampe, D. J., & Jacobs-Lorena, M. (2012). Fighting malaria with engineered symbiotic bacteria from vector mosquitoes. *Proceedings of the National Academy of Sciences*, 109(31), 12734–12739. <https://doi.org/10.1073/pnas.1204158109>
- Wang, S., & Jacobs-Lorena, M. (2013). Genetic approaches to interfere with malaria transmission by vector mosquitoes. *Trends in Biotechnology*, 31(3), 185–193. <https://doi.org/10.1016/j.tibtech.2013.01.001>
- Wang, Y., Gilbreath, T. M., Kukutla, P., Yan, G., & Xu, J. (2011). Dynamic gut microbiome across life history of the malaria mosquito *Anopheles gambiae* in Kenya. *PLoS ONE*, 6(9):e244767. <https://doi.org/10.1371/journal.pone.0024767>
- Wiebe, A., Longbottom, J., Gleave, K., Shearer, F. M., Sinka, M. E., Massey, N. C., Cameron, E., Bhatt, S., Gething, P. W., Hemingway, J., Smith, D. L., Coleman, M., & Moyes, C. L. (2017). Geographical distributions of African malaria vector sibling species and evidence for insecticide resistance. *Malaria Journal*, 16(1):85. <https://doi.org/10.1186/s12936-017-1734-y>
- Wijesinghe, G., Dilhari, A., Gayani, B., Kottegoda, N., Samaranayake, L., & Weerasekera, M. (2019). Influence of Laboratory Culture Media on *in vitro* Growth, Adhesion, and Biofilm Formation of *Pseudomonas aeruginosa* and *Staphylococcus aureus*. *Medical Principles and Practice*, 28(1), 28–35. <https://doi.org/10.1159/000494757>
- Wikipedia Contributors. (2019, December 3). *Resazurin*. Wikipedia; Wikimedia Foundation. <https://en.wikipedia.org/wiki/Resazurin>. Date of access: 29/09/2023

- Wilke, A. B. B., & Marrelli, M. T. (2015). Paratransgenesis: A promising new strategy for mosquito vector control. *Parasites and Vectors*, 8(1):342. <https://doi.org/10.1186/s13071-015-0959-2>
- Wood, T. L., Gong, T., Zhu, L., Miller, J., Miller, D. S., Yin, B., & Wood, T. K. (2018). Rhamnolipids from *Pseudomonas aeruginosa* disperse the biofilms of sulfate-reducing bacteria. *Npj Biofilms and Microbiomes*, 4(1):22. <https://doi.org/10.1038/s41522-018-0066-1>
- World Health Organization. (2022). *World malaria report 2022*. <https://www.wipo.int/amc/en/>
- Yan, J., & Bassler, B. L. (2019). Surviving as a Community: Antibiotic Tolerance and Persistence in Bacterial Biofilms. *Cell Host and Microbe*, 26(1), 15–21. <https://doi.org/10.1016/j.chom.2019.06.002>
- Yin, R., Cheng, J., Wang, J., Li, P., & Lin, J. (2022). Treatment of *Pseudomonas aeruginosa* infectious biofilms: Challenges and strategies. *Frontiers in Microbiology*, 13:955286. <https://doi.org/10.3389/fmicb.2022.955286>
- Yordanova, I. A., Zakovic, S., Rausch, S., Costa, G., Levashina, E., & Hartmann, S. (2018). Micromanaging Immunity in the Murine Host vs. The Mosquito Vector: Microbiota-Dependent Immune Responses to Intestinal Parasites. *Frontiers in Cellular and Infection Microbiology*, 8:308. <https://doi.org/10.3389/fcimb.2018.00308>
- Zoure, A. A., Sare, A. R., Yameogo, F., Somda, Z., Massart, S., Badolo, A., & Francis, F. (2020). Bacterial communities associated with the midgut microbiota of wild *Anopheles gambiae* complex in Burkina Faso. *Molecular Biology Reports*, 47(1), 211–224. <https://doi.org/10.1007/s11033-019-05121-x>

## 6. Annexes

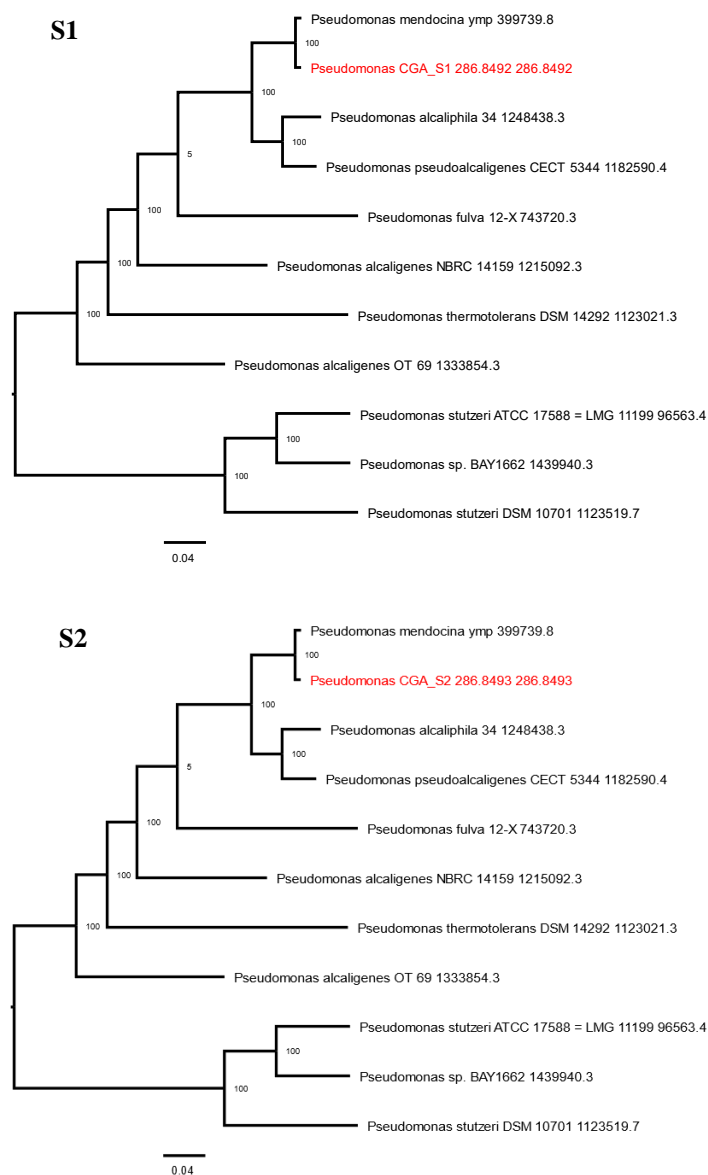


**Figure S1 - Phylogenetic Analysis** resulting from the Comprehensive Genome Analysis Service of the BV-BRC online program, referring to the *P. mendocina* isolate for which whole genome sequencing was conducted: S1 - *Pseudomonas* sp. isolated from *An. gambiae*; S2 - *Pseudomonas* sp. isolate recovered after the colonization experiment on *An. stephensi*.

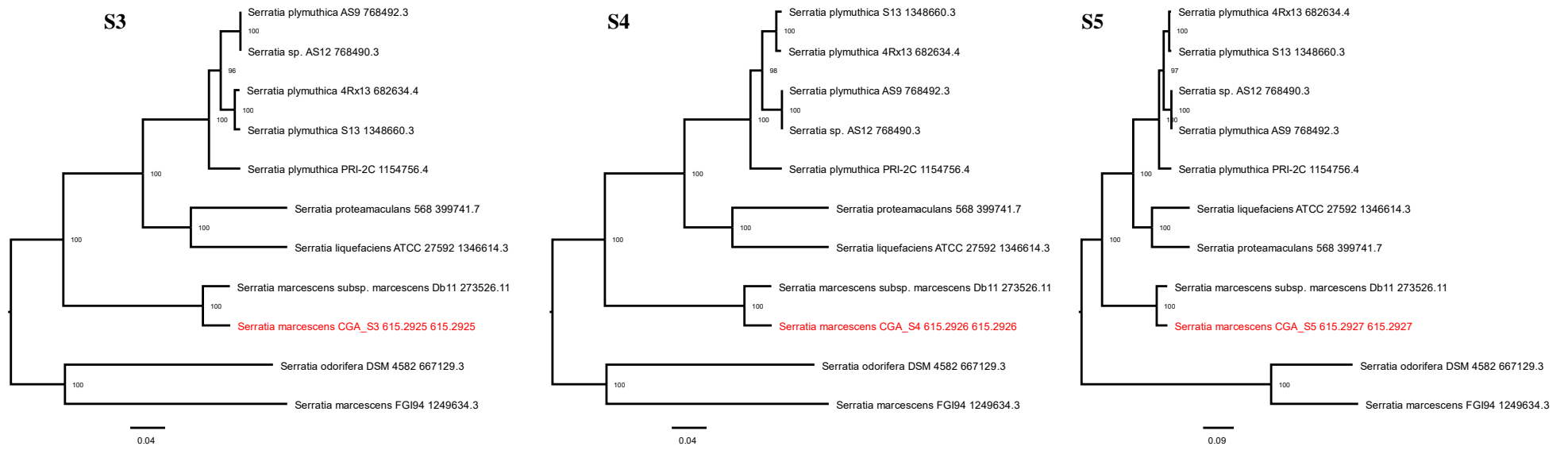


**Figure S2 - Phylogenetic Analysis** resulting from the Comprehensive Genome Analysis Service of the BV-BRC online program, referring to the *S. marcescens* isolates for which whole genome sequencing was conducted: S3 – *S. marcescens* An. steph A1-C1 isolated from *An. stephensi*; S4 – *S. marcescens* An. steph A7-A1 isolated from *An. stephensi*; S5 – *S. marcescens* An. col A9-C4 isolated from *An. coluzzii*.

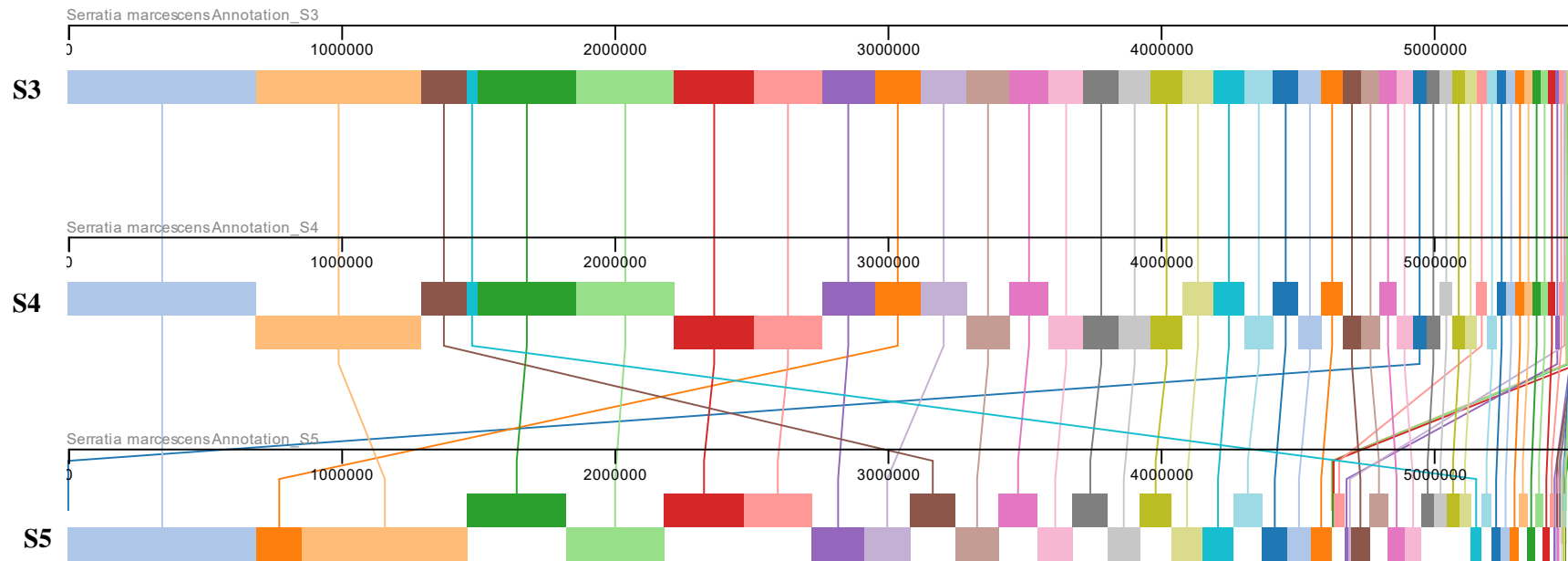


**Figure S3 - Schematic representation of the genomic alignment between the sequences of the *S. marcescens* isolates resulting from whole genome sequencing.** The sequences were assembled and then entered into the Genome Alignment (Mauve) tool in the BV-BRC software. The sequences are identified by a simplifying nomenclature: S3 – *S. marcescens* An. steph A1-C1 isolated from *An. stephensi*; S4 – *S. marcescens* An. steph A7-A1 isolated from *An. stephensi*; S5 – *S. marcescens* An. col A9-C4 isolated from *An. coluzzii*.

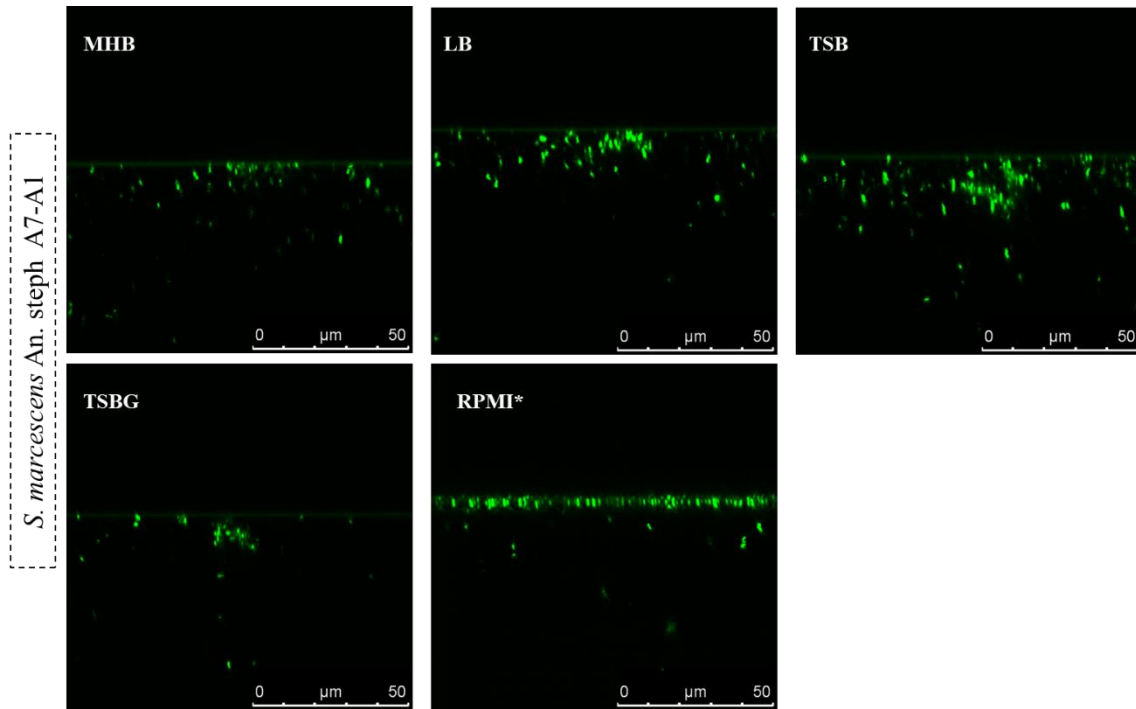


**Figure S4 - Representative confocal microscopy images of 24 hours *S. marcescens* An. steph A7-A1 biofilms.** The biofilms were labeled with the probe SYTO 9 and visualized using a Leica TCS SP5 inverted confocal microscope (Leica Microsystems CMS GmbH, Mannheim, Germany). The images depicted in the Figure correspond to the xzy plane view. Each image corresponds to different biofilm culture conditions.

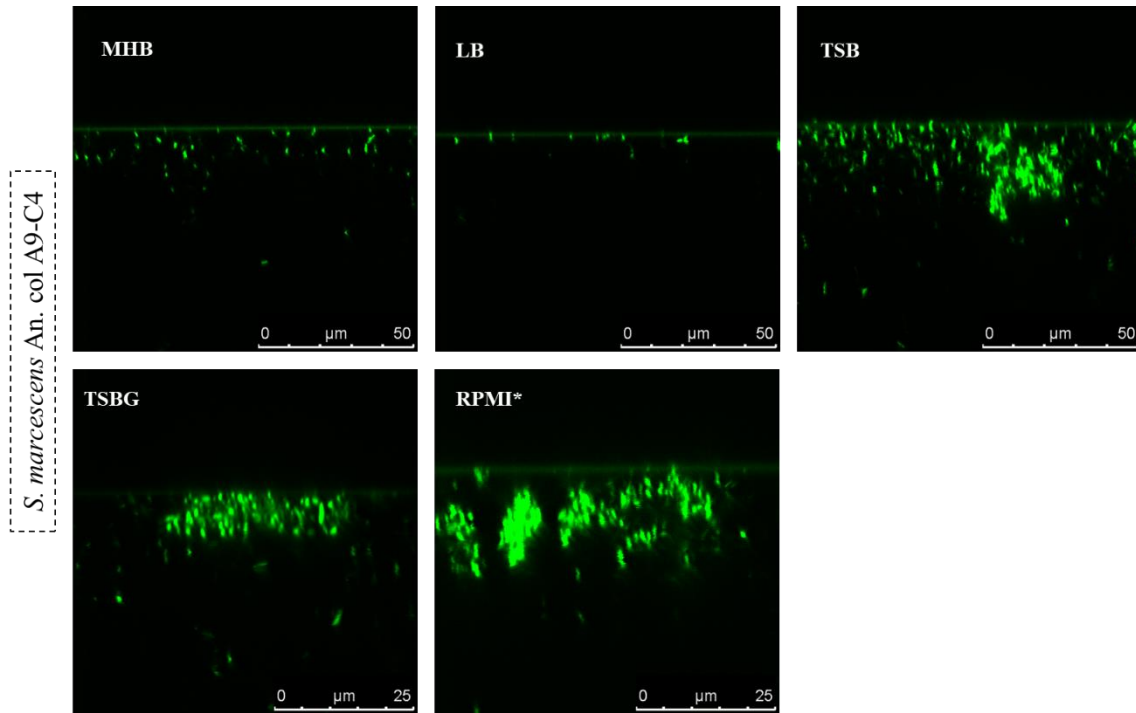


**Figure S5 - Representative confocal microscopy images of 24 hours *S. marcescens* An. col A9-C4 biofilms.** The biofilms were labeled with the probe SYTO 9 and visualized using a Leica TCS SP5 inverted confocal microscope (Leica Microsystems CMS GmbH, Mannheim, Germany). The images depicted in the Figure correspond to the xzy plane view. Each image corresponds to different biofilm culture conditions.

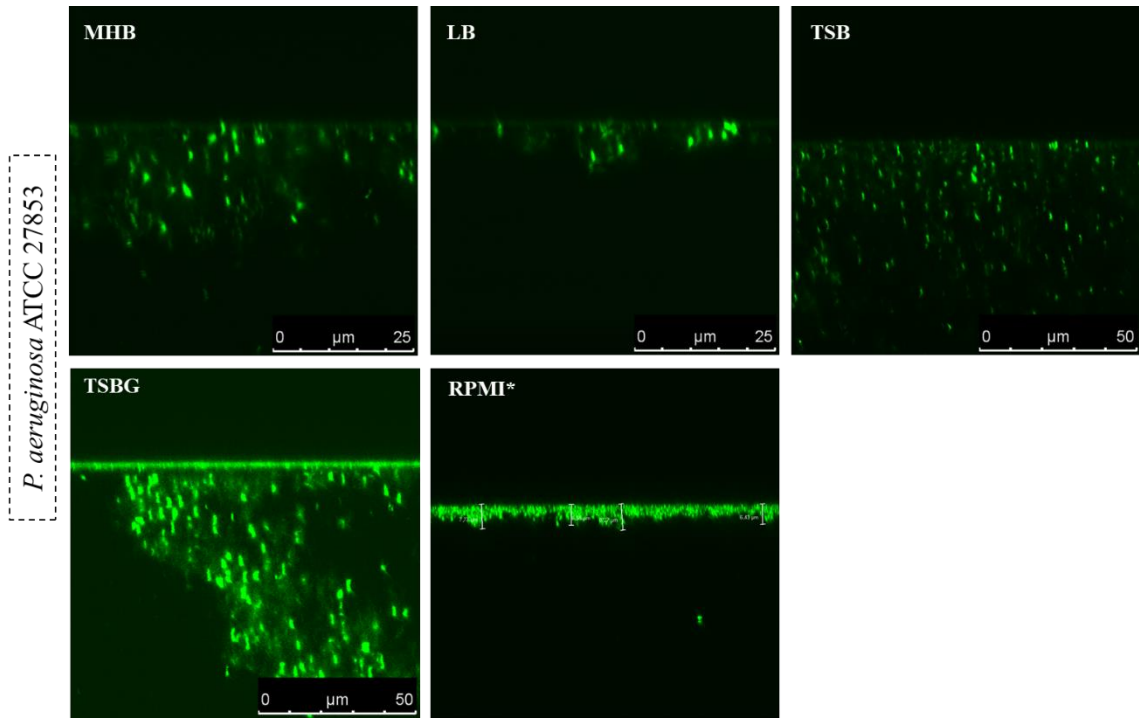


**Figure S6 - Representative confocal microscopy images of 24 hours *P. aeruginosa* ATCC 27853 biofilms.** The biofilms were labeled with the probe SYTO 9 and visualized using a Leica TCS SP5 inverted confocal microscope (Leica Microsystems CMS GmbH, Mannheim, Germany). The images depicted in the Figure correspond to the xzy plane view. Each image corresponds to different biofilm culture conditions.



**NOVA**

UNIVERSIDADE NOVA  
DE LISBOA